

# Engineering Extracellular Matrix Scaffolds Derived from Vascularized Composite Allografts and Vascularized Peripheral Nerves Grafts

Master Thesis Molecular Life Sciences  
Faculty of Science, University of Bern

Handed in by  
Tsering Wüthrich  
February 2018

Thesis Supervisors  
Prof. Dr. R. Rieben  
Dr. phil. nat. A. Taddeo

As knowledge increases, wonder deepens.

Charles L. Morgan

## Table of Contents

<b>1. Abstract .....</b>	<b>7</b>
<b>2. Introduction.....</b>	<b>9</b>
2.1 Tissue Engineering.....	9
2.1.1 Regenerative Medicine and Tissue Engineering .....	9
2.1.2 Regenerative Medicine .....	9
2.1.3 Definition of Tissue Engineering.....	10
2.1.4 History of Tissue Engineering.....	10
2.1.5 Biomaterials .....	12
2.1.6 Extracellular matrix scaffolds - ECMS .....	12
Extracellular matrix – ECM.....	13
Proteoglycans and Glycosaminoglycans.....	13
Other non-fibrous proteins of the ECM .....	14
Fibrous proteins: collagen .....	15
Fibrous proteins: elastin.....	15
2.1.7 Importance of vascularization in engineered tissues.....	15
2.2 Decellularization.....	17
2.2.1 The dawn of the decellularization technology .....	18
2.2.2 Methods for decellularization.....	18
2.2.3 Bioreactors .....	19
2.2.4 Chemical decellularization .....	20
Ionic, non-ionic and zwitterionic agents .....	20
Acids, bases, hyper- and hypotonic solutions .....	20
Alcohols.....	21
Miscellaneous solvents .....	21
2.2.5 Biological decellularization.....	21
Enzymes .....	21
Miscellaneous biologics .....	22
2.2.6 Physical and miscellaneous agents .....	22
Temperature.....	22
Force and pressure .....	22
Electricity.....	23
2.2.7 Techniques for Decellularization .....	23
Whole organ perfusion .....	23
Pressure gradient.....	24
Supercritical cell clearance.....	24

Immersion and agitation .....	25
2.3 Clinical aspects .....	26
2.3.1 Rationale for using ECMS in the clinics.....	26
2.3.2 Administered ECMS in patients.....	26
2.4 Limitations of TE.....	28
2.4.1 Alternatives to ECMS-TE .....	29
3D bioprinting – a brief introduction .....	29
Crossing kingdoms – of extended horizons.....	29
2.5 Future of TE.....	32
2.6. Vasclularized Composite Allograft Engineering.....	35
2.6.1 Vascularized composite allografts - VCA .....	35
2.6.2 The challenges of VCA.....	36
2.6.3 Overcoming the challenges.....	36
2.6.4 Vascularized composite allograft-engineering: VCE.....	37
2.7.1 Tissue engineering of peripheral nerve .....	38
2.7.2 The need for peripheral nerve TE.....	38
2.7.3 Peripheral nerve ECMS .....	38
2.7.4 A tissue engineering approach for the repair of peripheral nerve injuries .....	39
<b>3. Aim of the study .....</b>	<b>41</b>
<b>4. Methods .....</b>	<b>42</b>
4.1 Graft acquisition.....	42
4.1.1 VCE grafts – face and ear grafts .....	42
4.1.2 Porcine nerve grafts.....	42
4.1.3 Surgical sciatic nerve collection of pigs .....	42
4.2 Decellularization.....	43
4.2.1 Perfusion decellularization of face and ear grafts .....	43
4.2.2 Perfusion decellularization of porcine sciatic nerve grafts.....	44
4.3 Scaffold analysis .....	44
4.3.1 Agiography .....	44
4.3.2 DNA quantification .....	44
4.3.3 sGAG quantification.....	45
4.3.4 Sampling for protein extraction .....	45
Biopsies Human ear .....	45
Biopsies Human face.....	45
4.3.5 Protein extraction.....	46
4.3.6 Protein quantification.....	46
4.4 Cytokine quantification .....	47

4.4.1 Human face and ear.....	47
4.4.2 Porcine nerves.....	48
4.5 Cryosectioning.....	49
4.5.1 Ear.....	49
4.5.2 Nerve.....	49
4.6 Immunofluorescence staining.....	49
4.7 Histology.....	51
4.8 Recellularization of the porcine nerve grafts.....	51
4.8.1 Porcine aortic endothelial cells.....	51
4.8.2 Fluorescent membrane labelling.....	51
4.8.3 Perfusion-recellularization with wtPAEC.....	52
4.9 Statistical analysis.....	52
<b>5. Results.....</b>	<b>53</b>
5.1 Characterization of Human Ear VCE.....	53
5.1.1 Effectiveness of perfusion decellularization protocol.....	53
5.1.2. Preservation of cytokines in the ear ECMS.....	54
5.1.3 Coagulation associated factors in the ear.....	57
5.2 Characterization of Human Face ECMS.....	59
5.2.1 Preservation of cytokines in the face ECMS.....	59
5.2.2 Comparison of ear and face ECMS.....	61
5.3 Development of a vascularized peripheral nerve ECMS.....	63
5.3.1 Morphology and tissue architecture of the peripheral nerve ECMS.....	63
5.3.2 Assessment of internal vascularization of the peripheral nerve graft.....	68
5.3.3 Characterization of cytokine preservation decellularized nerve ECMS.....	71
5.3.4 Re-endothelialization of the nerve ECMS.....	75
<b>6. Discussion.....</b>	<b>78</b>
6.1 Discussion of VCE results.....	79
6.1.1 Preservation of Cytokines after decellularization.....	79
6.1.2 Body parts show individual preservation patterns.....	79
6.1.3 Analyzing different layers of the VCE.....	80
6.1.4 Coagulation associated factors in the ear ECMS.....	80
6.1.5 Limitations of the study.....	81
6.2 Discussion of the engineered vascularized peripheral nerve ECMS.....	83
6.2.1 Structural assessment.....	83
6.2.2 Vasculature.....	84
6.2.3 Decellularization and DNA content.....	84
6.2.4 Preservation of nerve structures.....	85

6.2.5 Characterization of cytokine retention patterns ..... 85

6.2.6 Re-endothelialization..... 86

**7. Conclusion ..... 87**

7.1 VCA experiments ..... 87

7.2 Peripheral nerve experiments ..... 87

**8. Outlook..... 88**

8.1 Vascularized composite engineering..... 88

8.2 Peripheral nerve engineering ..... 88

**9. References ..... 90**

**10. Declaration of consent ..... 90**

**11. Acknowledgements ..... 99**

# 1. Abstract

The worldwide imbalance between supply and demand of transplants has led to new approaches for creation of engineered grafts and refinement of existing techniques. In order to scientifically contribute to help solving the tremendous donor organ shortage, we addressed refinement of two different types of transplants, namely vascularized composite allografts (VCA) and peripheral nerve grafts. VCA transplants, such as hand and face grafts, are known for having the highest rates of acute rejection amongst all kinds of transplants. Vascularized composite engineering is the development of VCA scaffolds, in which recipient cells can be grown before implantation. Therefore, this might be an effective solution to decrease the immunological response to the graft and to reduce the need for strong immunosuppression, while at the same time expanding the donor pool. However, the immunologic characteristics of decellularized extracellular matrix scaffolds (ECMS) of VCA have been barely investigated. A deeper understanding of such ECMS might create the base for enhanced development of engineered VCA transplants. Therefore, in this study, we analyzed the cytokine content of human ear and face ECMS, that have been cleared from cells using perfusion decellularization. Starting from the experience gained from the development and characterization of the face and ear ECMS, we then developed an acellular vascularized peripheral nerve ECMS that was re-endothelialized. This innovative model of re-endothelialized decellularized nerve grafts may help to overcome the current limitation of 2-3 cm gap length in peripheral nerve bridging by providing vascularization of the graft. Re-endothelialized vessels could potentially be anastomosed to the recipients' vascularization and the graft is expected to present improved blood perfusion leading to increased oxygenation and nutrient supply in the nerve, which will enhance tissue regeneration and increase functional outcome. Our data confirmed that in the VCA as well as in the peripheral nerve grafts a variety of important cytokines (e.g. growth factors and angiogenic proteins) as well as important ECM molecules are preserved at considerably high retention rates and that the cell-empty ECM scaffolds of peripheral nerves can be re-endothelialized.

## Genesis 2:21- 23 from ‘The creation of Man and Woman’

21 So the Lord God caused a deep sleep to fall upon the man, and while he slept **took one of his ribs and closed up its place with flesh.**

22 And the rib that the Lord God had taken from the man he **made into a woman** and brought her to the man.

23 Then the man said, “This at last is **bone of my bones and flesh of my flesh;** she shall be called Woman, because **she was taken out of Man.**”

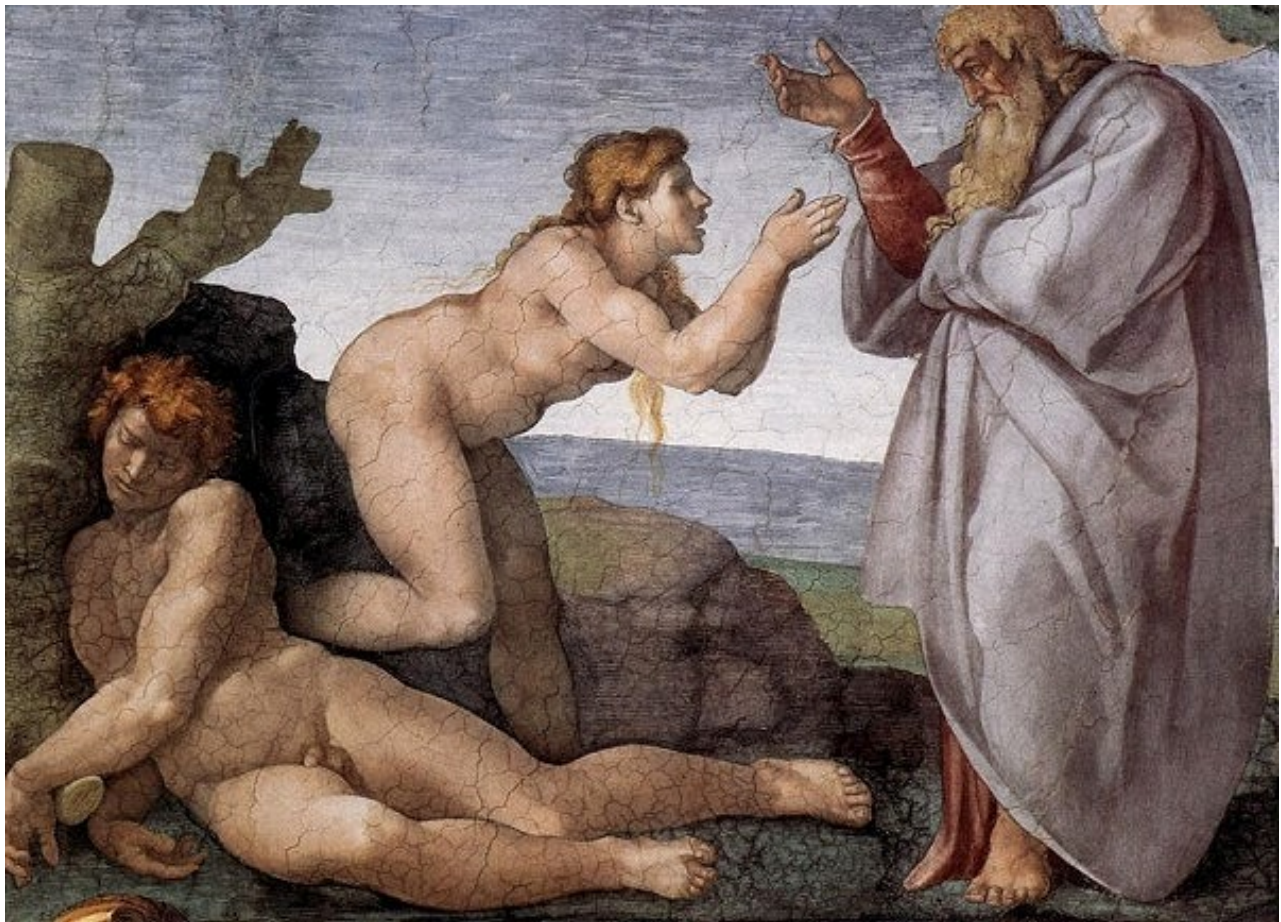


**Figure 1. The creation of Eve.** Fresco by Michelangelo Buonarroti in the Sistine Chapel, Vatican City, 1512. The depiction is linked to Genesis 2:21-23. This biblical passage can be interpreted as the first written reference of tissue engineering.

## 2. Introduction

### 2.1 Tissue Engineering

#### 2.1.1 Regenerative Medicine and Tissue Engineering

Regenerative Medicine and Tissue Engineering share a common goal that is, functional restoration of tissues, organs or entire body parts. A more detailed definition says that Regenerative Medicine (RM) and Tissue Engineering (TE) desire to replace diseased, malformed or damaged tissue through the design and development of biological substitutes that rehabilitate and maintain normal function of the tissue<sup>1</sup>. Both fields desire to increase or enhance the body's regenerative ability. However, their way to achieve this differs not only in philosophy, but they also use distinct methods and collaborate with dissimilar scientific fields<sup>2</sup>. Although there is a huge overlap of the two fields, they are considered as individual scientific domains.

#### 2.1.2 Regenerative Medicine

The main instrument of Regenerative Medicine are human cells. These may originate from different sources and come in varying differentiation stages. Many types of cells are being investigated, ranging from somatic cells, adult stem cells (e.g. mesenchymal stem cells, MSC), embryonic stem cells (ESC), pluripotent stem cells (also progenitor cells)<sup>3</sup> or the latest described induced pluripotent stem cells (iPSC). RM involves mainly cell culturing, directed cell growth and cell manipulation. Therefore, collaboration with other fields such as stem cell research, molecular biology and gene therapy lead to cell-based therapies, that are directed to restoration of function by (assisted) regeneration. Such therapies usually include cell transplantation and have shown great promise for therapy of diseases like macular degeneration (i.e. Holoclar®, an autologous limbal stem cell transplantation), leukemia, myeloma and lymphoma (i.e. by hematopoietic stem cell transplantation or bone marrow transplantation) and Parkinson's disease (transplanted human fetal brain cells)<sup>4</sup>. Holoclar® was the first stem cell based product on the European market and has been approved by the European Committee for medical application in the European Union in February 2015<sup>5,6</sup>. Modified cells or stem cells can also be applied into a scaffold, where an overlap with the sector of TE occurs. Sometimes autologous cells are expanded, stimulated or manipulated and then injected back into the original organ, to enhance intrinsic regenerative abilities.

However, this thesis was conducted under the aspect of scaffold production and Tissue Engineering. Therefore, no further details about Regenerative Medicine will be discussed.

### 2.1.3 Definition of Tissue Engineering

Tissue Engineering can be described as the development of biologic tissue substitutes using cells in combination with a supporting scaffold in order to restore, maintain or improve tissue function<sup>1</sup>. The lattices used to form the scaffold may also be bio-absorbable to let the cells remodel their own environment after implantation. It is a very interdisciplinary field that combines aspects from life sciences, material sciences, engineering, biomedical engineering and molecular biology.

### 2.1.4 History of Tissue Engineering

The first scientific articles about TE were published before the Second World War. In 1935 Alexis Carrel and Charles A. Lindbergh published the article *“The Culture of Whole Organs”* in the journal *Science*<sup>7</sup>. In 1938, Alexis Carrel and Charles A. Lindbergh produced a book (*The Culture of Organs*, New York, 1938), simultaneously to the scientific duo Raimond C. Parker and Paul B. Herber (*Methods of Tissue Culture*, New York, 1938). Alexis Carrel was awarded the 1912 Nobel Prize in Physiology or Medicine *“in recognition of his work on vascular suture and the transplantation of blood vessels and organs”*<sup>8</sup>. Some concepts of modern vessel engineering are based on his work in the early 20<sup>th</sup> century. Nevertheless, it took around sixty years until the first big series of TE experiments was carried out. These experiments attempted the generation of new cartilage tissue and had been conducted in the 1970's by the pioneer Dr. William Green at the Children's Hospital, Boston<sup>9</sup>. Although his experiments were unsuccessful, he correctly concluded, that with newly emerging biomaterials it would be possible to let cells grow in a certain shape to generate a new tissue<sup>2</sup>. At that time, the term *“Tissue Engineering”* was not clearly defined and its use was ambiguously applied to similar fields as for example Reconstructive Surgery and Regenerative Medicine. In the coming years - the 1980's - the number of reports of successful experiments rose. Collagen matrices were used to support the growth of dermal fibroblasts, sheets of keratinocytes were used to treat burn patients<sup>10</sup> and the first *“collagen gels”* were developed<sup>11</sup>. In 1988, a milestone was achieved when Dr. Joseph Vacanti (Children's Hospital, Boston) and Dr. Robert Langer (MIT, Boston), published the concept of designing cell-delivery scaffolds with defined features in vitro to support cell growth and enable environmental remodeling after in vivo implantation<sup>12</sup>. They introduced the concept of artificial bio-absorbable polymers and matrices as scaffolds for cell growth<sup>13</sup>. A decade later,

in 1997, they published their very famous work on production of a tissue engineered collagen auricle by seeding chondrocytes into a polymer-cell scaffold with subsequent in vivo implantation onto to back of a mouse<sup>14</sup>, thereby creating the so-called “Vacanti mouse” (figure 2). Therefrom, the engineering aspect found its way into the field of TE, which by then had matured into its modern essence as defined above. As research increased, the field expanded, and numbers of published articles rose. In 1994 the journal “Tissue Engineering” was founded. On the other hand, several centers for TE were launched worldwide in the 1990’s. Originating in the Boston (US) area, the first centers arose in the United States of America and soon, the wave swept over to Mexico and Europe. Centers in London, Giessen, Innsbruck, Freiburg and other locations were opened. By the late 1990’s, Asian centers were inaugurated in Tokyo, Nagoya and Shanghai<sup>2</sup> and by the turn of the millennia, TE centers had been spread all over the world at universities, foundations and private ventures and several Associations and Societies had been founded. Finally, the biggest of all Societies, i.e. the Tissue Engineering and Regenerative Medicine International Society (TERMIS), was founded in 2005.



**Figure 2. The Vacanti mouse.** Athymic male mouse (*nu/nu*) with a subcutaneously implanted polymer scaffold shaped like a human auricle and seeded with chondrocytes<sup>14</sup>. Modified from <http://www.newsweek.com/tissue-surgeon-ear-mouse-human-organs-transplant-cell-phones-666082>, (published 16.9.2017, accessed 9.2.2018).

### 2.1.5 Biomaterials

It is a common mistake to confound biomaterials with biologic materials. However, it is very essential to understand that they are not the same. A biologic material is a material that was produced by a biological system and is considered “alive” (i.e. viable material, capable of living, like cellular agglomerations, cells and tissues). Whereas according to the journal “Biomaterial” *“A biomaterial is now defined as a substance that has been engineered to take a form which, alone or as part of a complex system, is used to direct, by control of interactions with components of living systems, the course of any therapeutic or diagnostic procedure.”* (Citation from the journal “Biomaterials”, Editor-in-Chief K.W. Leong, [www.journals.elsevier.com/biomaterials/](http://www.journals.elsevier.com/biomaterials/), (23.01.2018), Copyright © 2018 Elsevier B.V.). This essentially means that a biomaterial is a non-living material that is compatible and able to interact with biologic systems and does not cause any irritation, inflammatory reaction or trigger any other malignant changes in the living tissue (e.g. capsule formation or neoplasms). A biomaterial can be of natural source or artificially fabricated. Some are bioactive (interact with biology of recipient) and some are only stationary. The most commonly used biomaterials are metals, ceramics, polymers (e.g. contact lenses), composite biomaterials (carbon products or fiber reinforced bone cement), biodegradable polymers, biologic biomaterials (tissue-derived, e.g. collagen or silk) and various kinds of hydrogels (agarose, alginate, collagen, peptides, polyethylene glycol). As there is a huge variety of biomaterials, the scaffolds that originate from them are also very unique and differ a lot in their features. A scaffold can be very jelly, porous or solid and as a second feature either biodegradable or persistent, depending on the type of biomaterial and the fabrication technique that was used to manufacture it. That allows for many combinatory possibilities and tailor-made implants. Therefore, in theory any tissue can be replaced. Although this is not yet practicable for all the bodies’ tissues (e.g. brain, heart or nerve tissue not), nevertheless, the current applications do cover a wide selection of tissue replacements, ranging from porous bone to solid teeth, and to soft tissues like elastic skin grafts. For the main experiments of this thesis, a type of biologic biomaterial was used, namely decellularized extracellular matrix scaffolds (ECMS) of human face, human ear and porcine sciatic nerves.

### 2.1.6 Extracellular matrix scaffolds - ECMS

In case of a transplantation the ideal graft would be made of the very same components as the lost tissue. Therefore, in terms of morphology and immunology, an autograft with the same shape and function would be required. TE strives for developing such grafts. The base

of any graft is the scaffold, which determines the size and shape of the engineered transplant. The natural scaffold of any multicellular organism is the ECM. The evolution of ECM was a major breakthrough in the history of all metazoa (multicellular organisms). In fact, it is a very preserved feature that actually is necessary for an organism to classify as metazoan. Due to extreme genetic preservation across species, variations in ECM composition are limited and the biomaterial is very biocompatible across species barrier<sup>15,16</sup>. The ECM is a secreted product from its resident cells which constantly change and adjust their microenvironment. Reciprocally, the ECM influences local cells and provides cues for cell proliferation, migration and differentiation<sup>17,18,19,20</sup>. There is a specific protein class to describe ECM components that are not primarily responsible for structural support but rather for cell-ECM interactions and cell function: the matricellular proteins<sup>17,21,22</sup>. The process of decellularization clears the ECM of all cellular components, leaving behind an empty ECM scaffold (ECMS). Depending on the type of tissue, the obtained ECMS has different structural features and molecular compositions. A graft that is composed of several types of tissues presents an increased complexity for decellularization methods and further procurement (i.e. recellularization).

### Extracellular matrix – ECM

The term ECM by default includes everything that is on the outside of cells, which includes not only the skeletal proteins but also associated molecules such as matricellular proteins, receptors, integrins, growth factors, cytokines and others. The ECM is not merely a dead structure or an environment that ensures stability of the tissue, but it has different functions and it also regulates tissue development, function and homeostasis by regulating pH, the abundance of receptors and growth factors, adjusting local hydration levels and initiating signaling cascades. Via such processes, the ECM plays an important role in establishment, separation and maintenance of organs and entire body parts<sup>23</sup>. ECM activity starts very early in ontogenesis and is involved in the development of the embryo and its organogenesis<sup>24</sup>. It is therefore self-evident, that the molecules that constitute the ECM have evolved to show structural and biochemical properties that are specifically tailored to their biological functions<sup>25</sup>. The ECM is composed of two major classes of macromolecules: glycoproteins and fibrous proteins. The glycoproteins include fibronectin, proteoglycans and laminin. The main fibrous proteins are the collagens and elastins<sup>25</sup>.

### Proteoglycans and Glycosaminoglycans

The majority of the interstitial space is filled with a gelatinous substance that retains a considerable quantity of water. This hydrated gel is made of many glycosaminoglycans (GAG) that are attached to a core protein via linker protein to form proteoglycans. This

structure and the enormous hydration allows for tissue buffering and mechanical force-resistance. The classification of PG is based upon the differences in the core proteins, the GAG content and localization. Three main families have been identified: 1) small leucine rich PG (SLRPs), 2) modular PG and 3) cell-surface PG<sup>26</sup>. GAGs on the other hand are unbranched polysaccharide chains composed of repeating disaccharide units [sulfated *N*-acetylglucosamine or *N*-acetylgalactosamine, *D*-glucuronic or *L*-iduronic acid and galactose (–4 *N*-acetylglucosamine- $\beta$ 1,3-galactose- $\beta$ 1)]. GAGs can be subdivided into further subclasses: sulfated GAGs (sGAG) and non-sulfated GAGs. Representatives of the sGAG include heparin sulfate, chondroitin sulfate and keratin sulfate. The non-sulfated GAGs are referred to as hyaluronic acid<sup>26</sup>. GAGs in general are highly hydrophilic and therefore, adopt extremely extended conformations that allow for hydrogel formation, which can bear high compressive forces. In terms of TE, retention of GAGs could be beneficial when it comes to tissue architecture and maintenance of mechanical properties of the decellularized graft.

#### Other non-fibrous proteins of the ECM

Another member of the non-fibrous protein family is fibronectin. It plays an important role in directing architecture of the interstitial ECM and cell attachment and cell function. It is secreted as a dimer conjoined by two disulfide bonds C-terminally. Fibronectin has several binding sites to other fibronectin dimers, to the cell-surface molecule integrin, to collagen and to heparin<sup>27</sup>. Its interaction with integrin influences migration and the behavior of the cell in a pleiotropic way. Fibronectin also serves as an extracellular mechano-receptor for the cell.

Laminins also interact with cell surface receptors like integrin. They are mainly associated with the basal lamina of tissues and are composed of large glycoproteins of globular nature. Laminins consist of laminin-type epidermal growth factor (EGF)-like repeats as well as alpha-helical domains. They are mainly known for bridging between other molecules<sup>28</sup>. The basal lamina is a very important type of epithelial and endothelial ECM, as it allows cells to attach and grow on it. Another member of the family is tenascin, which also exerts pleiotropic effects on cells that include fibroblast migration during wound healing and cellular behavior. Such molecules can be very useful in TE and their preservation can help to increase recellularization rate and facilitate tissue regeneration. As they naturally occur in the ECM, it is estimated that they would be very beneficial in engineered ECMS, too.

### Fibrous proteins: collagen

The most abundant protein in a multicellular organism is collagen and it can constitute up to 30% of the total protein mass of an organism<sup>29</sup>. Collagens are secreted by fibroblasts and are the main components to direct structural tissue architecture. However, they do not only provide tensile strength, but they also regulate cell adhesion, migration and chemotaxis and they can direct tissue development<sup>29</sup>. A study from 2010 found, that up to that date, 28 different types of collagenous proteins had been identified<sup>30</sup>. Most of the collagenous fibrils are formed by three triple-stranded helical collagen molecules winded up with each other. A standard collagen molecule has an amino- and a carboxy-terminal propeptide sequence at the ends and the middle is a simple series of Gly-X-Y repeats. On average, every third amino acid in these repeats is a glycine and although the X and Y components can be any other amino acid, they frequently are proline and hydroxyproline. A high glycine content is necessary for the 3D structure of the fibrils and their stabilization. It allows a close association of the fibers, which leads to facilitated formation of intramolecular hydrogen bonds and intermolecular cross-links<sup>31</sup>. The assembly into the triple helical structure (procollagen) occurs intracellularly and depending on the type of collagen different post-translational modifications and cleavages can occur when secreted into the extracellular space (conversion to mature collagen). In TE, collagen is the major component of ECMS and therefore, needs to be preserved very carefully during decellularization. There are many protocols that have different impact on the retention of collagen. Therefore, the decellularization protocol should be adjusted to the purpose and the tissue of origin of the ECMS. However, in any protocol it is very important to preserve collagen as it can help to guide the cells and regenerate the tissue with its intrinsic functions.

### Fibrous proteins: elastin

Elastin is another major fibrous ECM protein of tissues. They are associated with collagens and have the function to recoil in tissues that are exposed to immense tensile forces, i.e. stretches (e.g. connective tissue). Like collagens, elastin is secreted as tropoelastin (precursor of elastin) and assembles into fibers that get crosslinked to one another at their lysine residues.

## 2.1.7 Importance of vascularization in engineered tissues

The vascularization of a tissue has many tasks, with the two most important clearly being the oxygenation of the tissue and the removal of waste products. So far, clinical success of implanted TE grafts has been restricted to structurally thin and simple, as well as acellular tissues. Avascularity of the graft restricts the size and thickness of the tissue, as the natural

diffusion zone ends after 100 – 200  $\mu\text{m}$ <sup>32</sup>. Therefore, passive neovascularization from the surrounding tissue into the graft must be deep enough to provide the right amount of nutrients. However, neovascularization is usually limited to a penetration of 10 mm into the tissue. It has been observed, that the network formation of neovascularization in vitro is denser when cells are cultured in tri-cultures (endothelial cells, myoblasts and embryonic fibroblasts) rather than in co-culture (endothelial cells and myoblasts)<sup>33</sup>. Hence, a study concluded that perivascular cells (i.e. myoblasts, fibroblasts and other cells in proximity to vessels) seem to be equally important as endothelial cells for vessel formation<sup>34</sup>. Not only do they provide physical support for the endothelial cells, but they also create the appropriate environment, i.e. release of factors, like for example vascular endothelial growth factor (VEGF). Hence, TE protocols aiming at increasing angiogenesis should consider the important role of perivascular cells, too. A study has demonstrated, that in vitro produced vascularization helps to increase blood supply into the tissues of the graft and reduces cell death after in vivo implantation. Furthermore, 41% of the engineered CD31<sup>+</sup> vessels transported blood<sup>33</sup>. Although these findings are remarkable, it is not enough data to prove actual “functionality” of the vessels. This would include the assessment of responsiveness to physiologic signs from organs and the perivascular environment and to other vasoactive stimuli, tissue oxygenation and vascular permeability in vivo. Improper functionality of blood vessels can lead to edema, hypertension, acute respiratory distress syndrome and septic shock. When the vascular permeability gets too low, oncotic pressure can cause edema and lymphatic vessels will be needed to remove the extravascular fluid<sup>35</sup>. Therefore, it is advised to take the lymphatic system into consideration when designing ECMS and imply lymphangiogenic provisions, too. For the future, it will be important to assess the functional status of engineered vessels, to evaluate vascular remodeling in vivo and to determine the fate of the unperfused engineered vessels.

## 2.2 Decellularization

Decellularization stands for complete physical clearance of the tissue from any cellular compartments like cells, membranes, DNA fragments and any other component that is not considered as part of the ECM. Decellularization of a tissue leads therefore to an empty ECM 3D structure, which creates a so-called “ghost-organ”. As described above, such decellularized tissues are known as extracellular matrix scaffolds (ECMS). Almost any type of tissue can be decellularized. The remaining ECMS can directly be used as implants, or they can be biochemically (e.g. growth factor treatment) and biologically (recellularization) modified before application. As none of the below described methods and techniques are able to remove 100% of all cellular traces, lipids and DNA bits, the term decellularization has not been defined by quantitative metrics. However, some authors have put together certain thresholds that became generally accepted as guidelines. These numbers are based upon several studies, that included in vivo experiments which did not show any adverse effects. An ECMS can be considered as “decellularized” after the following three thresholds by Crapo et al., 2011<sup>36</sup>:

- < 50ng DNA per mg ECMS dry weight
- < 200bp length of DNA fragments
- absence of visible nuclear staining in tissue sections by H&E or DAPI (4',6-diamidino-2-phenylindole)

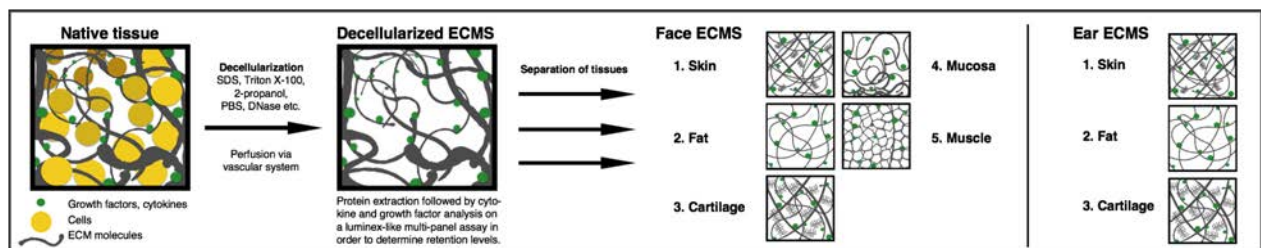


**Figure 3. Schematic overview of the decellularization process** and further sampling methods used for experiments in this thesis. Native grafts were perfusion decellularized and analyzed according to their different types of tissues. Design by Tsering Wüthrich.

### 2.2.1 The dawn of the decellularization technology

The principle of decellularization had been considered already in the early 20<sup>th</sup> century when W. E. Gallie in 1918 proposed to use boiled bone allografts in operative surgery<sup>37</sup>. It was only until 29 years later, when the next article considering the use of boiled bone grafts was published<sup>38</sup> and pointed out, that it still needed to be determined whether such boiled bone grafts were actually cleared of all living elements (i.e. cellular residues). Another 20 to 30 years later, in the 1970's and 1980's, orthopedic surgeons slowly began to pay attention to immune reactions against the devitalized but not decellularized, bone grafts (the boiled bone marrow was dead but not cleared out of the bone allografts). However, by the 1960's, the orthopedic surgeons had already been overtaken by researchers that had interest in soft tissues. They produced the first acellular small bowel grafts (by vigorously scraping the tissue with gauze) to successfully replace blood vessels in dogs. Although the dog trials were successful, a first in men study ended in decease of the patient 13 days after surgery, most probably due to the fact, that the graft was only partially decellularized<sup>39</sup>. Another early series of first in human trials had been carried out in the 1980's when chemically modified tracheas were implanted into two patients to close tracheal defects. These scaffolds were acellular and healed well in both patients<sup>40</sup>. Almost 30 years later, in 2008, decellularized trachea were used as scaffold. However, the novelty of this transplantation was, that the ECMS had been repopulated with autologous epithelial and mesenchymal stem cell-derived chondrocytes<sup>41</sup>. The outcome for the patient seemed outstanding. However, in 2017, six publications from the same authors (not the here cited paper) had been retracted due to scientific misconduct. Since the 1990's various decellularization protocols have been used to generate acellular collagen scaffolds and several were tested in animal experiments<sup>42,43</sup>. Another decellularization milestone was achieved in 2008, when the concept of perfusion decellularization by decellularization of a whole heart had been described for the first time by the group of Dr. Harald Ott<sup>44</sup>. In the past ten years, perfusion decellularization has become accepted as standard method for decellularization of organs with vascular access and a complex 3D structure.

### 2.2.2 Methods for decellularization

A variety of decellularization protocols has been developed and they can be divided into three main subtypes: chemical, biological and physical protocols. An overview of the most common techniques follows in the paragraphs below. However, before any decellularization protocol is started, the procurement of the graft should be adequately provided. Target structures need to be carefully surgically exposed (e.g. vessels from inside of

an amputated limb for perfusion decellularization) and the bioreactor setup should be established and sterilized in advance. Generally, the length of the decellularization process is proportional to the complexity (i.e. VCA vs. kidney) and the thickness as well as the size and structural nature of the tissue or organ<sup>36</sup>.

### 2.2.3 Bioreactors

A bioreactor is an apparatus that is used to carry out any type of bioprocesses (e.g. fermenters or enzyme reactors)<sup>45</sup>. Bioreactors are engineered or manufactured devices that are required to support a biologically active process. The most evident example of a bioreactor is the sewage purification plant where wastewater gets clarified. As the following paragraphs will describe, there are many techniques to obtain decellularization of a graft. As much as these techniques differ, the bioreactors must have different features and provide various environments. For example, in the experiments of this thesis, the bioreactors were selfmade and used for perfusion decellularization and recellularization. To enable perfusion and flow of the decellularizing solutions, a peristaltic pump was conjoined to the bioreactor system. Other protocols may include rigid agitation of the graft and therefore, the bioreactor must be vibration-proof or include a mobile compartment that allows for the motion. More complex types of bioreactors for example, must allow for pressure gradient formation in order to perform mesenchymal recellularization (cells migrate into the tissue along the pressure gradient). It is evident, that the bioreactor must be specifically tailored for the type of experiment that will be conducted in it. The humongous specificity of features that bioreactors have to provide leads to the fact, that most laboratories develop a self-engineered, selfmade specimen that is adequate for their type of experiments.

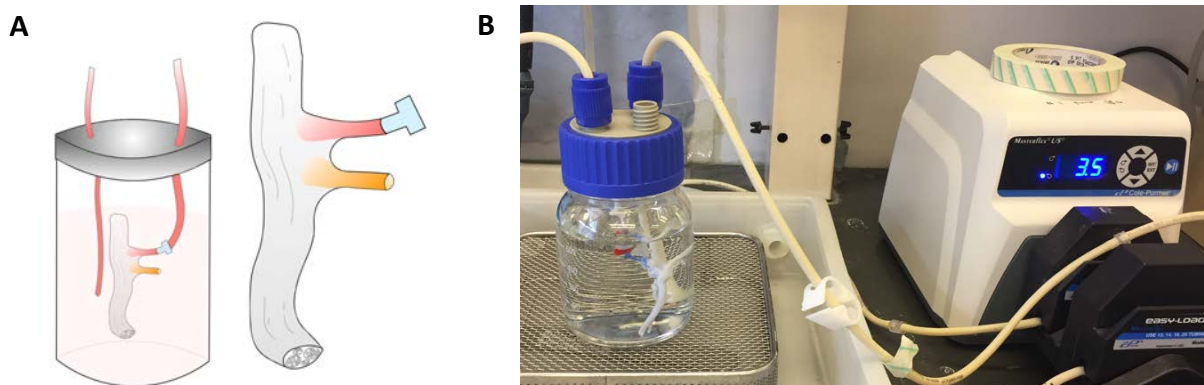


**Figure 4. A) Depiction of selfmade bioreactor** used for the experiments in this thesis. The nerve graft's artery was cannulated, attached to a microtubing system and placed in the bioreactor for perfusion decellularization. **B)** A peristaltic pump enabled flow of decellularizing solutions through the vascular tree of the graft in a closed-circuit manner. Source: A) design by Tsering Wüthrich, B) Courtesy of Jérôme Duisit.

## 2.2.4 Chemical decellularization

### Ionic, non-ionic and zwitterionic agents

Chemical decellularization protocols are the most commonly used. They can be applied to a wide variety of tissues, ranging from skin sheets to whole organ grafts. The “classic” decellularization protocols for soft and composed tissues are usually detergent-based. Detergents - be it ionic, non-ionic or zwitterionic - disintegrate the cellmembranes and disrupt the cellular entity. If motion is applied (i.e. agitation, flushing or perfusion), the cellular debris gets washed away and cleared out of the tissue. Most chemical decellularization protocols include cycles of different detergents like Triton X-100 or sodium dodecyl sulfate (SDS). It has been shown that Triton X-100 removes cell residues more effectively<sup>46</sup> while SDS is more efficient in removing cell nuclei<sup>47</sup> from thicker tissues. Therefore, most protocols include a combination of different chemicals, sometimes also different types of decellularization methods. For example, they can include a first chemical part and a second biological or physical part. For delipidation of the graft, non-ionic detergents (e.g. Triton X-100) are more effective than ionic ones (e.g. deoxycholate). Zwitterionic detergents (e.g. 3-[(3-cholamidopropyl)dimethylammonio]-1-propanesulfonate or CHAPS) are rarely used and are more effective for thinner sheet-like tissues like lung<sup>48</sup>. A study from 2004 showed better preservation of peripheral nerve ECM architecture when non-ionic and zwitterionic detergents were used rather than ionic chemicals<sup>49</sup>. In order to apply a decellularized graft to a patient, it is important to change the ECM structure and composition as little as possible and to use chemicals, that have the least impact on the recipient. Also, chemicals that are easy to clear out of the decellularized graft should be chosen over such that might be more efficient in decellularizing but then cannot be removed fully.

### Acids, bases, hyper- and hypotonic solutions

Other commonly used chemical decellularization agents are different kinds of acids and bases and hypo- or hypertonic solutions. Peracetic acid is commonly used as a disinfectant and, therefore, usually applied at the end of the decellularization process. Additionally, it removes remaining nucleic acids from the tissue by hydrolysis, with minimal damage to the ECM's molecular composition and structure<sup>50,51</sup>. However, it does slightly affect collagen stability but has no impact on sulfated proteoglycans (sGAG)<sup>52</sup>. Strong bases (calcium hydroxide, sodium sulphide and sodium hydroxide) are usually used for hair removal of dermis samples and therefore, commonly used in early stages of decellularization. However, bases reduce mechanical properties of the ECMS by cleaving collagen fibers and disruption of their crosslinks. Hence, bases reduce the ECMS stability more than any other chemical or enzymatic agent and it has been reported that they eliminate growth factors to a big extent<sup>53</sup>. Fewer protocols include hypertonic solutions. They can be applied to dissociate proteins

from DNA. Hypotonic solutions on the other hand, lyse the cells simply by osmotic effects. The ECMS gets minimally modified and the molecular composition is not affected<sup>54</sup>. Some protocols include several cycles of hyper- and hypotonic baths (depending on the protocol up to 5-6 cycles). However, if the tissue reaches a certain thickness this method can be of limited efficacy.

### Alcohols

Another group of chemicals that are used for decellularization are the alcohols. Many agents from this group have been used, such as glycerol, chloroform, ethanol, methanol and isopropanol. They dehydrate the cells and, eventually, lyse them. Some alcohols (ethanol, methanol, isopropanol etc.) also eliminate phospholipids and they have been proven to be more effective than lipases in doing so<sup>55,56</sup>. However, some alcohols are traditionally used for tissue fixation and are known to damage the ECM's molecular structure. Therefore, they should be used with precaution in decellularization protocols.

### Miscellaneous solvents

Other agents that have been used include acetone and tributyl phosphate (TBP). The same concerns as for the alcohols also apply for acetone and it is not very foresightful when it comes to clinical application of the resulting graft. On the other hand, TBP seems to be very efficient for decellularization of dense tissues like tendon, even more than Triton X-100 and SDS. An advantage of TBP is that it has viricidal properties but the effects on the ECM and molecule retention varies between studies<sup>15</sup>.

## 2.2.5 Biological decellularization

### Enzymes

Enzymes have a very high specificity when it comes to cleavage of desired molecules. They are therefore very effective in clearing the tissue of cells or digesting the ECMS. Many different enzymes have been reported to be part of decellularization protocols, such as collagenases, lipases, dispases, nucleases, trypsin, thermolysin and alpha-galactosidase. Nevertheless, complete cellular removal is not achievable with only enzymatic treatment. Additionally, enzymatic residues could interfere with implantation into the recipient or recellularization. However, it is very common to integrate a step of nuclease immersion into the decellularization protocols, to degrade remaining nucleic acids after gross cell clearance. The integration of biological decellularizing agents should thoroughly be considered, as some (e.g. trypsin) may attack ECM components (i.e. elastin and collagen) more intensely than chemical agents<sup>57</sup>, which can have an impact on the mechanical feature of the produced ECMS<sup>58</sup>. Collagenase should only be applied when tissue architecture is

nonessential and a lipase only treatment is not effective enough for complete delipidation of the entire graft. Enzymes like dispase and thermolysin can be used as sole decellularization agents on the surface of a tissue (e.g. skin graft) but they might require mechanical chafing for final cell removal. Alpha-galactosidase can be applied to remove the cell surface antigen galactose- $\alpha$ -(1,3)-galactose (Gal epitope) in xenogenic grafts<sup>59</sup>.

### Miscellaneous biologics

There are numerous other biological agents, that are not of enzymatic nature. Chelating agents for example, are believed to weaken protein-protein interactions, which is beneficial in context of decellularization. However, these changes in protein connections are very subtle and chelating agents have to be applied in combination with other biological or chemical compounds. A smart way of getting rid of the cell is to use naturally occurring cytotoxins. A representative for example is the family of the latrunculins, which have been shown to be effective in removing residual DNA and intracellular proteins in a protocol, that only applied hyper- and hypotonic solutions, latrunculin B and DNase<sup>60</sup>.

## 2.2.6 Physical and miscellaneous agents

### Temperature

Freeze-thawing cycles are a well established method for decellularization. Especially the rigid bone grafts undergo such physical treatments. However, the cellular compartments need to be removed in further processing. Multiple freeze-thaw cycles do not seem to have a tremendous impact on ECM composition. However, it does produce small cracks in the ECM structure, although the loss of stability is not significant<sup>61,62</sup>. In soft tissues, rapid crystallization of liquids may disrupt ECM architecture.

### Force and pressure

Cells of superficial tissue layers, e.g. from urinary bladders, skin, small intestine or heart valves, can be removed by mechanical abrasion in combination with enzymes or other decellularizing agents (i.e. chemicals). However, direct application of mechanical forces can damage and disrupt the basal lamina<sup>63</sup>. If the scaffold is used for recellularization or implantation into a living organism, the basal lamina should be as preserved as possible, as it presents a good environment for cell attachment and growth. Another physical method is sonication decellularization. The cells get disintegrated via ultrasound (e.g. 40kHz) and then again, flushed with liquid chemical agents<sup>64</sup>.

## Electricity

Non-thermal irreversible electroporation (NTIRE) disrupts the cellular membranes by destabilizing the electrical potential of the cell membrane, which leads to micropore formation. Due to the applied microsecond electrical pulses the cell disintegrates and its homeostasis is lost – the cell dies. However, the tissue still needs to be washed out and it is not entirely clear how well this approach is applicable to large and thick tissues<sup>65</sup>.

### 2.2.7 Techniques for Decellularization

It is evident, that the decellularization process has to be carefully elected when it comes to clinical application of the ECMS. Depending on the purpose of the ECMS (only scaffolding purpose, only temporal application, partial or full recellularization etc.) and the type of tissue, not only the decellularization protocol but also the decellularization technique needs to be adjusted. The major factor however, is the type and thickness of the target tissue. In case of the decellularization process one's entire creativity may be tapped and many DIY (do it yourself) skills are required.

### Whole organ perfusion

To reach each corner of the tissue evenly, decellularizing agents can be applied via the innate vascular system of organs and grafts<sup>66</sup>. This method is very efficient and known as perfusion decellularization. It is also the method that had been used for the experiments of this thesis. The flow can either be applied anterograde or retrograde. However, although this method is very physiologic and preserves the 3D structure of the ECM very well<sup>67</sup>, it is not necessary to choose this technique in order to obtain a stable ECMS. Nevertheless, perfusion decellularization appears to be very gentle to the structure and the outcome is astonishingly similar to the original graft, except the whiteish translucency (known as “ghost organs”). To date, perfusion decellularization has been applied to many organs and composite tissues such as heart<sup>68</sup>, lung<sup>48</sup>, liver<sup>69</sup>, kidneys<sup>70</sup>, face<sup>71</sup>, ear<sup>72</sup>, digits and for the first time, here in this thesis vascularized peripheral nerve grafts.



**Figure 5. Native and perfusion decellularized vascularized composite face graft that was analyzed in this thesis. A)** Depiction of native face graft with cannulated vascular network. Arterial cannulas allowed inlet of decellularizing agents into the graft, whilst venous cannulas assured outlet of the liquids. Middle picture depicts internal structures of the face and origin of the vascular tree. Right image represents immersion of the graft in the bioreactor. **B)** The same situations as described in A after perfusion decellularization, respectively. Due to the even distribution via the vascular network, the tissue got cleared very efficiently and even facial hair was removed. Data published<sup>71</sup>. Courtesy of Jérôme Duisit.

### Pressure gradient

Inducing a pressure gradient across the tissue can enhance enzymatic decellularization treatment. This technique is recommended when a tissue with a hollow cavity (e.g. bladder or lung) is being decellularized. It has been shown to be less harmful to collagen than agitation decellularization, however, some intracellular proteins may be retained in the ECMS<sup>36</sup>.

### Supercritical cell clearance

Supercritical carbon dioxide can be passed through a tissue to remove cellular residues. This method is not very widely used, however it has the advantage of completely dry graft procurement (prolongs storage and limits probability of contamination) and it is extremely fast (a few hours)<sup>73</sup> compared to other techniques (e.g. days for freeze-thaw cycles, weeks for perfusion decellularization). It follows a similar principle as the protocols for critical drying of tissues.

### Immersion and agitation

For tissues that do not have vascular access (eg. cartilage), agitation decellularization might be an option. The most common strategy is, to immerse the graft into decellularizing solutions and to set the bioreactor in agitation in order to “wash” the cells out, just like a washing machine does with the dirt in the fabric. This method has been used for quite a variety of tissues: heart valves<sup>46</sup>, blood vessels<sup>74</sup>, tendons<sup>75</sup>, cartilage<sup>62</sup>, meniscus<sup>76</sup>, skeletal muscle<sup>77</sup>, peripheral nerve<sup>78,79</sup>, spinal cord<sup>80</sup>, trachea<sup>41</sup>, esophagus<sup>81</sup>, dermis<sup>53</sup> and urinary bladder<sup>47</sup>. The duration of agitation decellularization protocols is dependent on the thickness of the tissue and the agents used (dense tissue like tendon or cartilage can take up to several weeks to complete full decellularization).

## 2.3 Clinical aspects

### 2.3.1 Rationale for using ECMS in the clinics

As mentioned, using ECM products for transplantation is reasonable as biocompatibility is excellent, even across species. Besides increasing human donor availability, it may in the future potentially enlarge donor range by enabling xenotransplantation<sup>15</sup>. Moreover, as addressed above, ECM influences cell mitogenesis, chemotaxis, cell differentiation and other processes as tissue remodeling<sup>17,18,19,20,21,22</sup>. Furthermore, in vitro preparation (i.e. vascularization and recellularization) can lead to faster healing and better recovery. All these features are already included in the native ECM and do not need to be extensively manufactured. Moreover, the procurement of an ECMS is relatively cheap and fast, as the preparation principles are very straightforward. Additionally, excellent biocompatibility of ECMS has been proven<sup>15,16</sup>. Therefore, natural ECMS have many advantages over artificially constructed scaffolds or traditional allografts.

### 2.3.2 Administered ECMS in patients

There is a number of ECMS that has already been used in the clinic. Some only for first in human studies, other already at a large scale. The first ones to be used in human patients were 2D acellular scaffolds like decellularized ECMS and collagen lattices. They were mainly used for skin grafting and could be applied to superficial and full-thickness grafts, as well as second degree burns. Such scaffolds were very well compatible with the patient's biology and they showed gratifying results in wound healing. By the time, there is a tremendous amount of products on the market – with and without cells, most of them being skin grafting products. Another early product was CARTICEL (Genzyme Corporation) for cartilage repair, which was approved by the FDA in 1997. Shortly after, the first 3D scaffolds were implanted into human patients. Antony Atala pioneered the urinary bladder engineering and reported his first in human implantation of a biomaterial scaffold in 1996 (urethra) and the first in human trial of an engineered bladder in 1999<sup>82</sup>. Up to date, he has been refining his methods and developing new techniques<sup>83</sup> and his patients show great results. The product Neo-Bladder Augment by Tengion, was launched in third phase 2 clinical trials in 2008. Furthermore, Neo-Urinary Conduit<sup>84</sup>, also manufactured by Tengion, currently shows more promising results. Other successful examples include the trachea transplants that are described in the paragraph “The dawn of decellularization technique”. In 2001 the first engineered vessel was implanted into a 4 year old child in Japan. By 2004, 25 more children had been treated by the same group and showed promising results. In

2012, the FDA approved the use of this technique in adults in the USA<sup>85</sup>. In Germany, over 11 patients have been treated with a similar method for heart-valves. However, no long-term studies exist yet. Another example of a EMCS in clinical use is Avance Nerfe Graft by AxoGen. It can be used for gapping of peripheral nerve injuries. Other commonly used grafts are dental grafts, bone grafts and collagen sponges, that are infused with autologous hematopoietic stem cells.

## 2.4 Limitations of TE

A major limitation in TE is the lack of functional vascularization of the currently available ECM-grafts. The engineered tissues need to be oxygenated properly and nutrients have to reach the cells – otherwise the cells in the graft are bound to die. As the vicinity of natural diffusion is relatively limited, current grafts have to rely on passive vascularization by surrounding tissues. This of course, limits the maintainable size and shape of the graft enormously (see paragraph “Importance of vascularization in engineered tissues”). Moreover, depending on the technique for graft engineering, limitations may vary. A common problem is the use of cells for (re)cellularization of the scaffolds. Over the course of time, cells typically lose their efficacy and change their original phenotype during in vitro cultivation. Besides the differentiation state, the amount of cells needed for repopulating the scaffold is a huge logistic problem since an enormous number of cells is needed. Therefore, scaling up scaffold production is a difficulty and might be addressed in large-scale production sites.

Another major concern related to cell seeding of the scaffolds is represented by the type and the source of the cells to be used for repopulation of TE organs. Obviously, autologous cells seem to be the best option due to low probability of immunologic adverse reaction. However, it is not known yet, if it is more beneficial to use autologous differentiated cells, adult stem cells, embryonic stem cells (ESC) or induced Pluripotent stem cells (iPSC) in the long term. All these cells have been used and tested in several studies and each of them has different advantages and disadvantages and their own ethical and scientific concerns, but discussing them here would trespass the scope of this paragraph. Additionally, some specific cells of organs cannot be grown in culture. Another problem that had been reported upon in vivo implantation, is that a portion of the cells in the scaffold die off. They start to die during the implantation process and the exacerbation of apoptosis is driven by the hostile environment of hypoxia, inflammation and scarring<sup>86</sup>. So even in case of a successful implantation and wound healing, many cells in the graft die.

Another remaining challenge is related to the necessity to find the appropriate biomaterial for each graft with a specific purpose and function. Not every material might be suitable for every part of the tissue, i.e. coral skeletons cannot be applied as vascular grafts, but they might be a useful biologic material for bone or the bulk of tooth grafting.

Furthermore, although the field of TE has had its first successful transplantations over twenty years ago, not enough long-term studies exist yet, especially not about the more complex

3D structured grafts. Therefore, only limited knowledge about long-term side effects, e.g. cancer and other more chronic diseases, cannot be assessed yet.

TE is an older field than one might think at the first glance and it has generated some impressive breakthroughs for modern medicine. However, the technologies are very complex and interdisciplinary and the translation to clinical products is by far not an easy task. Therefore, much research is needed in the future to address the above-mentioned issues and open questions.

### 2.4.1 Alternatives to ECMS-TE

In the field of TE creativity is an appreciated quality and therefore, many different approaches to the generation of grafts have evolved. Reams of different methods to produce and enhance bio-artificial scaffolds (e.g. hydrogels, growth factor delivery systems, electro-spun nanofibers, glass or ceramic nanoparticles etc.) have been developed. However, this thesis is focused on the engineering of vascularized composite scaffolds and nerve ECMS using perfusion decellularization techniques and, therefore, not all approaches can be discussed. We will limit our discussion to two additional methods, which function in a similar manner in order to highlight the plethora of creative methods that scientists have been developing within the field of TE.

#### 3D bioprinting – a brief introduction

Recent advances have enabled to print biocompatible materials together with supporting components and living cells into a stable 3D structure. The aim of 3D bioprinting is, to print a graft, that is mimicking the cellular microenvironment from molecular to macroscopic structures<sup>87</sup>. Such manufactured grafts have already been implanted into human patients (tracheal splints, heart tissue, cartilage, bone, vascular grafts and multilayered skin tissue<sup>88</sup>). 3D models for research, drug delivery and toxicology include other meaningful purposes of such manufactured tissues. This approach has great potential to minimize in vivo animal experiments in the future. However, the use of 3D printed scaffold has several limitations such as speed of the production process, necessity to increase printing resolution, validation of the acquired tissue function and maturation, adjusting vascularization and innervation, to name just a few of them.

#### Crossing kingdoms – of extended horizons

As mentioned, one of the major limitations of engineered tissues is the lack of a proper functional vascularization network. In search of new ideas to develop inventive methods for

vascularization of scaffolds, in February 2017, Joshua R. Gershlak (Worcester Polytechnic Institute, United States) and colleagues published a paper in *Biomaterials* describing the use of decellularized plant scaffolds to engineer vascularization networks<sup>32</sup>. Prior to that, pectin<sup>89</sup>, cellulose<sup>90</sup> and hemicellulose<sup>91</sup> had been shown to be biocompatible and to promote wound healing. However, decellularized plant ECM was never explored as potential vascularized scaffold. Gershlak et al. were able to show the surprising similarities between the plant's nutrient transport system (xylem and phloem) and the mammalian vascularity (both follow Murray's law). They performed further experiments to determine the size of spheres that the decellularized plant network is able to transport. On their chosen model organism, spinach leaves (*Spinacia oleracea*), they were able to show that the decellularized network is suitable for engineering capillaries, as they smoothly transported spheres of 1 – 10  $\mu\text{m}$  size (red blood cell size  $\sim 7 \mu\text{m}$ ) without any difficulty. In a series of repopulating experiments, they succeeded to show adhesion and survival, and even cluster formation of three different human cell types after fibronectin coating (HUVEC, human embryonic stem cell-derived cardiomyocytes (hPS-CM) and mesenchymal stem cells (hMSC)).

Another group lead by Daniel J. Modulevsky (University of Ottawa, Canada), also crossed the borders within the Eukarya domain and has been working on decellularized 3D scaffolds originating from the outer hypanthium of McIntosh Red apples (*Canada Fancy*). In 2014 they published a paper that described the production of a decellularized apple scaffold with subsequent recellularization by C2C12 mouse myoblasts, NIH3T3 mouse fibroblasts and HeLa cells. All cell types were able to adhere, invade and proliferate in the cellulose scaffolds<sup>92</sup>. Excellent biocompatibility of such scaffolds has been proven in animal experiments<sup>93</sup>. Currently, the group is working on recellularization of apple-derived ear-shaped ECMS and they already have produced promising results (data not yet scientifically published, <https://ideas.ted.com/a-promising-way-to-grow-body-parts-using-an-apple/>, accessed 31.01.2018).

These studies showed that plants make a good source of diverse engineering materials and can hence be used for many different purposes, thanks to their variability of transport networks and tissue structure (e.g. bigger vs. small vessels or dense vs. loose networks). Furthermore, they are a very abundant and sustainable resource with limited cost in procurement and large-scale culture and fast growth.

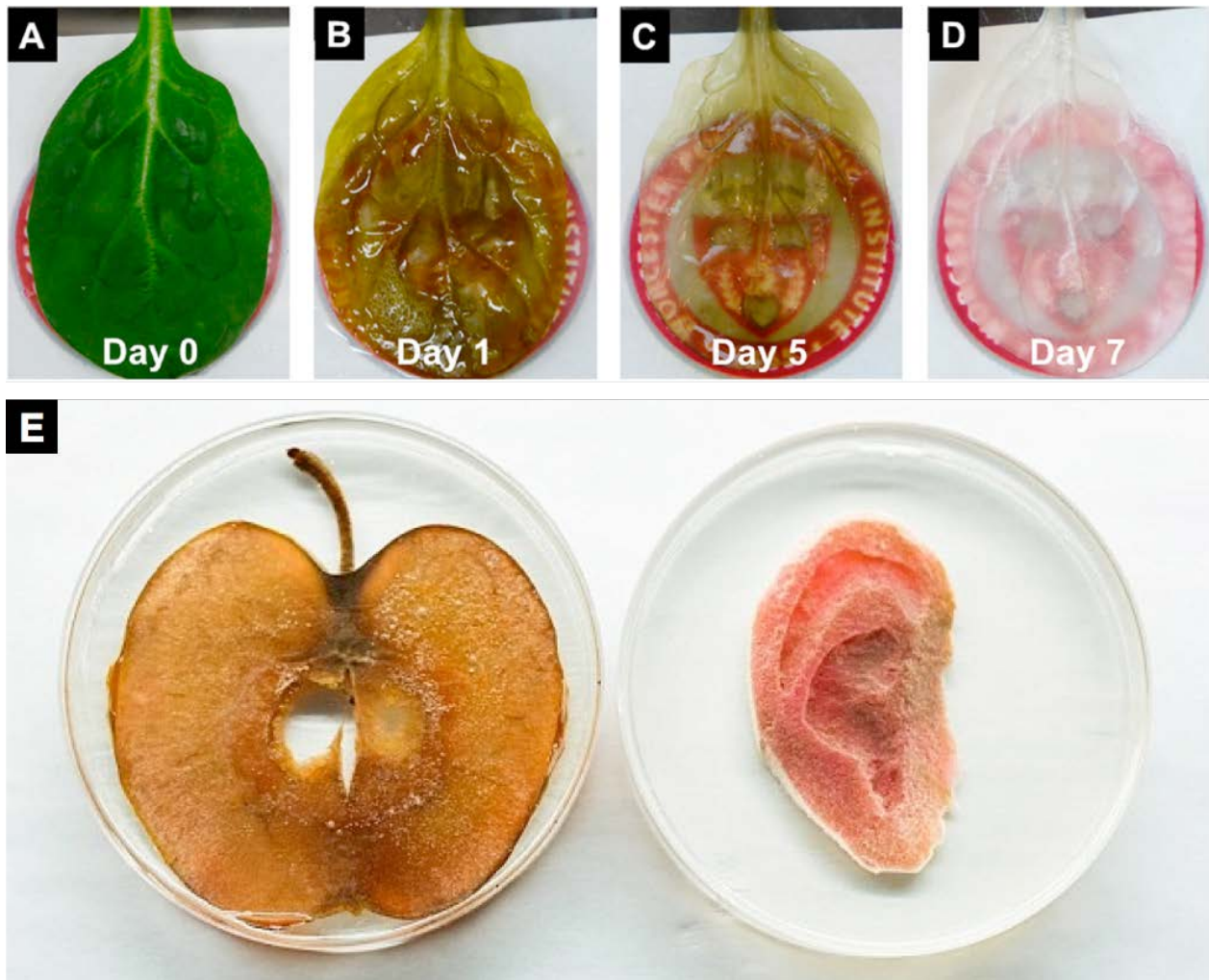


**Figure 6. Plant scaffolds. A) - D)** Perfusion decellularization process of a spinach leaf, published by Gershlak et al.<sup>32</sup> Complete decellularization is achieved on day 7. **E)** Apple slice on the left of which auricular scaffolds are carved out (depicted on the right). Photo credit Bonnie Findley. Modified from <http://www.dailymail.co.uk/sciencetech/article-3644581/The-mad-scientist-wants-grow-ears-APPLES-Bizarre-project-create-cheap-body-parts-leftover-produce.html>, (published 16.6.2016, accessed 9.2.2018).

## 2.5 Future of TE

For the future, it will be important to tackle the remaining problems of vascularization and oxygen as well as nutrient supply to the tissue, as discussed above. A good vascularization is key feature to living tissue and a functioning graft and therefore, more research should be invested in plants as a natural source of pre-vascularized scaffolds as well as in the determination of vessel functionality.

In order to be able to repopulate engineered grafts with a variety of cells, it is important to overcome the limitations of cell culturing, i.e. cell isolation (e.g. liver, pancreatic cells or cardiomyocytes) and in vitro cell expansion. If we cannot overcome the cell culture limitations (e.g. aging, loss of function or phenotype), we will not be able to grow entire tissues and organs in a physiologic way. Therefore, besides research in basic cell culture, more potential should be invested in engineering bioreactors that exhibit very specific conditions for a successful culture of different cell types and whole organs. Another aspect of bioreactor engineering is the refinement of recellularization protocols. Many destroy the ECMS partially by injecting cells into the matrix. In the future, more gentle and elaborate methods will be applied, as the mentioned example with pressure gradient.

Other challenges include manufacturing a stable yet flexible and functional scaffold that may adopt to the patient's anatomy and clinical needs. Concerning the scaffolds, there are many points that need to be investigated further. For example, the use of smart biomaterials that are not simply degrading over time, but also influencing the recipient's inflammatory reactions delivering cues for wound healing and tissue integration. Such smart biomaterials will be designed at the molecular level to be in situ utilized by the body to accelerate the healing process. Considering that, close collaboration with research fields like nanoscience and material science will be required to understand and exploit the unique characteristics of nanomaterials. Some scientists call it "adding 4-dimensionality" to the engineered grafts. Factors for tissue healing might include physical cues like 3D topology, specific nano- and microstructures or surface tension. Such factors could be adjusted a time of designing the scaffolds. Inclusion of biochemical triggers like cellular signal proteins (e.g. growth factors, bone morphogenetic protein 2 (BMP2) etc.) that are released or activated in a spatial and temporal manner could enhance the "smartness" of the scaffolds. In that context, four-dimensionality means, that the three-dimensional functional scaffolds are endowed with the ability to manage real-time responses (e.g. maintenance and maturation of the ECM molecules) over extended lifespans<sup>94</sup>. Another issue concerning biomaterials is the need to overcome regulatory hurdles, in order to be translated into the clinics. There is a tremendous barrier for materials, to meet the authorities' approval criteria and at the same time being

easily translatable into clinical applications. Therefore, regulations need to be adapted to the scientific progress.

However, not only new biomaterials but also new methodologies will be needed. On the one hand, existing technologies like bio-printers, incubators and bioreactors are to be refined. On the other hand, new approaches have to be incorporated into TE. The keyword is big data. Holistic research and data mining for example, could revolutionize the search for new scaffold designs (materiomics). In combination with bioinformatics and computational modeling such approaches can lead to unprecedented strategies and discoveries.

My personal opinion is, that for future progress in the field of TE, deeper knowledge of every aspect is required. In order to be able to mimic Mother Nature, one has to recreate in vitro, what evolution achieved in 4.6 billion years. This might seem impossible, but I believe that for some applications, we will achieve outstanding results. Therefore, I propose a very close collaboration between all the involved scientific disciplines and their available technologies (biology, physiology, physics, biochemistry, chemistry, material sciences, medicine, but also bioinformatics, engineering so on). Also, we might have to increase our mental horizons and look for solutions where we had not dared to in the past. Infinite creativity and the same time attention to details will bring success.



**Figure 7. A verger's dream:** Saints Cosmas and Damian performing a miraculous cure by transplantation of a leg. Oil painting by the Master of Las Balbases, Spain 1495. Representation of a verger's vision described in the book *Legenda aurea* (The golden legend) 1275 in Rome by Jacobus de Voragine. The vision was received by a verger in Rome, who had a flesh-eating disease in his leg. Church of Saint Cosmas and Damian, Burgos, northern Spain.

## 2.6. Vasclularized Composite Allograft Engineering

### 2.6.1 Vascularized composite allografts - VCA

Vascularized composite allografts are transplants that are composed of different types of tissues such as bone, cartilage, muscle, fat, connective tissues and skin. Such a graft is essentially a whole body part with all its necessary layers and functional tissues. VCA transplants are commonly applied to improve an individual's quality of life rather than prolonging it. VCA includes body parts such as hand, arm, face, abdominal wall, leg, trachea, larynx, uterus and penile transplants. Currently, the most transplanted type of VCA are upper extremities (hand, forearm) and faces<sup>95,96</sup>. At the time of writing this thesis, over 130 face and hand transplantations had been conducted worldwide<sup>97</sup>. However, the use of prosthesis remains the most common intervention for limb loss. A study aimed to compare the outcome of patient's with modern prostheses versus patients with VCA transplants<sup>98</sup> reported that there is no significant functional difference between the two groups. However, about 20% of prosthetic users abandon their device due to irritations in the stump regions originating from daily use in grooming and housekeeping<sup>99</sup>. Further patient complaints about prosthesis include high acquisition and maintenance costs, discomfort, excessive weight, constant need for repair or service, lack of functional benefit and most importantly, lack of neurologic feedback. The absence of sensation is one of the major limitations of prosthetic limbs. Psychological effects can have a tremendous impact on a patient's condition. Seeing a limb but not being able to feel it can cause major mental disconcertment leading to discontinuation of prosthesis use. Beside the still relatively small number of VCA patients, it seems that, as compared to prosthesis, VCA may promote a better neurologic restoration along with increasing functionality over time<sup>100</sup>. Hence, especially in bilateral amputees, the benefits from motor and sensory restoration can outweigh the side effects of transplantation and immunosuppression (more information below). Nevertheless, all considerations for treatment should individually be adapted to the patient and his/her psychological state of mind.

However, VCA remain not vitally important body parts. That is all the more reason to carefully calculate the risks of potential side effects. Such may include immunologic adverse reactions against the allograft (see paragraph "The challenges of VCA"), consequences of immunosuppressive drugs or ethical questions. Despite the pending issues, VCA transplants were amended to be acknowledged as "organs" due to legitimate and regulatory concerns<sup>101</sup> and were approved as such by the United Network for Organ Sharing<sup>102</sup> in 2014.

## 2.6.2 The challenges of VCA

As VCA consist of different tissues, they also present a variety of immunologic loads for the immune system of the recipient. Due to low donor availability, optimal HLA-matching is not always possible in case of a VCA transplantation. These challenges make VCA the grafts with the highest risk for acute rejection amongst all sorts of transplants - including solid organs. Acute rejection has been described in over 80% of the cases in face and hand transplants<sup>102,103</sup> and presents as the most prevalent and most feared complication, that has resulted in several graft losses and deaths<sup>104</sup>. These risks are specifically high for patients with face transplants. On the other hand, antibody-mediated rejection (AMR) and chronic rejection occur less frequently. Nevertheless, over the past few years reports of AMR have increased and several cases were described<sup>105,106,107</sup>. Chronic rejection remains yet to be defined in VCA<sup>108</sup>. There are fewer reports on chronic allograft deterioration, not lastly due to lack of long-term follow up studies that include a significant number of individuals. However, the importance of chronic changes in the grafts have become more of a focus over the past few years. Furthermore, under the regiment of immunosuppressive drugs necessary for the management of acute and chronic rejection, VCA patients are very susceptible to nephrotoxicity, metabolic disorders, risk of malignancies and infections. The side effects of immunosuppression and the risk of acute, antibody-mediated or chronic rejection pose critical challenges to the field<sup>103, 104,105</sup>. Additionally, unsolved ethical issues are still being discussed. One of the unsolved ethical dilemmas for example is, whether it is reasonable or not to transplant non-lifesaving “organs” with an utterly high certainty of rejection episodes. To date, VCA is not considered as standard treatment for loss of distal body parts and it is applied only after thorough evaluation of the patient’s individual needs, his/her psychological state of mind and the risks of secondary to life-long immunosuppression.

## 2.6.3 Overcoming the challenges

Protocols for improving the outcome of VCA transplantation are generally derived from solid organ transplantation. They include pharmacological treatments like to avoid graft rejection such as induction therapy (e.g. T-cell depletion, antithymocyte globulin treatment (ATG) and other non-myeloablative approaches), maintenance therapy (immunosuppressive drugs), rescue therapy (administration of increased maintenance and pulsed steroid medication) and AMR therapy (total plasma exchange and subsequent intravenous immunoglobulin injection)<sup>102</sup>. Recently, new approaches of allograft procurement are being developed, in order to reduce graft damage and improve the clinical outcome. Such may be prevention of graft injury by extra-corporal perfusion devices<sup>109</sup>, expanded donor availability for a better

HLA-matching, determination of biomarkers for early detection of rejection<sup>110</sup> and consequent adaptation of therapy. Moreover, new therapeutic approaches for the management of acute and chronic rejection have been developed such as cell-based therapies for immunosuppression, tolerance induction through the establishment of chimerism, site-specific immunosuppression, controlled activation of innate immunity (i.e. anti-ischemic treatments, downregulation of pro-inflammatory production by targeting NF- $\kappa$ b etc.), complement inhibition, targeting of adhesion-molecules or knock down of specific genes by cleaving complementary mRNA using small interfering RNA (siRNA)<sup>102</sup>. However, all of the above mentioned potential treatments could fix the problem only partially, reducing graft damage and the need of immunosuppression. Indeed, the currently available therapeutic options do not cover the whole range of complications. This is particularly problematic in the context of VCA where the ethical and immunological challenge described above require a global and effective approach that would allow VCA to become standard of care. VCA entails several significant side effects and therefore, solving one of the problems is not enough to ensure physical recovery devoid of further complications. Thus, the ideal option would be a custom-made VCA that resembles the recipient's lost body part not only on a morphological but also on a molecular level.

#### **2.6.4 Vascularized composite allograft-engineering: VCE**

In theory, editing and adapting the allograft to its recipient might overcome most of the severe side-effects. This is the very goal of tissue engineers in the field of VCA. Adapting the allografts to its future recipient helps to lower immunogenicity and hence, might be a way to overcome immunosuppressive drug therapy along with rejection episodes. Additionally, the grafts can be harvested from recently deceased donors which solves the problem of low availability of life-donors and general donor shortage. The field of vascularized composite allograft-engineering (VCE) has recently been growing and a lot of research is being performed at the time. It has been stated, that in future years, VCE might fully replace traditional VCA in the clinic<sup>111</sup>. The structurally complicated nature of VCA however, leads to many challenges when it comes to growing functional tissue in the laboratory. Find more information about TE in the chapter "Tissue Engineering".

## 2.7.1 Tissue engineering of peripheral nerve

One of the aims of this thesis was to construct a vascularized nerve graft by perfusion decellularization with subsequent re-endothelialisation of the vascular tree. Therefore, in the following paragraphs, we will introduce the clinical problems associated with peripheral nerve injuries and we will describe the TE approach developed for the management of such injuries.

## 2.7.2 The need for peripheral nerve TE

Millions of people in the United States and Europe suffer from traumatic nerve injuries every year<sup>112</sup> with an estimated frequency of 1 in 1000 people in Europe. The incidence rate is especially high in the population of working adults<sup>113</sup>. Severe peripheral nerve injuries can have a tremendous impact on an individual's life ranging from psychologic stress and social constraints to loss of functionality and hence, can lead to invalidity. Due to Wallerian degeneration and the limited capability of self-regeneration the peripheral nervous system is susceptible to poor healing and exiguous recovery<sup>115</sup>. In the presence of significant gaps of over 2-3 cm, tension-free anastomosis might not be practicable<sup>116</sup>. In such cases autologous nerve grafting is considered the gold standard although it comes at a high cost for the individual. Disadvantages like a second surgery with tissue loss, limited graft availability, donor site morbidity, scarcity and mismatching nerve morphologies can be restricting factors to autografting. Alternatively, allografts can be applied to fill the gap between the proximal and the distal blunt ends of the affected nerve. However, allografts come at an even higher cost with the undesirable concomitant of immunosuppression and the risk of rejection<sup>117</sup>. In order to find substitutes, the fields of regenerative medicine and tissue engineering have produced a plethora of meaningful contributions on nerve tissue engineering and improved nerve grafts in the recent years<sup>118</sup>.

## 2.7.3 Peripheral nerve ECMS

Several types of nerve conduits consisting of a variety of materials have been developed and various studies have demonstrated proof-of-principle<sup>119</sup> for nerve regeneration. The most promising candidates however, were found to be degradable collagen tubes<sup>120,121,122</sup> closely followed by extracellular matrix conduits<sup>120,121,123,124,125,126,127,128</sup>. These biologic materials are absorbable and can be remodeled by newly populating cells. This is in consistency with the isomorphous tissue replacement model, where the time of scaffold residency must be

approximately equal to the duration of natural tissue regeneration<sup>129,129,130</sup>. As with almost any type of tissue in TE, decellularization protocols have been applied to peripheral nerve grafts. Decellularized peripheral nerve ECMS bring the optimal environment for nerve regeneration. Not only biologic and biochemical but also three-dimensional and physical parameters are given in an appropriate physiologic environment<sup>17,131</sup>, e.g. the maintenance of channel-like structures for axonal growth. Currently there is only one decellularized nerve ECMS product on the market (Avance<sup>®</sup> Nerve Graft, AxoGen). Studies with this decellularized nerve from cadaveric source demonstrated promising results for large nerve gaps of 2-3 cm<sup>132,133</sup> and calibers of over 5 mm<sup>134</sup>. Despite remarkable improvements there are still limitations and restrictions to the application of decellularized nerve allografts. Although scaffolds like Avance<sup>®</sup> Nerve Graft seem to show an improvement in the treatment they still do not overcome the current limit of significant gaps (> 3 cm)<sup>132,133,134</sup>. Other techniques such as plain nerve conduits, application of neurotropic growth factors, cell transplantation and gene engineering are difficult to establish and do not show any better outcome with neurologic recovery not exceeding more than 70 %<sup>135</sup>. So far, all the described techniques are not yet implemented in the clinical routine and the gold standard remains transplantation of autologous nerve grafts<sup>116,136</sup>.

#### 2.7.4 A tissue engineering approach for the repair of peripheral nerve injuries

In order to improve decellularized nerve allografts and the clinical outcome of the patients we hypothesize, that a physiologic decellularization protocol and a re-endothelialized vascularization of the decellularized nerve graft could help to ameliorate and speed up the healing process by providing nutrients from within the tissue.

In pursuance of obtaining a maximally natural decellularized scaffold we made use of the innate delivery system of the tissue by using perfusion decellularization techniques that insert the decellularizing solutions into the graft via the vascular tree under physiologic flow. In that way, the solutions follow the natural flow of the tissue and maximal decellularization is obtained<sup>66</sup>. Besides, this method is very sustainable and gentle to the vascular tree which remains intact<sup>67</sup>. The importance of a good blood supply in nerve regeneration has been observed before<sup>137,138,139,140</sup> but no vascularized extracellular matrix nerve scaffolds exist yet. It has been shown that the direct supply of nutrients and other important regenerative agents is a key factor in nerve regeneration<sup>137,138</sup>. This could be achieved by direct anastomosis of recellularized vessels from the nerve graft to the recipient, rather than via passive vascularization from surrounding tissues. The importance of tissue-engineered

revascularization of decellularized grafts has been described before<sup>141</sup>, nevertheless no vascularized extracellular matrix nerve scaffolds exist yet.

We present for the first time a porcine model on the engineering of a vascularized extracellular matrix nerve scaffold using perfusion decellularization and recellularization of the intrinsic vascul

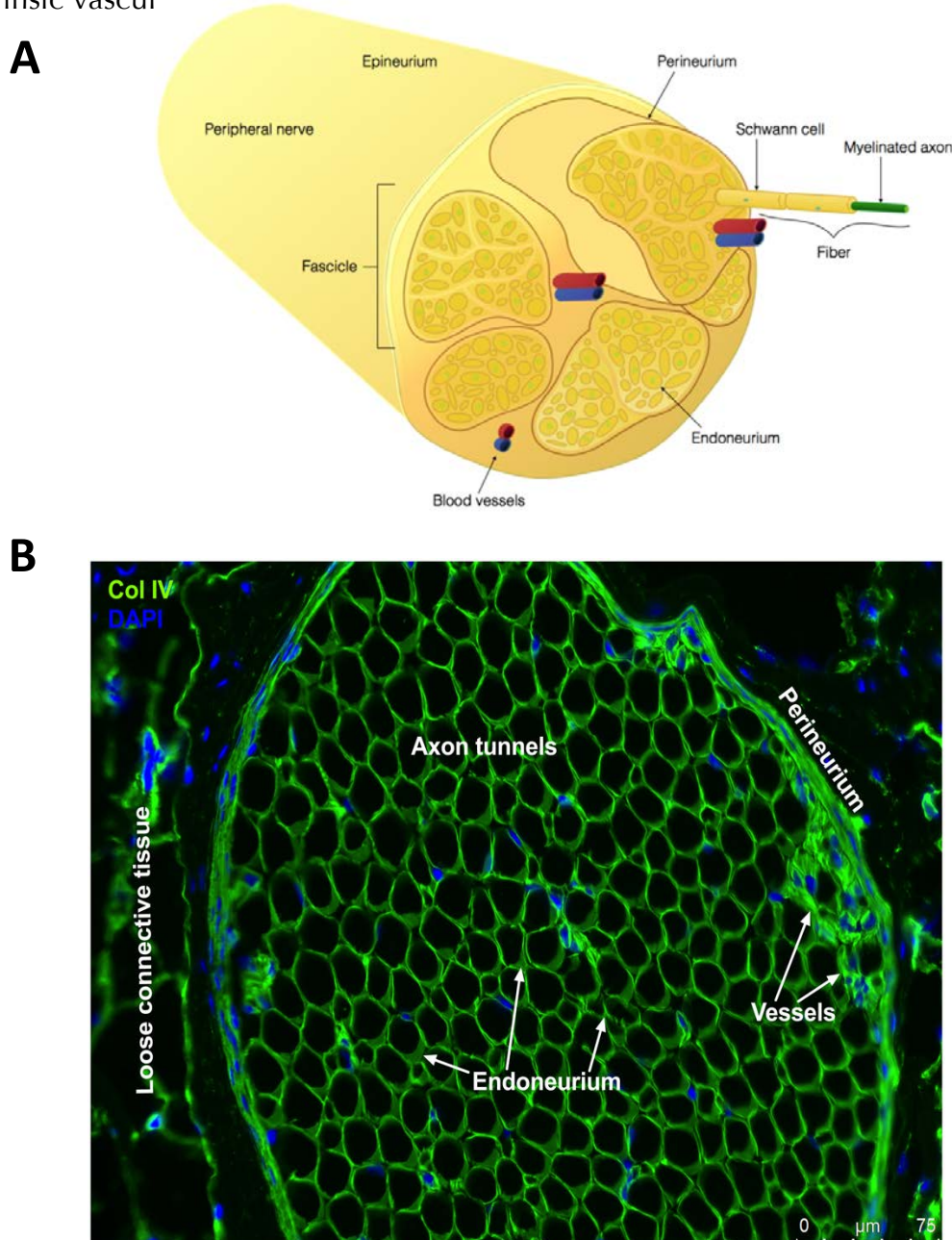


**Figure 8. Anatomy of a peripheral myelinated nerve. A)** The illustration depicts a transversal cut through a peripheral nerve. The experiments of this thesis aimed for perfusion decellularization with subsequent perfusion re-endothelialization of the intrinsic vascularization of porcine sciatic nerves. Design by Tsering Wüthrich. **B)** Immunofluorescent staining of native nerve in a transversal cut. Structures are indicated. The similarity to the illustration in A confirms the internal structure of the peripheral nerves used in the experiments for this thesis.

### 3. Aim of the study

- 1) Immunologic characterization of two types of vascularized composite engineered (VCE) allografts, namely human face and ear, according to their different tissue layers.
- 2) Development of a vascularized extracellular matrix scaffold (ECMS) of peripheral nerves using perfusion decellularization with subsequent perfusion re-endothelialization of the innate vascular system.

## 4. Methods

### 4.1 Graft acquisition

#### 4.1.1 VCE grafts – face and ear grafts

Body donation at the Université Catholique de Louvain (UCL) in Belgium enabled harvesting of the VCEs from fresh human cadavers. All the procedures were performed by the team of Prof. Lèngelé at the UCL. Time of harvesting was at a median of 50 hours post mortem (range 12 - 96). Median age of the donors was 82 (range 63 - 96). After decease, the cadavers were kept at 4°C until procurement of the graft. All procedures and experiments were approved by the local ethical committee.

#### 4.1.2 Porcine nerve grafts

7 sciatic nerves from common house pigs were collected, of which 4 originated from farmer pigs bought from a local butchery and 3 were obtained from ongoing animal experiments at University of Bern. All experiments were conducted agreement with the Swiss Animal Welfare Legislation.

#### 4.1.3 Surgical sciatic nerve collection of pigs

Shortly after euthanasia (electric shock at butchery, pharmacologically at University), the swine was placed in lateral decubitus and the hind limb was shaved and disinfected. A lazy-S incision was performed in the center of the proximal hind limb. After subcutaneous dissection and identification of the muscles, the musculus biceps femoris was disinserted from its distal attachment and everted posteriorly. The sciatic nerve, together with its 2 main branches (tibial and peroneal nerve), were dissected and the vascular pedicle (circumflexa femoris medialis artery and vein) and perforators identified. After preparation of the pedicle, the entire specimen was harvested and flushed through the arterial system with heparinized saline solution (5000 UI/100 ml saline) until clear fluid returned from the vein. The fibular branch was cut and taken as a separate sample for control purposes. Both vascularized and non-vascularized nerve specimens were weighed, measured and stored in 2%PS-PBS at 4°C.

## 4.2 Decellularization

### 4.2.1 Perfusion decellularization of face and ear grafts

The perfusion decellularization of face and ear grafts was performed at the Université Catholique de Louvain (UCL), by the team of Prof. Lèngelé. Briefly, arterial cannulas were incorporated to the graft's vascular system that was connected to a Masterflex® L/S® Series Peristaltic Pump (Cole-Parmer) using a 16G tubing. The graft was then immersed in a bioreactor and perfused through the vascular tree. Mean arterial pressure was held at physiological 80mmHg or below (monitoring on a Datex-Ohmeda S/5 monitor, Healthcare Life Sciences). The decellularization process split in three phases: 1) Decellularization: perfusion with 1.5L of heparinized saline (15 UI/ml) with 10 M adenosine (A-4036, Sigma-Aldrich), followed by 70L of 1% SDS, 6L de-ionized water, 9L 1% Triton-X 100 and 30L PBS. 2) Defatting: overnight stirring bath in 1L 2-propanol (ISO, VWR) followed by 2L ISO perfusion (closed circuit for 12 hours) and a second 1L overnight ISO stirring bath. Rehydration with 1L de-ionized water and 26L PBS perfusion. 3) Clearing: perfusion with 1.5L Type I bovine DNase in PBS (25 mg/L, Sigma-Aldrich) at 37°C with subsequent 10L PBS washing. Processing for analysis or storage at 4°C in PBS.

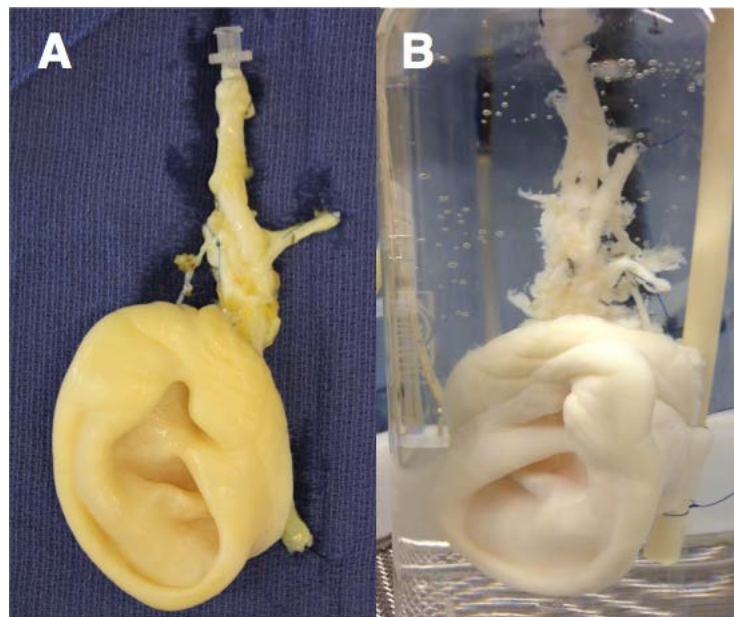


**Figure 9. Procurement of the ear graft. A)** Dissected native human ear graft prepared with appertaining vascular pedicle, that had been cannulated for the perfusion decellularization process. **B)** Human ear graft immersed in bioreactor after perfusion decellularization had been completed. The shape of the ECMS did not change noticeably. Data published<sup>72</sup>. Courtesy Jérôme Duisit.

## 4.2.2 Perfusion decellularization of porcine sciatic nerve grafts

Decellularization of the nerve grafts was performed by the team of Prof. Lèngelè similarly to what reported for human face and ear grafts. Arterial cannulas were incorporated to the graft's vascular system and via 16G tubing connected to a Masterflex® L/S® Series Peristaltic Pump (Cole-Parmer). The graft was then immersed in a bioreactor and perfused through the vascular tree. Mean arterial pressure was held at physiological 80mmHg or below (monitoring on a Datex-Ohmeda S/5 monitor, Healthcare Life Sciences). The decellularization process split in three phases: 1) Decellularization: perfusion with 350mL of heparinized saline (15 UL/mL) with 10 M adenosine (A-4036, Sigma-Aldrich), followed by 10.4 L of 1% SDS, 0.9L de-ionized water, 1.3L 1% Triton-X 100 and 10L PBS. 2) Defatting: overnight stirring bath in 1L 2-propanol (ISO, VWR) followed by 2L ISO perfusion (closed circuit for 12 hours) and a second 1L overnight ISO stirring bath. Rehydration with 1L de-ionized water and subsequent PBS perfusion. 3) Clearing: perfusion with 1.6L Type I bovine DNase in PBS (25 mg/L, Sigma-Aldrich) at 37°C with subsequent 630mL PBS washing. Processing for analysis or storage at 4°C in PBS.

## 4.3 Scaffold analysis

### 4.3.1 Angiography

The patency of the vascular pedicle, as well as the branching of the perforators supplying the nerve, were confirmed before and after decellularization through angiography by using lobitridol (Xenetix 300 mg/ml, Guerbet AG, Winterthurerstr. 92, CH-8006 Zürich) as contrast dye.

### 4.3.2 DNA quantification

DNA was extracted from native and decellularized biopsies with a mean weight of 22.40 mg (native, n= 7) and 21.07 mg (decellularized, n = 7), respectively. Purification from tissue was done with a commercially available kit (DNeasy Blood & Tissue Kit, 69504, QIAGEN) accordingly to the manufacturer's instructions for tissue samples. Quantification of isolated DNA levels were analyzed with a QuantiFluor® dsDNA Sample Kit (E2671, Promega) according to the manufacturer's instructions. Fluorescence intensity of the intercalating agent was measured on a plate reader (Tecan Reader Infinite M1000, Tecan) at  $504\text{nm}_{\text{Ex}}/531\text{nm}_{\text{Em}}$ .

### 4.3.3 sGAG quantification

Sulfated glycosaminoglycan contents of the native and decellularized nerve scaffolds were quantified using a commercially available kit (Glycosaminoglycan Assay, Blyscan™). All steps were performed according to the manufacturer's instructions. Briefly, scaffold biopsies (native n = 7, decellularized n = 7) were digested in a papain extraction reagent (papain from papaya latex, P3125 Sigma) for three hours at 65 °C. The supernatant was separated after centrifugation, blyscan dye reagent was added and complex formation between the dye and the analytes was allowed for 30 minutes under agitation at room temperature. Unbound dye was withdrawn in the supernatant after centrifugation and the pellet was air dried. Next, the dissociation reagent supplied by the kit was added and the tubes were heavily vortexed. Dissociation was allowed for 10 minutes. Samples were transferred in duplicates onto a flat transparent 96-well plate suitable for optical density measurements. Absorption was measured at 656 nm on a plate reader (Tecan Reader Infinite M1000, Tecan).

### 4.3.4 Sampling for protein extraction

#### Biopsies Human ear

Biopsies with a mean weight of 334.89g (n=32) were taken from the middle part of the ear according to the three different tissues skin, cartilage and fat. For each of the three tissues 4 native, 3 decellularized, 1 briefly reperfused and 1 briefly recellularized biopsies were taken. Sampling was done by Jérôme Duisit, (Université catholique de Louvain, Belgium) and shipped (4°C, 1%PS-PBS) to Switzerland for analysis.

#### Biopsies Human face

Biopsies with a mean weight of 117.14g (n=35) from the human face were taken from five different tissues: skin, mucosa, fat, cartilage and muscle. For each tissue 4 native and 3 decellularized biopsies were harvested. Sampling was done as above and shipped to Switzerland (4°C, 1%PS-PBS) for analysis.

### 4.3.5 Protein extraction

Biopsies were weighed and cut into small pieces with a surgical knife. The pieces were transferred into an M Tube (Miltenyi Biotec GmbH) filled with 10  $\mu\text{l}/\mu\text{g}$  of RIPA buffer (50mM Tris-HCl, pH 8.0, with 150mM sodium chloride, 1.0% Igepal CA-630 (NP40), 0.5% sodium deoxycholate and 0.1% sodium dodecyl sulfate) with 1:100 protease inhibitor cocktail (SIGMA P8340). The M tubes were promptly inverted and put on the gentleMACS Dissociator (Miltenyi Biotec GmbH). The program Protein\_01\_01 (M Tube) turned the biopsies into a mashed mass which was incubated on ice for 15 minutes. Sonication was carried out at output 3, duty cycle 20 for 10 pulses and further 5 pulses on output 5 and duty cycle 20. After a short centrifugal spin down the supernatant was transferred to smaller tubes for centrifugation at 13'000 rpm for 1 hour at 4°C. Again, the supernatant was transferred to a new tube for further analysis. The pellets were also transferred into new tubes and stored at -80°C for later analysis.

### 4.3.6 Protein quantification

For protein quantification a classical bicinchoninic acid (BCA) assay was performed. A bovine serum albumin standard (2.0mg/ml in 0.9% aqueous NaCl containing sodium azide, Prod# 23209, Thermo Fisher Scientific) with 7 dilutions was prepared by serial dilution and added to a flat transparent 96-well plate (Thermo Fisher Scientific). 5 $\mu\text{l}$  of sample were added to the wells and the assay was performed according to the DC™ Protein Assay kit instructions (Bio-Rad). The OD was measured at 750nm on a plate reader (Infinite® M1000 PRO) and interpolated by Prism 7.

#### Protein concentration

Twenty supernatants from the protein extraction of the ear (above) had to be concentrated because the evaluated total protein concentrations from the BCA assay were not sufficient for analysis with the standard curve. For this purpose, the Pierce Concentrator tubes (Thermo Fisher Scientific, 88512) were used according to the manufacturer's instructions.

## 4.4 Cytokine quantification

### 4.4.1 Human face and ear

Protein levels of 42 different cytokines were measured by Bio-Plex multiplex immunoassays. The Bio-Plex Pro™ Human Chemokine 40-Plex Panel (Bio-Rad) and the Bio-Plex Pro™ TGF- $\beta$  3-Plex kit (Bio-Rad) were used to analyze the supernatants of the protein extraction (above) and run on a FLEXMAP 3D® system (Luminex). The procedure was held after the original instruction manual of the manufacturer. Measured cytokine levels were normalized to the initial weight of the biopsies and expressed as pg protein per mg of tissue. Measured concentrations below or above detection limit were excluded and the remaining values underwent logarithmic transformation for heatmap display.

Pro-inflammatory cytokines	Growth factors	Chemokines
IL-1 $\beta$ , IL-6, IFN $\gamma$ , TNF- $\alpha$ , MIF	IL-2, IL-4, IL-8, IL-10, GM-CSF, TGF- $\beta$ 1, TGF- $\beta$ 3, CXCL5, CXCL12	IL-16, CCL1, CCL2, CCL3, CCL7, CCL8, CCL11, CCL13, CCL15, CCL17, CCL19, CCL20, CCL21, CCL22, CCL23, CCL24, CCL25, CCL26, CCL27, CXCL1, CXCL2, CXCL6, CXCL9, CXCL10, CXCL11, CXCL13, CXCL16, CX3CL1

**Figure 10. Cytokine allocation according to functional groups for the VCE analysis.** In order to better understand the retention pattern of the cytokines, they were allotted according to their reported functions. For the analysis of the VCE scaffolds, the three groups pro-inflammatory cytokines, growth factors and chemokines were established.

#### 4.4.2 Porcine nerves

For cytokine and growth factor analysis two different luminex-like protein detection assays were used. A nerve specific assay (EPX110-12170-901, ProcartaPlex) and a home-made developed porcine specific Bio-Plex multiplex immunoassay<sup>142</sup> were run on the FlexMap3D system (Luminex). The procedures were held according to the manufacturers and published instructions<sup>142</sup>. Analyte levels were normalized to the initial mass of the biopsies and displayed as pg protein per mg of tissue. Concentrations below or above detection limit were excluded, and the remaining values underwent  $\log_{10}$  transformation for heatmap display.

Pro-inflammatory	Complement	Angiogenic	Other	Nerve GF
IL-1 $\beta$ , IL-6, TNF- $\alpha$ ,	C5a, sC5b-9	IL-8, VEGF, bFGF, PDGF	IL-10, CCL2	LIF, SCF, HGF, EGF, bNGF, BDNF, FGF-2, PlGF-1, VEGF-A, VEGF-D, PDGF-BB

**Figure 11. Cytokine allocation according to functional groups for the nerve analysis.** In order to better understand the retention pattern of the cytokines, they were allotted according to their reported functions. For the analysis in the peripheral nerve the three groups pro-inflammatory cytokines, complement factors, angiogenic factors, nerve growth factors and other cytokines.

## 4.5 Cryosectioning

### 4.5.1 Ear

Six Tissue-Tek® O.C.T.™ Compound (Sakura Finetek) embedded human ear biopsies were shipped on dry ice from the Université catholique de Louvain to the University of Berne and stored at -80°C. Two of the biopsies were native tissues, two were halfway through the decellularization process i.e. pre-detergent and two were completely decellularized. The frozen OCT blocks were placed on a Hyrax C60 cryostat (Zeiss) and set to -16°C. The microtome was set to -17°C and sections of 5 to 6µm were cut. Temperature settings were adjusted by ± 2°C according to the samples. The emerging tissue sections were immediately caught on a glass slide and stored at -20°C until further processing.

### 4.5.2 Nerve

All nerve samples for cryosectioning were embedded, procured and stored the same way as the ear samples.

## 4.6 Immunofluorescence staining

The cut cryosections mentioned above were used for immunofluorescence staining with the antibodies listed below in table 1.

Target	Abb.	Type	Primary AB	Secondary AB	Channel
Human ear					
Antithrombin III	ATIII	Indirect IF	goat polyclonal IgG, sc-32453, Lot H1213, Santa Cruz	donkey anti-goat IgG (H+L) Alexa Fluor 488, A11055, Invitrogen	green
Fibrinogen-like protein 2	FGL2	Indirect IF	rabbit polyclonal IgG, orb183796, Lot Br3603, Biorbyt	goat anti-rabbit IgG (H+L) cross-adsorbed Alexa Fluor 633, A21071, Invitrogen	far red
Heparan Sulfate Proteoglycan	HSPG	Indirect IF	mouse IgM-α-10E4 epitope, 370255-1, Ambsbio	anti-mouse IgG F(ab') <sub>2</sub> fragment-Cy3, C2181, Sigma Aldrich	red
Plasminogen activator inhibitor-1	PAI-1	Indirect IF	mouse-α-human, MA-56A7C10, Hycult Biotech	anti-mouse IgG F(ab') <sub>2</sub> fragment-Cy3, C2181, Sigma Aldrich	red

Tissue factor	TF	Indirect IF	sheep- $\alpha$ -human, PAHTF-S, Haematologic Technologies	donkey anti-sheep IgG (H+L) cross-adsorbed Alexa Fluor 488, A11015, Invitrogen	green
Tissue plasminogen activator	tPA	Indirect IF	goat polyclonal IgG, sc-5241, Santa Cruz	donkey anti-goat IgG (H+L) Alexa Fluor 488, A11055, Invitrogen	green
Porcine nerve					
Collagen type IV	ColIV	Indirect IF	rabbit polyclonal anti-collagen IV, ab6586, Abcam	goat anti-rabbit IgG FITC, 4050-02, Southern Biotechnology	green
Heparan Sulfate Proteoglycan	HSPG	Indirect IF	mouse IgM- $\alpha$ -10E4 epitope, 370255-1, Ambsbio	goat anti-mouse Alexa488, 1082-08, Life Technologies	green
Laminin	Lam	Indirect IF	rabbit polyclonal anti-laminin, ab11575, Abcam	goat anti-rabbit IgG FITC, 4050-02, Southern Biotechnology	green
Platelet endothelial cell adhesion molecule 1	PECAM-1, CD31	Indirect IF	rat anti-porcine CD31, MAB33871, clone 377537, R&D systems	goat anti-rat IgG Alexa488, 3010-02, Southern Biotechnology	green

**Table 1. Overview of the used antibodies for the immunofluorescence staining.**

In order to stain the slides, they were left to dry at room temperature for about half an hour before fixation in  $-20^{\circ}\text{C}$  cold acetone for 10 minutes. After, the slides were left to dry again at room temperature and then rehydrated with 1x TBS for 5 minutes. Then the slides were slightly dried and confined by a line of hydrophobic pen (s2002, Dako) and placed in a wet chamber before applying 80 $\mu\text{l}$  of 3%BSA-TBS to block the samples for one hour at room temperature. Following that, the blocking solution was rinsed away with TBS and then the samples were covered with 80 $\mu\text{l}$  of primary antibody in TBS-PBS-1%BSA for an overnight incubation at  $4^{\circ}\text{C}$ . The following day the samples were rinsed and washed three times for 10 minutes in TBS, dried slightly and covered with 80 $\mu\text{l}$  of secondary antibody (1:500) and DAPI (4',6-Diamidin-2-phenylindol, 1:1000) diluted in TBS-PBS-1%BSA. Incubation was allowed for 90 minutes in a light protected wet chamber at room temperature. After that, the slides were rinsed again and washed three times 10 minutes in 1x TBS at room temperature. After removing the samples from the TBS bath, they were placed on a heating block set on  $42^{\circ}\text{C}$  in order to dry the tissues. Finally, the slides were mounted with a drop of pre-warmed glycergel (Dako, C0563) using usual coverslips. To clean the slides, they were rubbed with

a tissue that was wetted with 70% ethanol. Pictures were acquired on an immunofluorescence microscope (Leica DMI4000) on appropriately matched settings.

## 4.7 Histology

With a single transversal cut a section of approximately 8 mm thickness of each nerve scaffold (native  $n = 7$ , decellularized  $n = 7$ ) was severed and immediately fixed in formaldehyde followed by paraffin-embedding (FFPE). A classical hematoxylin and eosin (H&E) stain was performed. The resulting slides were scanned on a Panoramic 250 Flash ii scanner (3DHISTECH) in order to enable digital analysis. Slide observation, evaluation of histoarchitecture and structure preservation were carried out in the digital slide manager program CaseViewer 2.1 for Windows (3DHISTECH). Images were taken with the same program in unmanipulated as well as in Digital Differential Interference Contrast (DDIC) mode.

## 4.8 Recellularization of the porcine nerve grafts

### 4.8.1 Porcine aortic endothelial cells

Wild type porcine aortic endothelial cells (PAEC) were expanded in a T75 cell culture flask to the sixth passage under standard conditions (37°C, 5% CO<sub>2</sub>, 1%FBS-1%PS in DMEM) before cell membrane staining and introduction in to the vascular tree of the decellularized nerve scaffold (see below).

### 4.8.2 Fluorescent membrane labelling

Just before introduction into de decellularized nerve scaffold the PAEC were fluorescently labelled by a membrane staining (PKH26 Red Fluorescent Dye Kit, PKH26GL, Sigma-Aldrich). The procedure was held according to the manufacturer's instructions. In brief,  $2 \times 10^7$  cells were trypsinized and washed in serum free medium. After centrifugation, the supernatant was aspirated as much as possible and 1 ml of Diluent C contained in the kit was added and the cells resuspended. The dye solution was prepared by giving 4µl of PKH26 ethanolic dye solution to 1ml of Diluent C in a separate tube. Next the dye solution and the resuspended cells were combined and mixed well immediately. Incubation for 3 minutes with periodic mixing was allowed. Then the staining process was interrupted by adding 10ml of cell culture medium containing 1% BSA to bind excess dye. For the final washing steps, complete cell culture medium was used as well as for introduction into the graft.

### 4.8.3 Perfusion-recellularization with wtPAEC

Decellularized nerve scaffolds were sterilized by continuous perfusion with a peristaltic pump Minipuls 3 (Gilson) with 0.1% peracetic acid in PBS for 4 hours followed by 4 hours of washing with sterile PBS. All perfusion steps were held at a constant flow rate of approximately 2ml/min. Conditioning of the scaffold was also performed under constant perfusion with pure cell culture medium (DMEM) at 37 °C and 5% CO<sub>2</sub> overnight. The following day, the condition medium was removed and the ECMS disconnected from the perfusion system for injection of four times  $2.5 \times 10^6$  labelled PAEC over the course of two hours ( $2.5 \times 10^6$  cells every half an hour, totally  $1 \times 10^7$  cells) into the vascular tree via arterial cannula. Immediately before injection the PAEC were fluorescently labelled by PKH26 membrane labelling (PKH26 Red Fluorescent Dye Kit, PKH26GL, Sigma-Aldrich). After cell seeding, the perfusion system was reconnected to the arterial cannula and the flow slowly applied. Starting from less than 1 ml/min the flowrate was increased every half an hour up to 2ml/min. Cultivation of PAEC in the bioreactor under normal conditions at 37°C, 5% CO<sub>2</sub> with adding fresh medium (10% FBS – 1% PS in DMEM) every second to third day. After closing the experiment samples for analytical experiments were taken.

## 4.9 Statistical analysis

Data organization and storage as well as all calculations and quantifications were done on the software Excel for Mac version 15.22 (Microsoft Corporation) and are stored in their respective folders under “Masterthesis Tse” on the server of the University of Bern. Graphic presentation and statistical analysis was performed on Prism 7 for Mac OS X, Version 7.0a (GraphPad Software). Comparison between or within cytokines groups or tissues respectively, was done in relative proportions such as logarithmic transformations (ear log<sub>2</sub>, face log<sub>10</sub>, nerve log<sub>10</sub>), ratios and percentages and analyzed by ordinary one-way ANOVA with Tukey’s multiple comparisons tests. Absolute numbers are given in pg cytokine per mg tissue [pg/mg], µg sGAG per mg dry tissue [µg/mg] and in ng DNA per mg dry tissue [ng/mg]. The pg/mg (and µg/mg and ng/mg respectively) from native versus decellularized cytokines of a certain tissue were compared by unpaired two-tailed t-test. Heatmaps were analyzed by multiple unpaired two-tailed t-tests using the two-stage linear step up procedure of Benjamini, Krieger and Yekutieli, with Q = 1%. Each row was analyzed individually, without assuming a consistend SD. A p value of 0.05 or less was considered statistically significant: \*p ≤ 0.05, \*\*p ≤ 0.01, \*\*\*p ≤ 0.001, \*\*\*\*p ≤ 0.0001.

## 5. Results

### 5.1 Characterization of Human Ear VCE

#### 5.1.1 Effectiveness of perfusion decellularization protocol

In order to determine how effectively the perfusion decellularization protocol removed the immunogenic cellular part from the ECM an analysis of the fluorescence intensity of DAPI (4',6-diamidino-2-phenylindole), which is known to stain the nuclei of cells, was performed<sup>36</sup>. Samples were classified as “native”, “pre-detergent” and “decellularized” by our collaborators at UCL. “Pre-detergend” samples were treated up to and including SDS perfusion but no Triton X-100 treatment, while “decellularized” samples were treated with both detergents. As discussed above, Triton X-100 has been proven to remove cell residues more effectively than SDS<sup>46</sup>, while the latter is more efficient in removing the nuclei<sup>47</sup>. Nevertheless, both are classified as detergents, and therefore this classification is only assigned in order to differentiate the single and double detergent treatment. A significant reduction ( $*p \leq 0.05$ ) of fluorescence intensity was observed between the native and the decellularized pre-detergent and the finally decellularized samples, respectively. Almost no nuclei were observed in decellularized samples either before or after detergent treatment, whilst they were clearly visible in the native samples. We consequentially concluded that the cellular components were washed away very efficiently and that only the acellular ECM components remained as ECMS. These findings are in consistency with the DNA analysis that was done by our collaborators at the UCL (data not shown, manuscript under review).

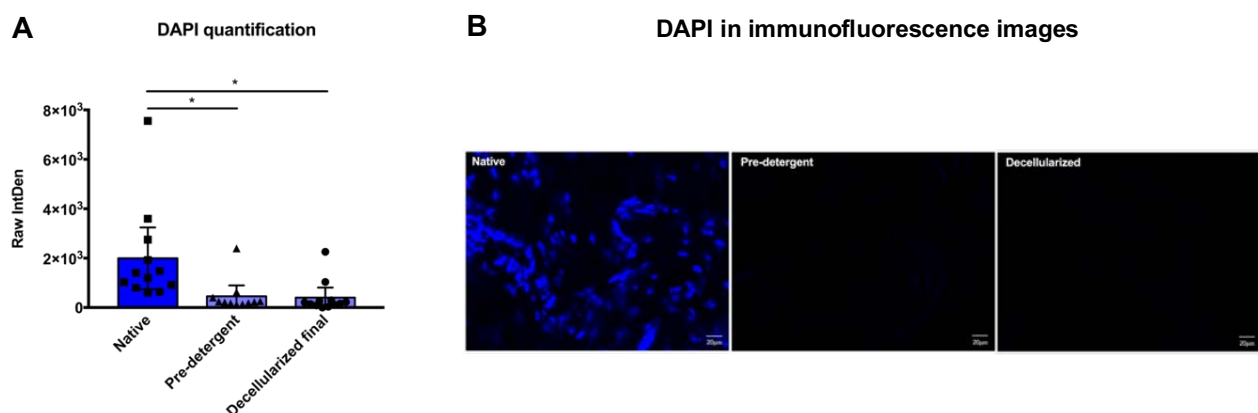


**Figure 12. DAPI quantification of the ear ECMS.** **A)** Quantification of the fluorescence signal of native, pre-detergent and finally decellularized samples (each n=1). Each data point represents one whole picture quantification of the blue channel. p-values were obtained by two-tailed unpaired t-test. Native vs. pre-detergent:  $p = 0.0223^*$ , native vs. decellularized final  $p = 0.0142^*$  and pre-detergent vs. decellularized = ns. **B)** Representative images of the blue channel used for quantification. In native samples the nuclei were clearly identifiable whilst absent in the pre-detergent and final decellularized samples.

### 5.1.2. Preservation of cytokines in the ear ECMS

For the VCA grafts, all cytokines were allocated to one of the three following groups: pro-inflammatory cytokines, migration-inducing cytokines (i.e. chemokines) and proliferation-inducing cytokines (growth factors, see figure 10). No double classifications were allowed. The cytokine analysis revealed that all the 42 tested cytokines were measurable in skin, cartilage and fat samples with the exception of IL-4 in fat tissue. In order to quantitatively characterize cytokine preservation in the different tissues of the scaffold, we analyzed the degree of change in each biological sample. As shown in figure 13A, all the measured cytokines in skin samples collected from the decellularized scaffold decreased significantly compared to native skin samples (only the IL-4 decrease was not significant). Conversely, only four of the measured cytokines decreased significantly by decellularization in fat tissue (MIF, CCL1, CXCL13 and CXCL16). The only undetected cytokine in fat tissue was IL-4 which was below detection level. Cartilage presented a middle behavior with 22/42 cytokines significantly decreased after decellularization compared to controls. To better understand how the decellularization process affected cytokines in the ear ECMS, we calculated the relative proportion of preservation for each cytokine in decellularized tissues expressed as percentage of the native mean abundance (figure 13B).

In order to investigate whether different cytokine subclasses were differentially affected by the decellularization process, the following cytokine groups were created according to cytokine function: 1. pro-inflammatory cytokines: IL-1 $\beta$ , IL-6, IFN $\gamma$ , TNF- $\alpha$ , MIF, 2. chemokines: IL-16, CCL1, CCL2, CCL3, CCL7, CCL8, CCL11, CCL13, CCL15, CCL17, CCL19, CCL20, CCL21, CCL22, CCL23, CCL24, CCL25, CCL26, CCL27, CXCL1, CXCL2, CXCL6, CXCL9, CXCL10, CXCL11 and 3. growth factors: IL-2, IL-4, IL-8, IL-10, GM-CSF, TGF- $\beta$ 1, TGF- $\beta$ 2, TGF- $\beta$ 3, CXCL5, CXCL12. As shown in figure 14, in decellularized skin total soluble protein preservation was  $8.75 \pm 4.07\%$  (mean + SD) with similar preservation of pro-inflammatory cytokines and chemokines ( $5.88 \pm 5.0\%$  and  $7.13 \pm 7.87\%$ , respectively). Growth factors showed a much higher percentage of preservation ( $152.68 \pm 213.84$ ) compared to pro-inflammatory cytokines and chemokines. Similar results were observed in cartilage ( $41.99 \pm 6.73\%$ ,  $19.48 \pm 11.21\%$ ,  $17.30 \pm 11.53\%$  and  $78.77 \pm 80.37$  of preservation of total protein, pro-inflammatory cytokines, chemokines and growth factor, respectively) and in fat ( $12.9 \pm 5.09\%$ ,  $31.74 \pm 21.65\%$ ,  $43.63 \pm 33.52\%$ ,  $255.94 \pm 275.28\%$  of preservation of total protein, pro-inflammatory cytokines, chemokines and growth factor, respectively). Interestingly, three of the 42 cytokines (i.e., TGF-beta1, TGF-beta3 and CXCL5) showed an increase in expression levels when comparing decellularized and native tissues of skin and cartilage. This is likely due to more efficient protein extraction in the cell-empty ECMS and the increase in the ratio of pg cytokine per total ECMS wet weight in the decellularized

tissues. In decellularized fat, six cytokines displayed relative increase as compared to native tissue (i.e., TGF- $\beta$ 1, TGF- $\beta$ 3, CXCL5, IL-2, CXCL2 and CCL24), confirming the higher capacity of the adipose tissue to retain growth factors during the decellularization process. Apart from TGF- $\beta$ 1, TGF- $\beta$ 3 and CXCL5 the most preserved cytokines across tissues were IL-2, GM-CSF, CCL1, CCL24 and CXCL2. In all three tissues, i.e. skin, fat and cartilage, growth factors were the most retained group of cytokines, followed by chemokines in skin and fat, and pro-inflammatory cytokines in cartilage, respectively.

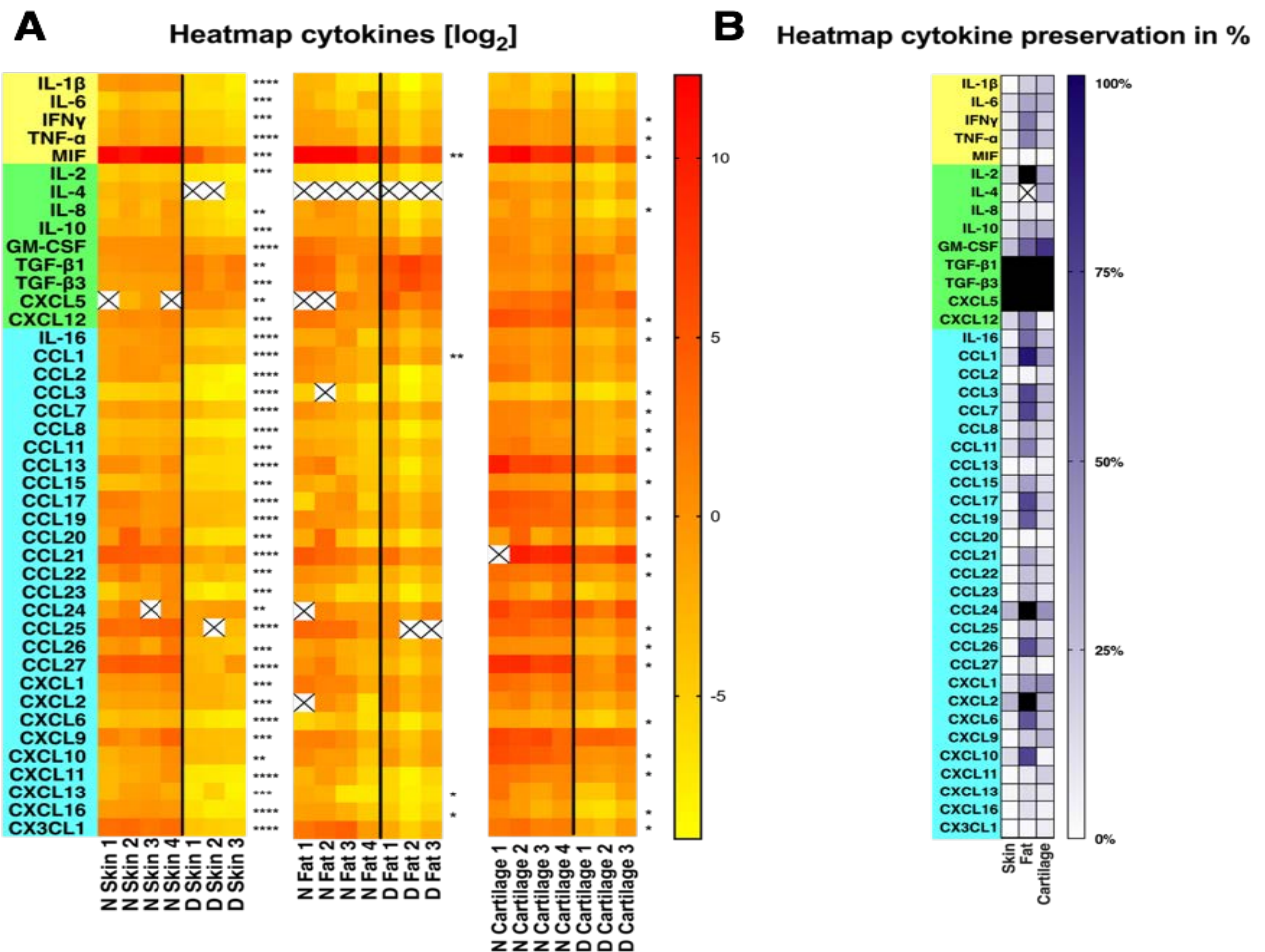


**Figure 13. Cytokine levels in the ear ECMS.** Cytokine levels were analyzed by Luminex-like multiplex assay. **A)** Heatmap shows  $\log_2$  transformed data for each individual sample in skin, fat and cartilage of native and ECMS ear. Each row shows separate measurements of native ( $n = 4$ ) and decellularized ( $n = 3$ ) samples. Significances were determined by multiple two-tailed unpaired t-tests using the two-stage linear step-up procedure of Benjamini, Krieger and Yekutieli, with  $Q = 1\%$ . Each row was analyzed individually, without assuming a consistent SD. \* $p < 0.05$ , \*\* $p < 0.01$ , \*\*\* $p < 0.001$ \*\*\*. **B)** Heat map showing the relative average preservation of every cytokine in each tissue displayed as percent [%] of mean native expression. Black cells indicate measurements out of range, indicating a relative increase after decellularization (> 100%). Figure modified from manuscript<sup>72</sup>.

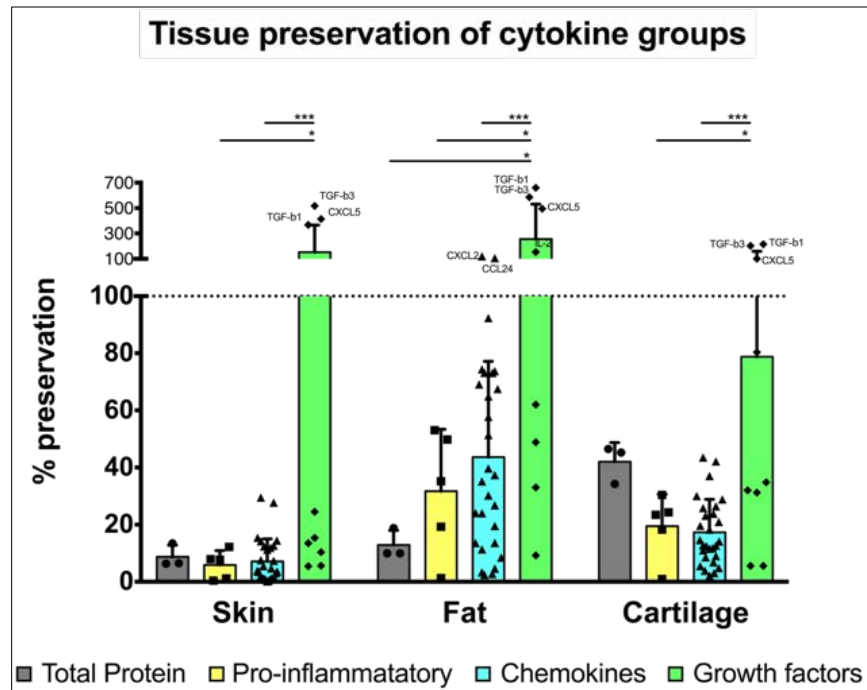


**Figure 14. Tissue preservation of total protein and the different cytokine groups after decellularization.** Cytokines were grouped based on their function and the relative preservation as compared to native mean expression of each subgroup was analyzed. Bar graph indicating mean + SD and individual data points. Cytokines with a relative increase in abundance show percentages of over 100%. Growth factors were significantly better preserved in all three tissues of the ear ECMS. Chemokines were the second most preserved in skin and fat, whereas pro-inflammatory cytokines were the second most preserved in cartilage. \* $p < 0.05$ , \*\* $p < 0.01$ , \*\*\* $p < 0.001$  by ordinary one-way ANOVA with Tukey's multiple comparisons tests. Figure modified from manuscript<sup>72</sup>.

### 5.1.3 Coagulation associated factors in the ear

In order to obtain a first impression of the coagulation status of the ear-ECMS, the following six factors that are associated with coagulation and endothelial cell activity were analyzed in an immunofluorescence staining in native, pre-detergent and final decellularized samples: antithrombin III (ATIII), fibrinogen-like protein 2 (FGL2), heparan sulfate proteoglycan (HSPG), plasminogen activator inhibitor-1 (PAI-1), tissue factor (TF) and tissue plasminogen activator (tPA). Immunofluorescence signal quantification was analyzed with the software ImageJ Version 1.0 and the data was depicted as raw integrated density (Raw IntDen). Data are presented as mean  $\pm$  SD scatter dot plots combined with a bar of color, to increase visual comprehension. Each dot represents one measurement. The signal intensity measurements for DAPI and the coagulation factors were whole picture quantifications. The data of native samples presented a generally higher variation in fluorescence intensity as the pre-detergent or the final decellularized samples. This is most likely due to higher variability of structures in the native tissue and therefore, also the distribution pattern of certain factors may vary across tissue sections (e.g. ATIII is found in the plasma, hence it is observed only in sections that include blood vessels). The pre-detergent and the decellularized groups showed less variation and also less fluorescence intensity. The expression of ATIII, FGL2 and tPA both groups were significantly reduced in the pre-detergent and decellularized samples as compared to the native samples. tPA, PAI-1 and TF showed no significant reduction in any case, however, their intrinsic expression levels in the native tissues were lower by nature (where less is, less can be reduced). However, there was no significant difference observed between the pre-detergent and the final decellularized group, which indicates that SDS seems to be a very potent chemical to decrease coagulation associated factors in perfusion decellularization protocols.

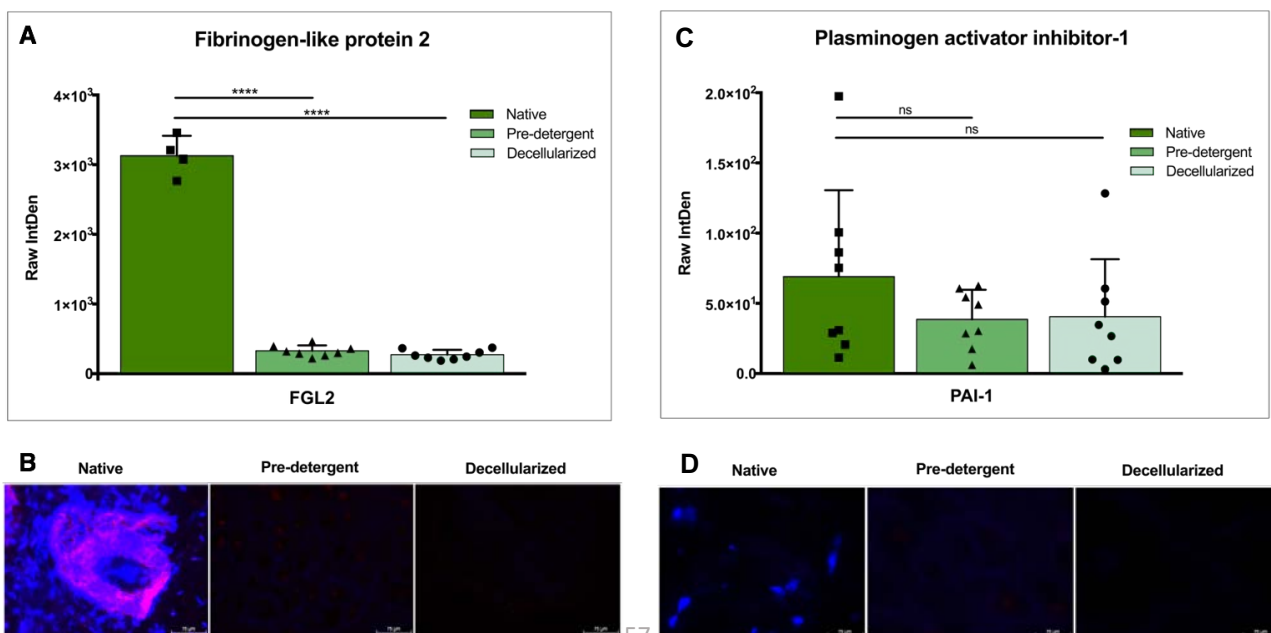
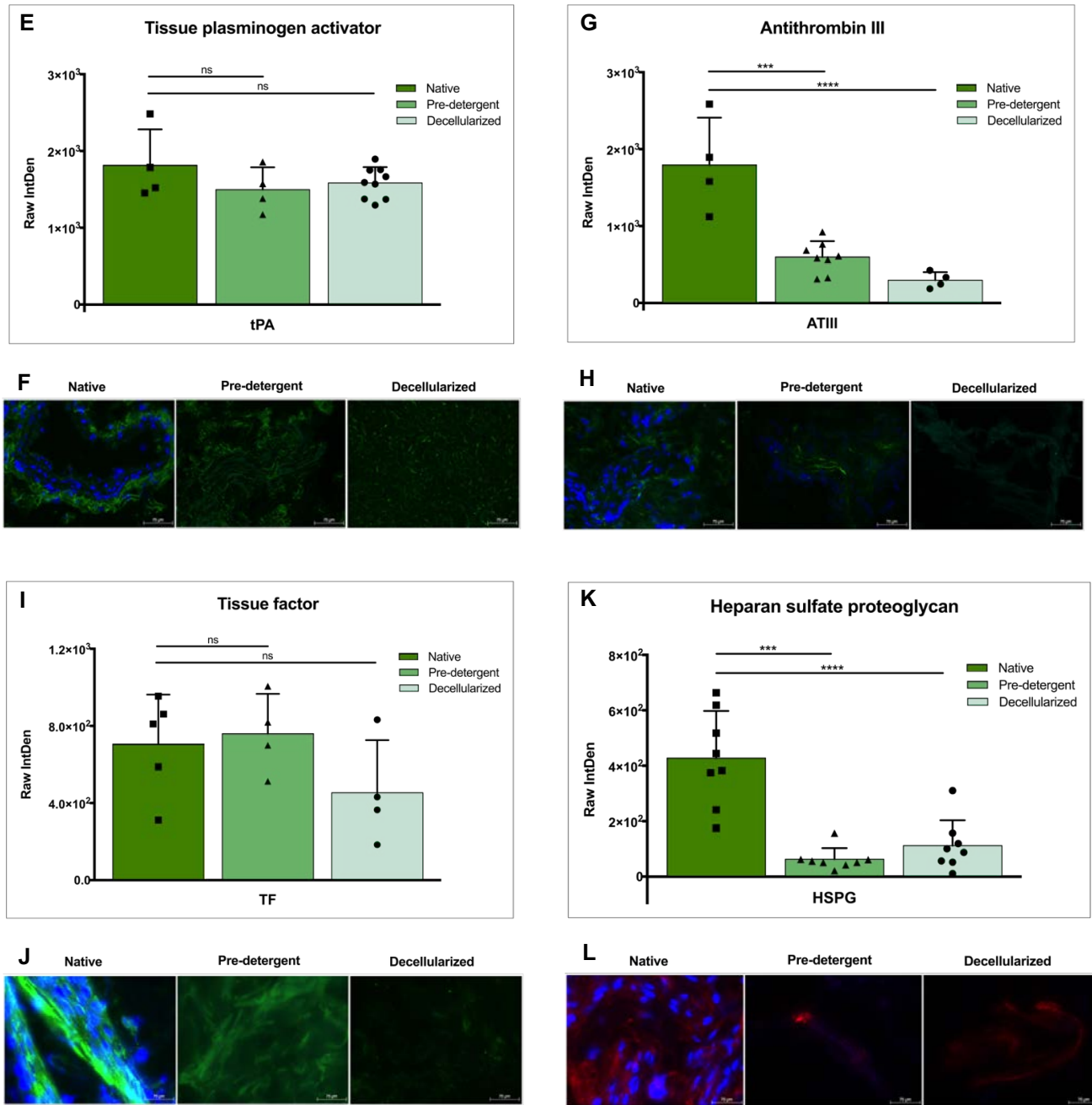


Figure continued on following page.



**Figure 15. Immunofluorescence staining and signal quantification of coagulation-associated factors in the ear ECMS (full thickness). B, D, F, H, J, L) Immunofluorescence staining of FGL2, PAI-1, tPA, ATIII, TF and HSPG. Each target was stained in native, pre-detergent and final decellularized samples (each n = 1). A, C, E, G, I, K) Quantification of the immunofluorescence signal intensities. Each data point represents one quantification. FGL2, ATIII and HSPG show significant reductions whereas PAI-1, tPA and TF were not significantly reduced. None of the targets showed a significant difference in fluorescence intensity between pre-detergent and final decellularized samples. Data analyzed with an ordinary one-way ANOVA with Tukey's multiple comparisons test. ns = not significant, \* p < 0.05, \*\*p < 0.01, \*\*\*p < 0.001, \*\*\*\*p < 0.0001.**

## 5.2 Characterization of Human Face ECMS

### 5.2.1 Preservation of cytokines in the face ECMS

Unlike in the ear ECMS, not all of the 42 measured cytokines were measurable in the face ECMS. Overall, less cytokines and lower levels were measured in the face ECMS. Two additional tissues were analyzed, namely mucosa and muscle. All cytokines were detected in skin and cartilage. In mucosa, only IL-4 was not measurable, in fat CXCL2 and IL-4 were not detected and in muscle IL-1 $\beta$ , IFN $\gamma$ , IL-4, CCL11 and CXCL2 remained undetected. Out of 42 measured cytokines, 31 were significantly reduced in cartilage and 29 in skin and mucosa. In muscle, 15 cytokines were significantly reduced and in fat only 9 (figure 16A). The relative proportion of preservation was calculated for each cytokine in every of the five tissues and expressed as percentage of the native mean abundance (figure 16B). Growth factors were the most preserved cytokine group in all five tissues. In order to compare the cytokines according to their functional activities, the same three cytokine groups as in the ear ECMS were analyzed, i.e. 1. pro-inflammatory cytokines (IL-1 $\beta$ , IL-6, IFN $\gamma$ , TNF- $\alpha$ , MIF), 2. chemokines (IL-16, CCL1, CCL2, CCL3, CCL7, CCL8, CCL11, CCL13, CCL15, CCL17, CCL19, CCL20, CCL21, CCL22, CCL23, CCL24, CCL25, CCL26, CCL27, CXCL1, CXCL2, CXCL6, CXCL9, CXCL10, CXCL11) and 3. growth factors (IL-2, IL-4, IL-8, IL-10, GM-CSF, TGF- $\beta$ 1, TGF- $\beta$ 2, TGF- $\beta$ 3, CXCL5, CXCL12).

As can be seen in figure 17, the total soluble protein preservation of the decellularized tissues was highest for fat (48.34 $\pm$ 8.85%, mean + SD), followed by cartilage (21.34 $\pm$ 7.53%), muscle (14.9 $\pm$ 3.70%), skin (8.31 $\pm$ 0.38%) and mucosa (5.20 $\pm$ 0.70%). Fat showed in all cytokine groups the highest retention levels: 36.38 $\pm$ 32.91% for chemokines, 44.04 $\pm$ 38.99% for pro-inflammatory cytokines and 389.88 $\pm$ 566.45% for growth factors, with the latter being the only group showing a tremendous relative increase of over 100%. Similar to ear ECMS, in the face ECMS the growth factors were the most preserved cytokine group across the tissues with the highest preservation in fat followed by muscle (20.98 $\pm$ 25.28%), skin, cartilage and mucosa (12.42 $\pm$ 22.14%, 12.34 $\pm$ 11.93% and 8.77 $\pm$ 11.04% respectively). The chemokines were generally better preserved than the pro-inflammatory cytokines, except in fat and muscle. Chemokines were most preserved in fat (36.38 $\pm$ 32.91%) followed by muscle (5.30 $\pm$ 4.61%), cartilage (3.08 $\pm$ 3.16), mucosa (1.48 $\pm$ 1.57%) and skin (1.23 $\pm$ 2.40%). The pro-inflammatory cytokines were the overall least preserved group with mean retention levels of 44.04 $\pm$ 38.99% in fat, 10.48 $\pm$ 14.53% in muscle, 1.64 $\pm$ 1.51% in cartilage, 1.11 $\pm$ 1.02% in mucosa and less than 1% in skin (0.66 $\pm$ 0.66%).

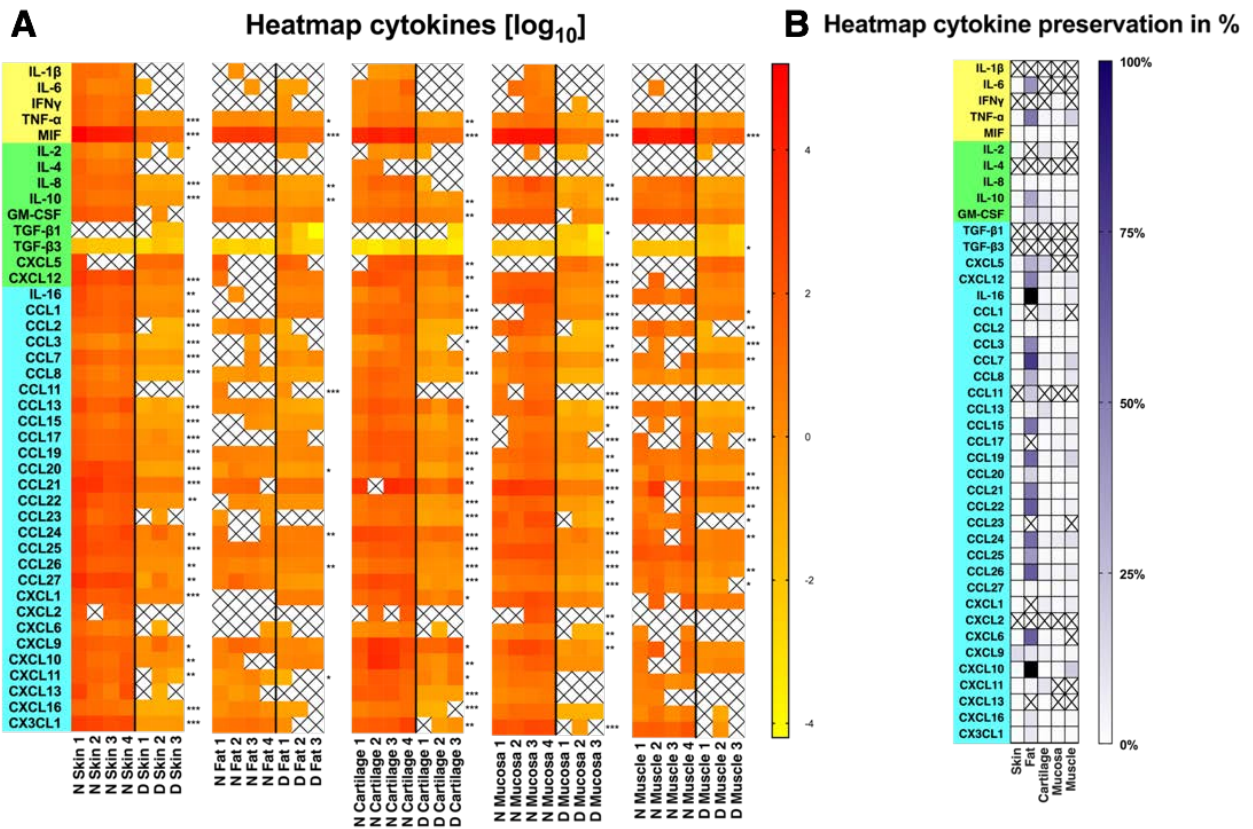


**Figure 16. Cytokine levels in the face ECMS.** Cytokine levels were analyzed by Luminex-like multiplex assay. **A)** Heatmap shows  $\log_{10}$  transformed data for each individual sample in skin, fat, cartilage, mucosa and muscle of native and ECMS face. Each row shows separate measurements of native ( $n = 4$ ) and decellularized ( $n = 3$ ) samples. Significances were determined by multiple two-tailed unpaired t-tests using the two-stage linear step-up procedure of Benjamini, Krieger and Yekutieli, with  $Q = 1\%$ . Each row was analyzed individually, without assuming a consistent SD. \* $p < 0.05$ , \*\* $p < 0.01$ , \*\*\* $p < 0.001$ , \*\*\*\* $p < 0.0001$ . **B)** Heat map showing the relative average preservation of every cytokine in each tissue displayed as percent [%] of mean native expression. Black cells indicate measurements out of range, indicating a relative increase after decellularization ( $> 100\%$ ). Figure modified from manuscript<sup>71</sup>.

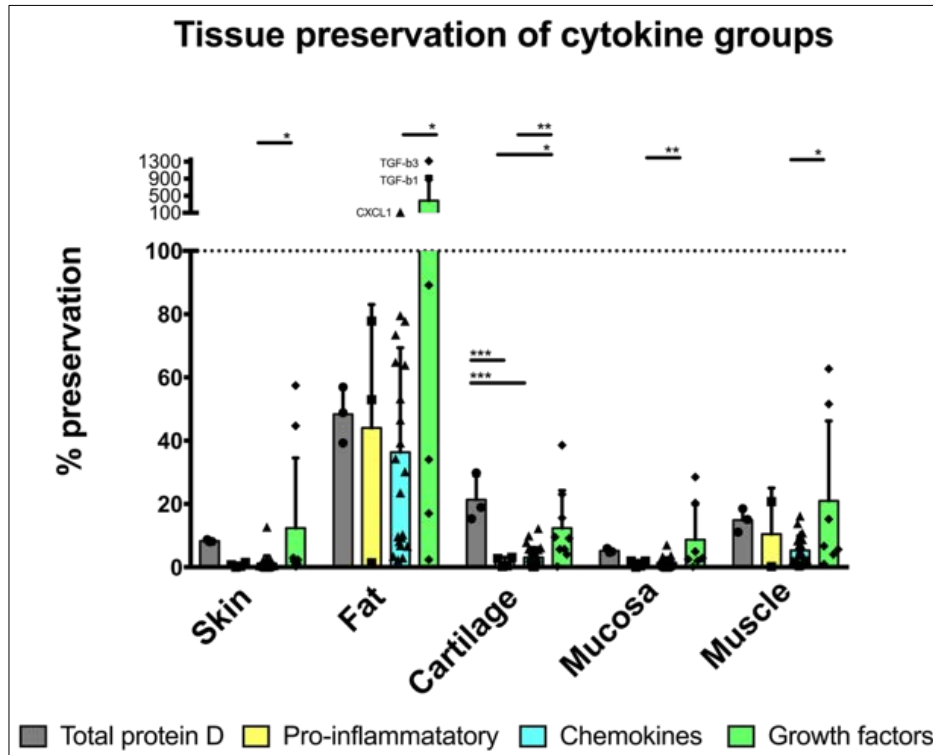


**Figure 17. Tissue preservation of total protein and the different cytokine groups after decellularization.** Cytokines were grouped based on their function and the relative preservation as compared to native mean expression of each subgroup was analyzed. Bar graph indicating mean + SD and individual data points. Cytokines with a relative increase in abundance show percentages of over 100%. Growth factors were significantly better preserved in all five tissues of the face ECMS. Chemokines were the second most preserved in skin, cartilage and mucosa whereas pro-inflammatory cytokines were the second most preserved in fat and muscle. \*p < 0.05, \*\*p < 0.01, \*\*\*p < 0.001 determined by ordinary one-way ANOVA with Tukey’s multiple comparisons tests. Figure modified from submitted manuscript<sup>71</sup>.

## 5.2.2 Comparison of ear and face ECMS

In order to compare cytokine preservation between the human ear and the human face ECMS, the expression levels of cytokines were compared in skin, fat and cartilage. Performing a  $\log_{10}$  transformation allowed to merge the data and it was observed that all the data points settled within a similar range. Native skin, fat and cartilage samples were not significantly different between ear and face grafts, suggesting that the two ECMS were comparable. Conversely, cytokine levels after decellularization were significantly different in fat and cartilage between face and ear, indicating a different response of the ear and the face scaffolds to the decellularization protocol. Skin however, did not significantly differ after perfusion decellularization. Tissue wise, skin and cartilage were better preserved in the ear ECMS whereas fat was more preserved in the face ECMS.

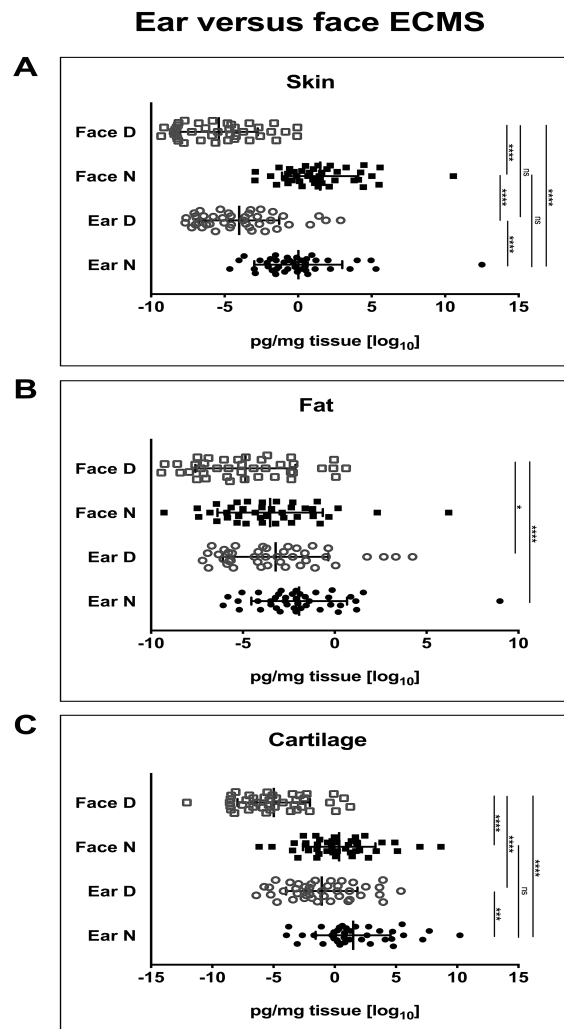


**Figure 18. Comparison of ear versus face ECMS in skin, fat and cartilage.** A, B and C)  $\log_{10}$  transformed data of measured pg cytokine/ mg of the respective tissue (i.e. skin, fat and cartilage) for native and decellularized samples. An ordinary one-way ANOVA analysis with Tukey's multiple comparisons test was used to perform the statistical analysis. ns = not significant, \* $p < 0.05$ , \*\* $p < 0.01$ , \*\*\* $p < 0.001$ , \*\*\*\* $p < 0.0001$ .

## 5.3 Development of a vascularized peripheral nerve ECMS

### 5.3.1 Morphology and tissue architecture of the peripheral nerve ECMS

Macroscopically, the grafts did not differ significantly before and after decellularization. The only macroscopic change after decellularization was that the overall structure appeared slightly looser and therefore, a mild decrease in length and a slight increase in circumference was observed (figure 19). Histologic examination revealed a strikingly well-preserved tissue architecture after decellularization. Although the cells were absent and the H&E staining less prominent in the decellularized samples, the tissue architecture remained the same and the structures, i.e. tissue orientation, connective tissue, epi- and perineurium, nerve fascicles and axonal tunnels, were well identifiable (figure 20). DNA contents in decellularized nerve was significantly lower than in native tissue (i.e. mean $\pm$ SD, 185.56 $\pm$ 109.29 ng/mg and 74.37 $\pm$ 39.76 ng/mg, respectively). In order to determine the length of the measured DNA fragments in the decellularized samples, a gelelectrophoresis was performed. Although the DNA concentration were lower in the decellularized samples, the length of the DNA fragments did not significantly differ and the DNA of decellularized presented the same length range as the native samples around 3000bp. A molecular analysis by immunofluorescence staining confirmed the lack of any nuclear staining in the decellularized samples and the preservation of the structural features and the molecular composition of the basal lamina (i.e. collagen type IV and laminin) of nerve fascicles. In terms of relative quantification, collagen type IV did differ in decellularized samples as compared to native tissue. Consistently, laminin expression was also slightly decreased in decellularized ECMS. To obtain more information about the molecular composition of the ECMS, the sulfated glucosaminoglycans (sGAG) were quantified. No significant decrease in sGAG content was detected in decellularized ECMS as compared to native tissue (4.44 $\pm$ 2.96 and 4.88 $\pm$ 4.13  $\mu$ g/mg dry tissue, respectively).

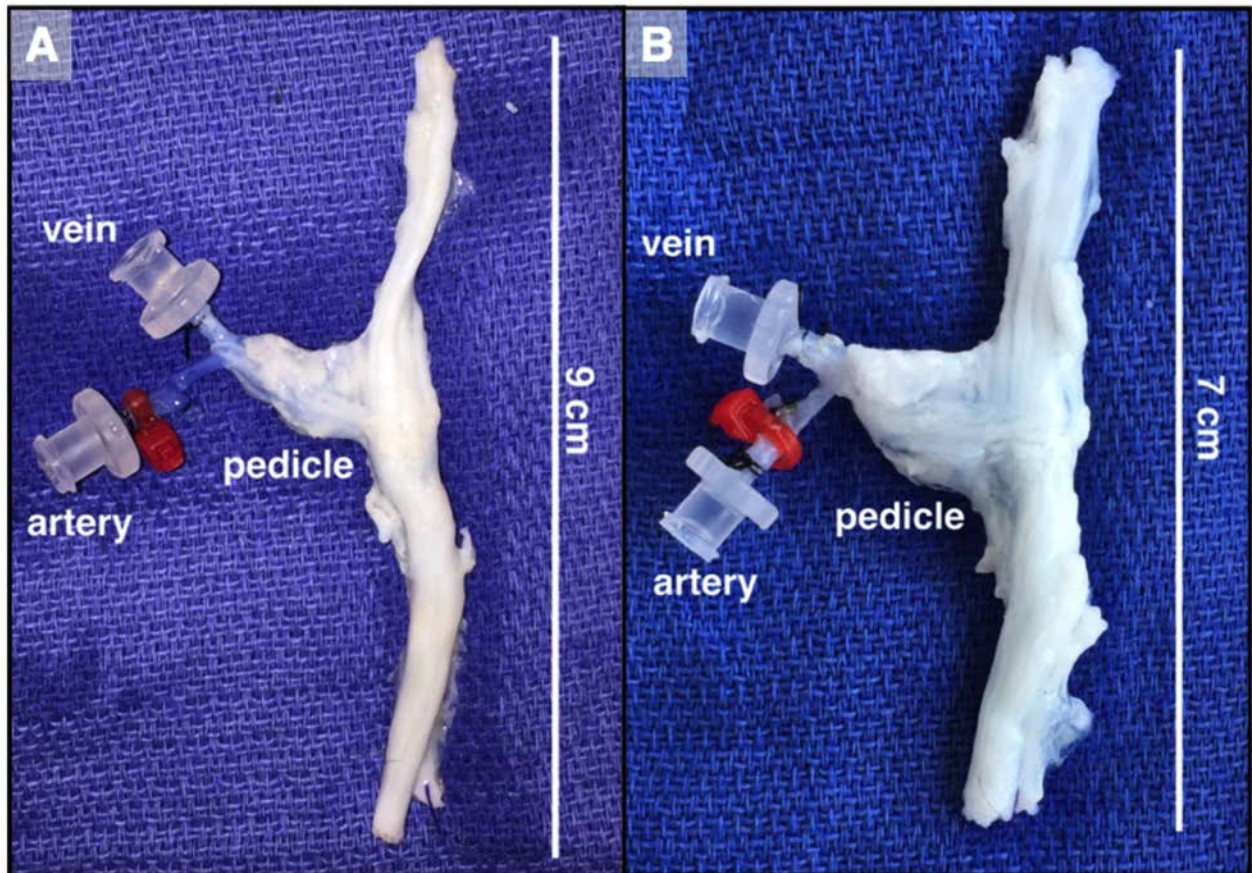


**Figure 19. Macroscopic structure of a native and decellularized vascularized peripheral nerve graft.** Representative pictures of the vascularized nerve scaffolds (n=7 native and n=7 decellularized). **A)** Native porcine sciatic nerve before procurement. Access to the vascular tree was ensured by cannulation of the artery and the vein of the main pedicle. Cannulas were connected to a Masterflex® L/S® Series Peristaltic Pump (Cole-Parmer) by 16G tubing, which allowed perfusion of the graft with decellularizing solutions. **B)** The same specimen after perfusion decellularization. The structure became slightly less defined and the graft's constitution got softened and showed reduced 3D stability and a slight increase in circumference and a slight decrease in length.

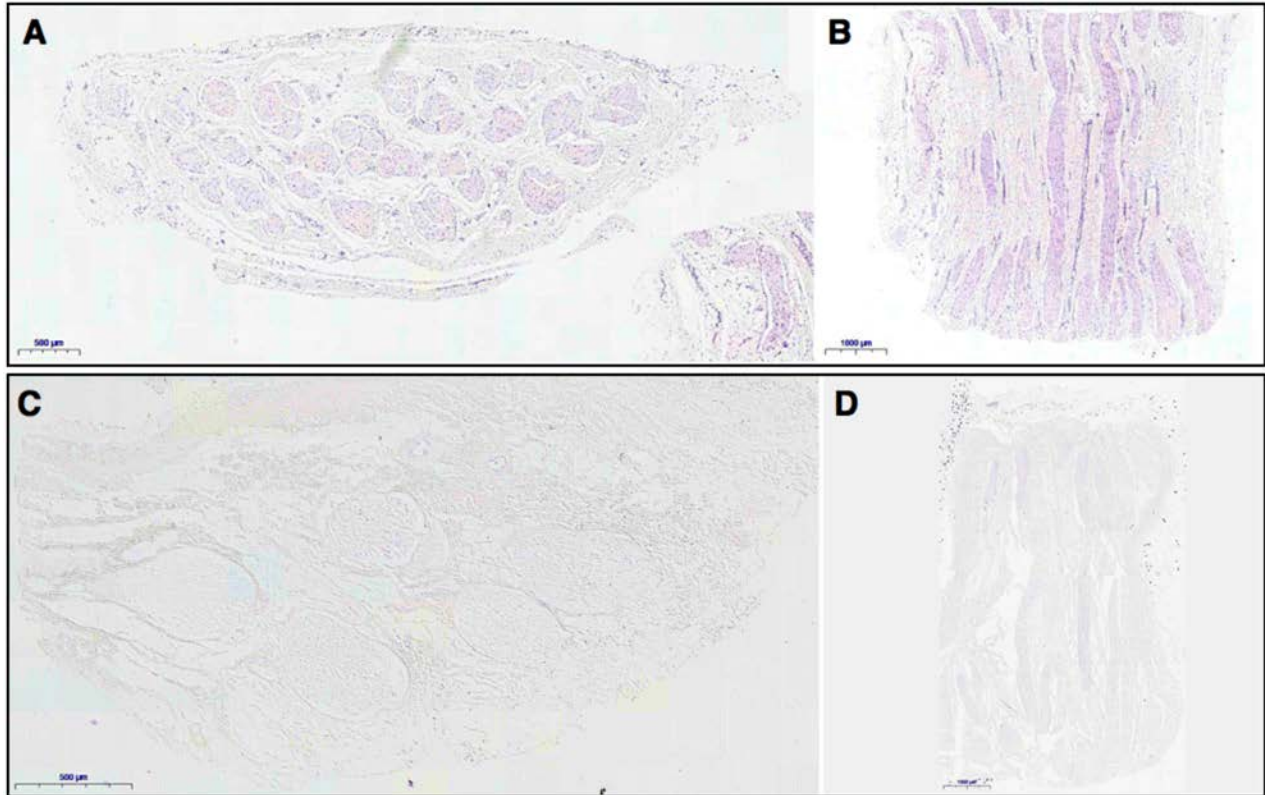
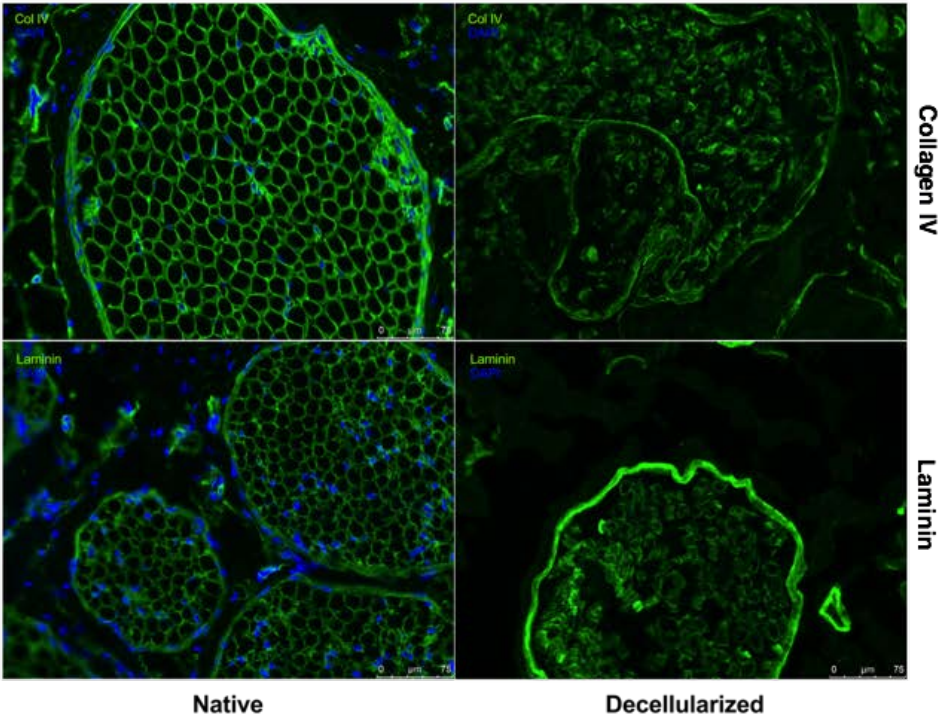
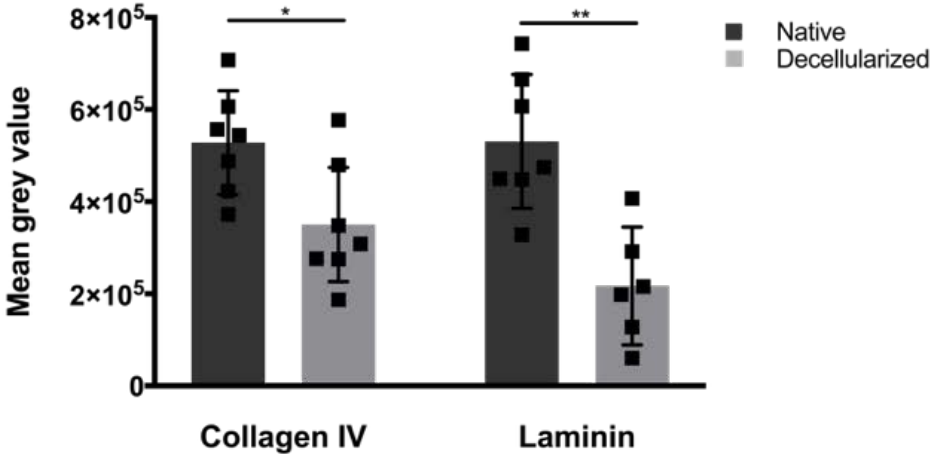


**Figure 20. Histological analysis of a native (A, B) and decellularized (C, D) vascularized peripheral nerve.** Representative pictures of H&E staining of histological sections of vascularized nerve ECMS (n=7 native and n=7 decellularized). **A)** Transversal section of the native porcine sciatic nerve after procurement. Epineurium, connective tissue and fascicles with perineurium are nicely identifiable and the interior of the fascicles, i.e. the axonal structures are stained. **B)** Longitudinal section of native porcine sciatic nerve. Layers of connective tissue and nerve fascicles are distinguishable. **C)** Transversal section of decellularized peripheral porcine sciatic nerve. The fascicular structures, the perineurium and the connective tissue are identifiable, with minimal changes of the tissue architecture after the perfusion decellularization process. **D)** Longitudinal section of a decellularized porcine sciatic nerve. The structural pattern is very similar to the native (cf. B). Remaining nucleic acid artifacts are located in the outer layer of the connective tissue with none identifiable within the nerve. All pictures were acquired on a panoramic slide scanner: A, B in classic light microscopy mode and C, D in digital differential interference contrast mode to enhance visibility of the almost translucent tissue. 40x magnification in all pictures.

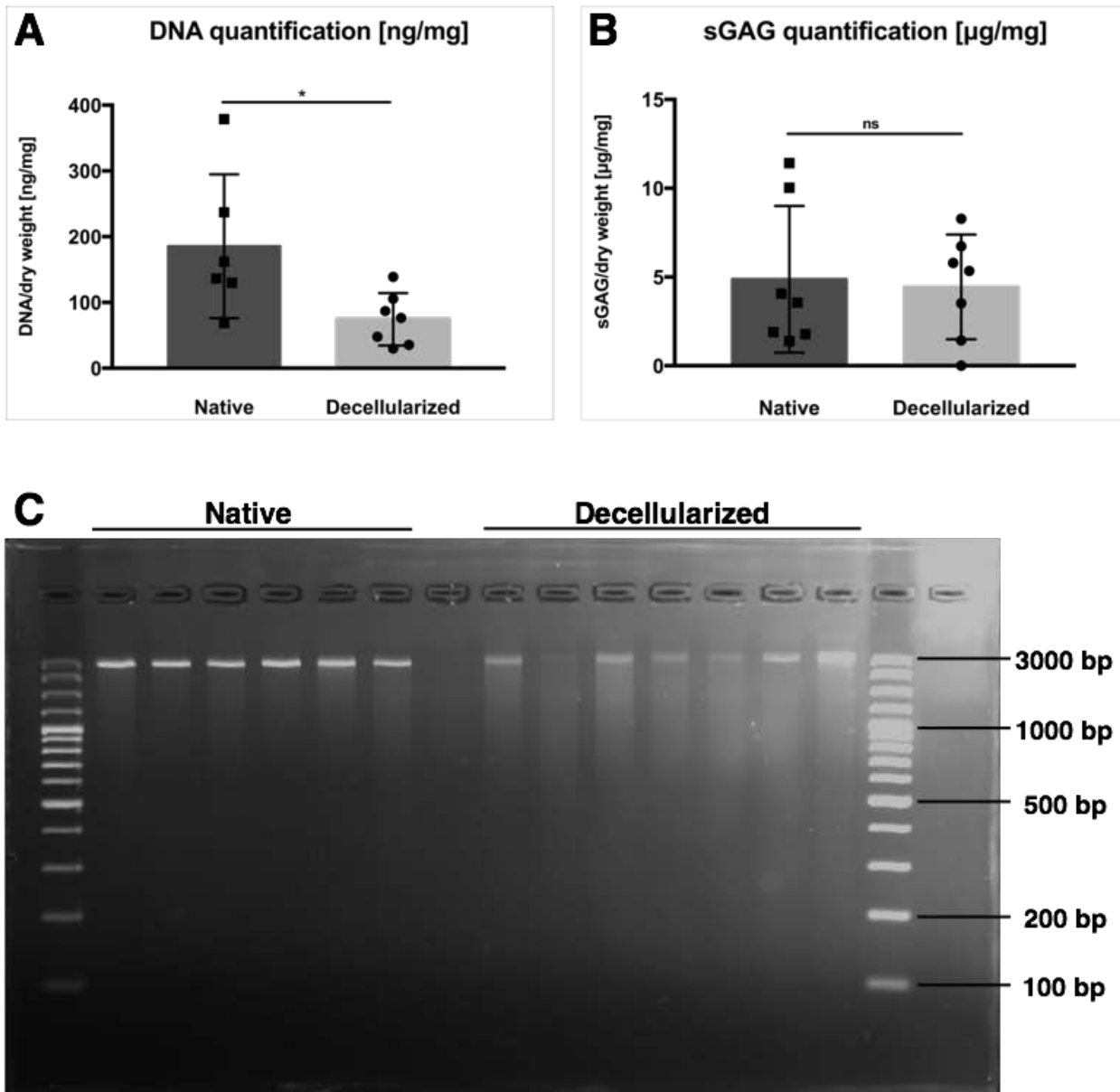
### A Immunofluorescence staining



### B Quantification of immunofluorescence staining



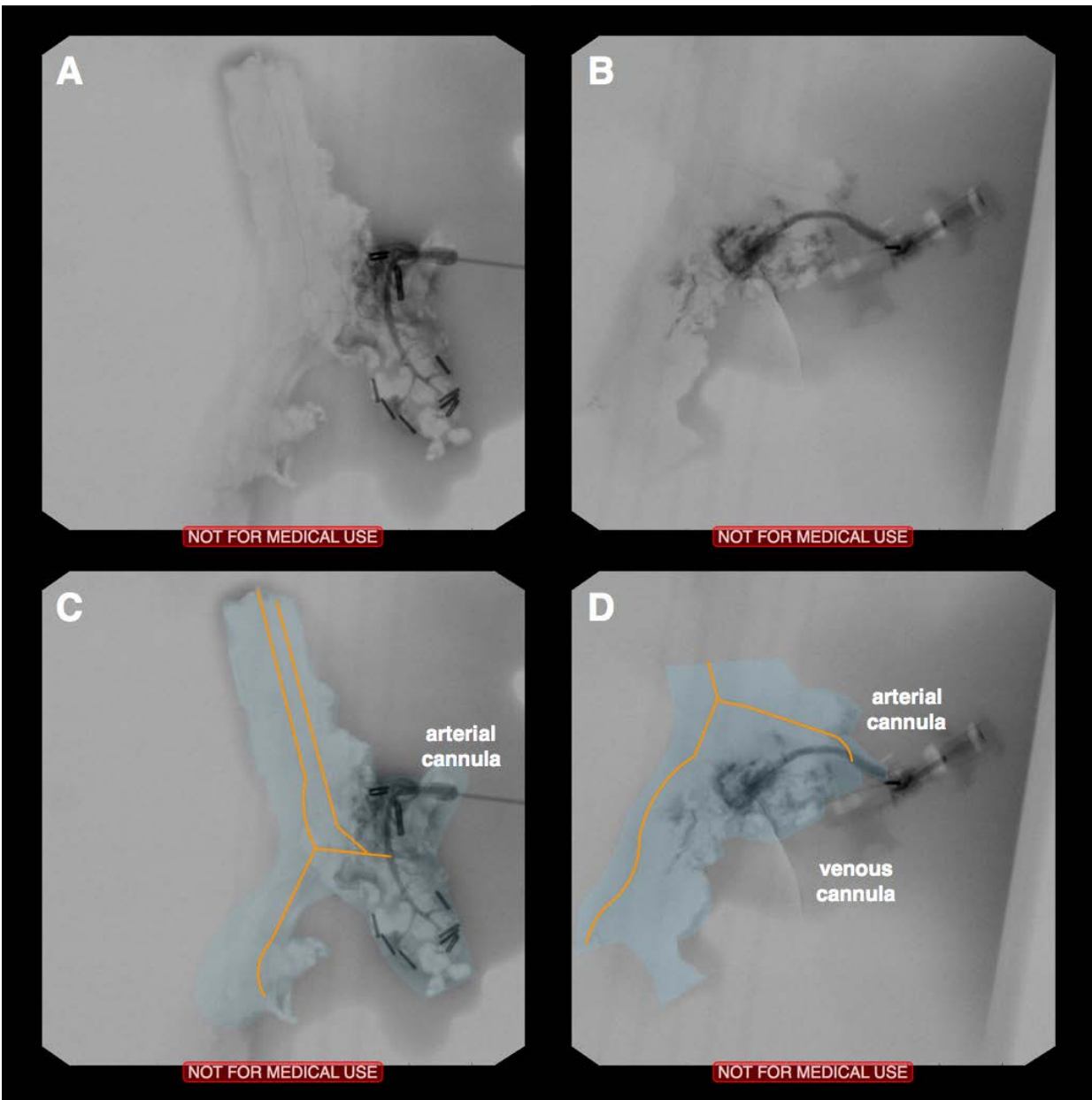
**Figure 21. Molecular structure of vascularized nerve ECMS. A)** Representative immunofluorescence pictures of collagen type IV (top row) and laminin (bottom row) each native (left, n=7) and perfusion decellularized (right, n=7). Preservation of tissue structure and of the two components of the basal lamina (i.e. collagen type IV and laminin) is confirmed. **B)** Quantification of the immunofluorescence signal (Raw IntDen) of collagen type IV and laminin, in native (n=7) and decellularized (n=7) nerves. Each data point corresponds to a mean of 5 to 6 quantifications for each nerve. Only area within the basal lamina was analyzed. Hence, one picture could produce one measurement, that was composed the additive sum from several sub-measurements (e.g. bottom left). Reduction of collagen type IV was observed to be significant ( $p = 0.020$ ) as well as reduction of laminin content ( $p = 0.002$ ). Data analyzed by two-tailed unpaired t-test. \* $p < 0.05$ , \*\* $p < 0.01$ .



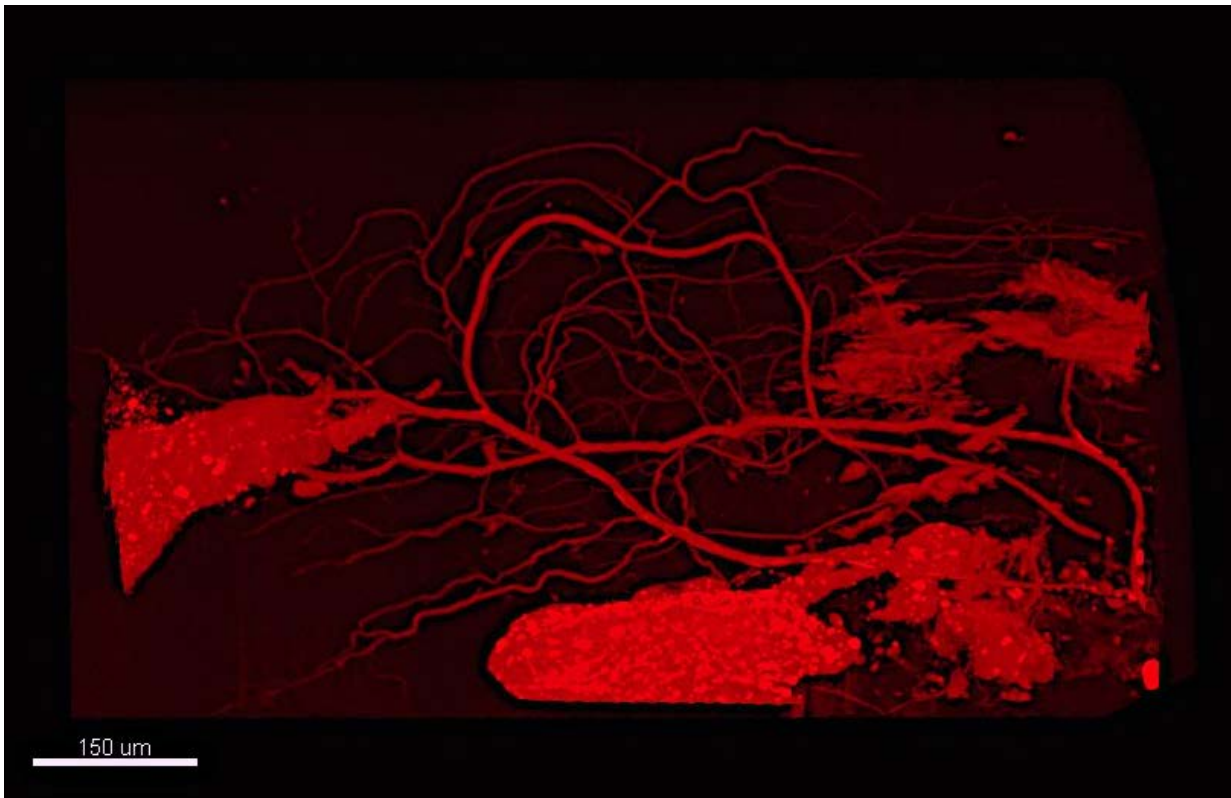
**Figure 22. Quantification of DNA and sGAG in the peripheral nerve ECMS before and after decellularization.** **A)** Quantification of DNA shown as ng/mg dry tissue. Native n=6, decellularized n=7. The native group showed a higher standard deviation (mean±SD, 185.56±109.29 ng/mg) as compared to the decellularized (74.37±39.76 ng/mg). Reduction of DNA content after decellularization was significant ( $p=0.029^*$ ). **B)** Quantification of sGAG given in µg/mg tissue. Native n=7, decellularized n=7. No significant reduction of the sGAG content was detected in decellularized ECMS as compared to native tissue (mean sGAG content 4.44±2.95 µg/mg and 4.88±4.13 µg/mg, respectively,  $p = 0.826$ ). ns = not significant,  $*p < 0.05$  by two-tailed unpaired t-test. **C)** Gelelectrophoresis (southern blot) of native and decellularized samples. 15 ng of DNA (native n=6, decellularized n=7) or less was loaded onto the gel. All samples aligned in the same region, at around 3000 bp. Hence, the DNA did not seem significantly fragmented and there was no obvious difference in length detectable between native and decellularized DNA isolates.

### 5.3.2 Assessment of internal vascularization of the peripheral nerve graft

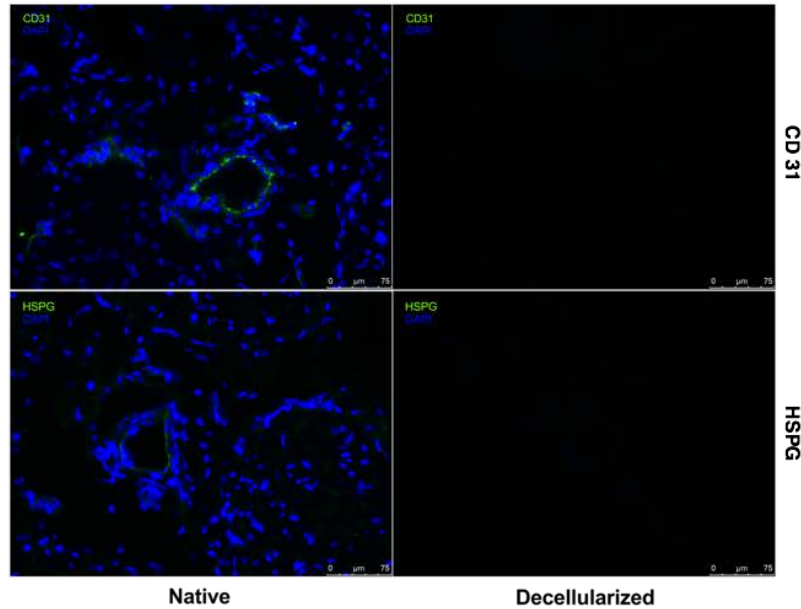
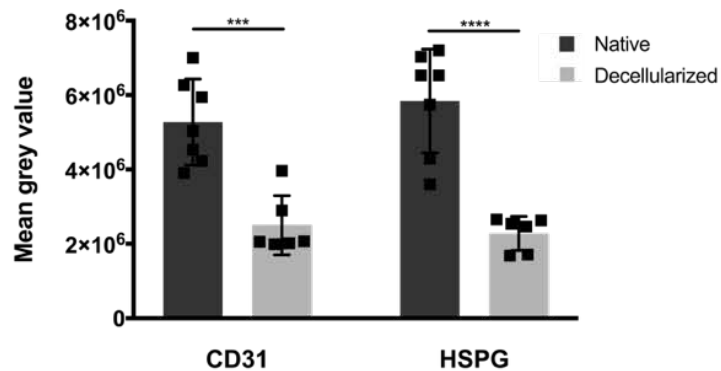
In order to address the preservation of the blood vessels in the vascularized grafts, the innate vascularization of the native nerves was analyzed by fluoroscopic angiography in freshly harvested native nerves and in the ECMS after the decellularization process had been completed. As shown in figure 23, the vascular structure inside the nerve was preserved and remained perfusable after decellularization. In order to obtain more information about the 3D structure of the vascular conduits inside the nerve, micro-angio-CT was performed. As presented in figure 24, a dense decellularized vascular network with preserved bifurcation was observed. To confirm the absence of endothelial cells, a CD31 immunofluorescence staining was performed. CD31 (or PECAM-1) is a widely used marker for endothelial cells<sup>143</sup>. The staining revealed a significant decrease of CD31 signal after decellularization. Along with CD31, HSPG (heparan sulfate proteoglycan) showed a significant decrease after the decellularizing treatment. As most HSPG types are either membrane-, ECM- or vesicle-bound<sup>144</sup>, this indicates, that the luminal layers of the vascular network as well as the rest of the tissue had been cleared out very efficiently. Nevertheless, the vascular system and its patency were preserved in the decellularized peripheral nerves, due to the presence of the structural ECM proteins of the endothelial basal membrane. The preservation of the acellular vascular tree in the graft provided the optimal condition for recellularization experiments.



**Figure 23. Fluoroscopic angiography of the innate vascular structure before and after decellularization.** **A)** Angiography of freshly harvested, native peripheral nerve. Fluoroscopic contrast fluid was injected into the nerve via the arterial cannula of the vascular system. A fine contrast along the midline of the nerve indicates the vascularization. **C)** Depicts the same picture as shown in A, but colored with the nerve area in light blue and the observed intraneural vascular structure in orange. **B)** Angiography of completely decellularized peripheral nerve. The same procedure as in A was used. A nice intraneural vascularization was detected and the patency of the vascular system seemed to be preserved. **D)** Shows the same image as in B, except with indication of nerve tissue in blue and the intraneural vessels in orange.



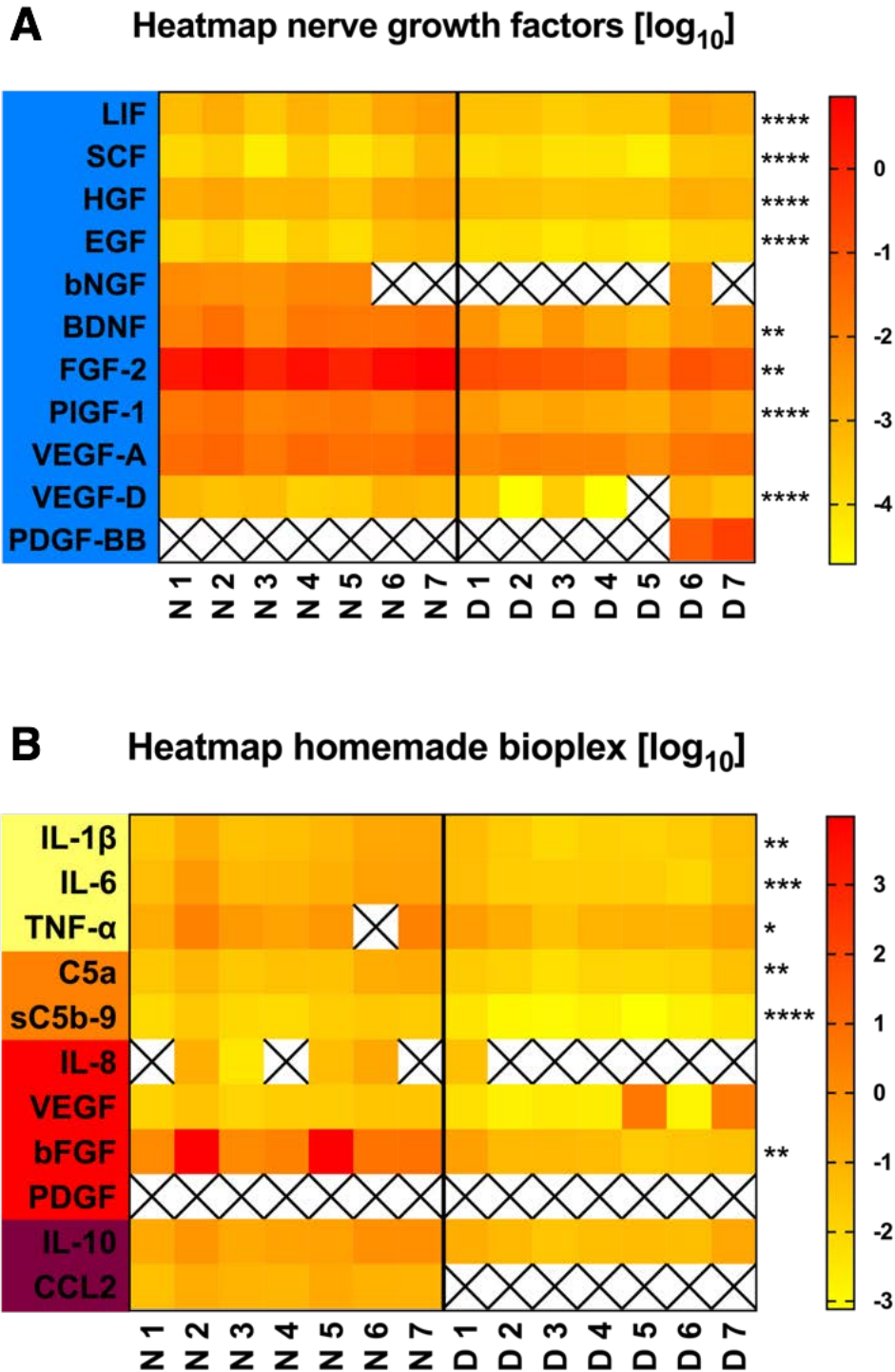
**Figure 24. Micro-Angio-Computertomography of a decellularized peripheral nerve.**  $\mu$ Angiofil® (Fumedica AG, Muri, AG, Switzerland), a polymerizing vascular contrast agent, was injected into the vascular tree via arterial cannula.  $\mu$ CT of the vascular system of a decellularized specimen shows a dense network of blood vessels with bifurcation. Some leakage was observed. More detailed information about the method can be found in the paper by Schaad et al.<sup>156</sup>.

**A Immunofluorescence staining****B Quantification of immunofluorescence staining**

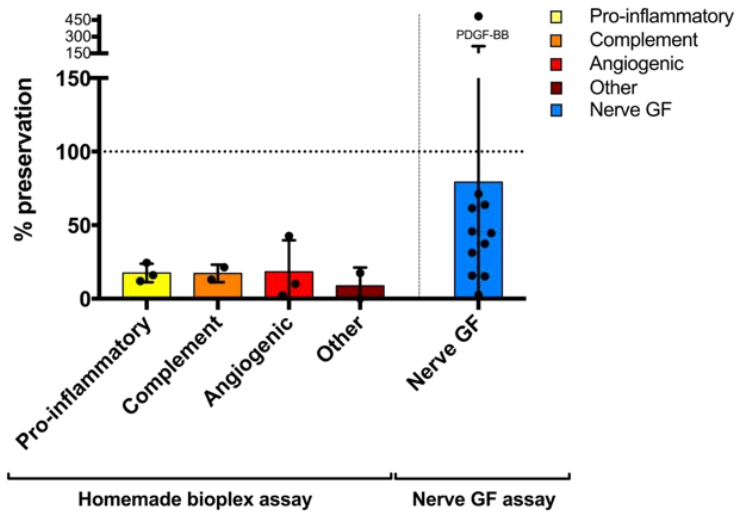
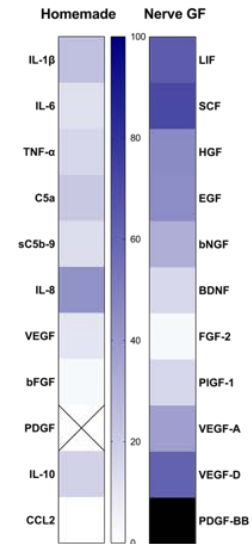
**Figure 25. Immunofluorescence staining and signal quantification of CD31 and HSPG in the native and decellularized peripheral nerve. A)** Representative immunofluorescence pictures of CD31 (top row) and HSPG (bottom row) each native (left, n=7) and perfusion decellularized (right, n=6). Clearance of cellular CD31 and HSPG in the ECM is confirmed. **B)** Quantification of the immunofluorescence signal (each dot represents a mean of 4 to 5 whole picture quantifications) of CD31 and HSPG, in native (n=7) and decellularized (n=6) nerves. Each data point corresponds to a mean of 3 to 4 whole picture quantifications for each nerve. Reduction of CD31 was observed to be significant ( $p = 0.0004$ ) as well as reduction of HSPG content ( $p < 0.0001$ ). Data analyzed by two-tailed unpaired t-test, \*\*\* $p < 0.001$ , \*\*\*\* $p < 0.0001$ .

### 5.3.3 Characterization of cytokine preservation decellularized nerve ECMS

For characterization of cytokine and growth factor content of the peripheral nerve ECMS, two different assays for cytokine analysis were performed. The first assay was a homemade production whose development that had been published before<sup>142</sup>. The second assay was commercially available and specifically designed for analysis of growth factors important in peripheral nerve biology (ProcartapPlex). Both were run on the same samples and the same machine (Flexmap3D). The cytokine group allocation was held after reported biologic activity of the proteins. In the first group all the nerve growth factors were included (i.e. LIF, SCF, HGF, EGF, bNGF, BDNF, FGF-2, PIGF-1, VEGF-A, VEGF-D, PDGF-BB, ProcartapPlex assay). The second group was composed of the pro-inflammatory cytokines of the homemade assay (i.e. IL-1 $\beta$ , IL-6, TNF- $\alpha$ , homemade assay). In the third group, the complement related proteins were assigned (i.e. C5a, sC5b-9, homemade assay) and in the fourth group the angiogenic proteins (i.e. IL-8, bFGF, VEGF, PDGF, homemade assay). The fifth group was composed of the remaining proteins that were merged into the group “other proteins” (i.e. IL-10 and CCL2, homemade assay). The most preserved group were clearly the nerve growth factors with a mean preservation of 79.33%. The second most preserved cytokine group were the angiogenic factors with a mean preservation of 18.35%, closely followed by the pro-inflammatory cytokines and the coagulation associated proteins (17.47% and 17.22%, respectively). The least retained group were the “other” proteins with a mean preservation of 8.78%. Looking at the nerve growth factor assay, 10/11 cytokines were measurable and 8 of them were significantly decreased when comparing the native and the decellularized samples. In the homemade assay, 9/11 cytokines were well detectable and 6 of them presented significantly decreased levels after perfusion decellularization. Some of the cytokines were measured in both assays. In particular, PDGF was part of the homemade and PDGF-BB was listed in the nerve growth factor assays. Both were not detectable in native tissue, which confirms the reproducibility of the experiments, even across assays. In decellularized samples, PDGF was not detected using the homemade assay (0% retention after decellularization). However, PDGF-BB was detected in two decellularized samples, affecting the calculation of the relative preservation with a relative increase of its expression over 100%. Moreover, the detection levels of VEGF-A and VEGF-D in the purchased assay were similar to the detection level of VEGF from the self-made assay. Another doubled measurement was bFGF in the homemade and FGF-2 in the purchased assay with relative retention levels of 2.40% and 2.64%, respectively. Thus, the two assays seemed to be comparable. The only cytokine with a retention level of 0% was CCL2.



**Figure 26. Cytokine retention in the peripheral nerve ECMS.** Heatmap showing cytokine measurements analyzed by Luminex-like multiplex assay. **A)** The heatmap shows  $\log_{10}$  transformed data of the determined pg growth factor per mg of tissue for each individual sample of native ( $n=7$ ) and decellularized ( $n=7$ ) specimen. Each row depicts 14 measurements of each nerve growth factor, according to graft status (native or decellularized). **B)** Heatmap depicting  $\log_{10}$  transformed data of the measured pg/mg tissue of the cytokines included in the homemade multiplex assay. Further information can be found in the publication of the assay<sup>142</sup>. Significances were determined by multiple two-tailed unpaired t-tests using the two-stage linear step-up procedure of Benjamini, Krieger and Yekutieli, with  $Q = 1\%$ . Each row was analyzed individually, without assuming a consistent SD. \* $p < 0.05$ , \*\* $p < 0.01$ , \*\*\* $p < 0.001$ , \*\*\*\* $p < 0.0001$ .

**A** Tissue preservation of both bioplex assays**B** Heatmap cytokine preservation [%]

**Figure 27. Relative protein retention in the decellularized nerve ECMS. A)** Bar graph with single data points of the homemade (left, yellow to red bars) and the nerve growth factor assay (right, blue bar). Data points represent average percentage of protein preservation calculated from native ( $n = 7$ ) and decellularized ( $n = 7$ ) samples. The homemade assay is split into the four different cytokine groups pro-inflammatory cytokines, complement factors, angiogenic factors and other proteins. The nerve growth factors are depicted in a single bar. One single analyte, namely PDGF-BB from the nerve growth factor group, presented a relative increase. However, this is believed to be due to measurement artifacts, as the analyte was only detected in 2 out of 7 decellularized samples, but not in any native samples (cf. figure ABD), hence creating a false positive increase in percentage ( $> 100\%$ ). No significances were detected neither between nor within the cytokine groups. Statistical analysis was performed using the ordinary one-way ANOVA with Tukey's multiple comparisons test. **B)** Relative average preservation of every cytokine in each tissue displayed in percent [%]. Black cells indicate measurements out of range, indicating a relative increase after decellularization ( $> 100\%$ ).

### 5.3.4 Re-endothelialization of the nerve ECMS

To prove that the engineered vascularized peripheral nerve ECMS has the potential to be recellularized before implantation, we administered perfusion re-endothelialization to the decellularized vascular tree. Re-endothelialization may be used to provide a functional vascular network, in which not only the basal membrane but also the cellular component is provided, aiming to improve blood supply within the nerve ECMS. Hence, wild type porcine aortic endothelial cells (*wtPAEC*) were expanded in culture, stained with a membrane labelling agent (PKH26), and then seeded into the nerve ECMS via the arterial cannula of the vascular tree. Microscopic pictures were taken on day 0 directly after cell-seeding, on day 1 after 24 hours of culture under flow and on day 7 of culture under flow (figure 28). After seeding, the PAEC settled inside the vessels, and already on day 1 of flow culture changed their appearance to a smoother surface and began to adapt to their environment. On day 7, vessel-like structures were observed inside the nerve with a very prominent 3D structure, indicating a successful re-endothelialization of the vascular structures. Immunofluorescent staining of the graft on day 7 confirmed a partial re-endothelialization of the vessels. The majority of cells settles in vessels that were located close to the pedicle, rather than in the periphery of the nerve. High amounts of collagen type IV and laminin were found where the cells occurred and also CD31 was observed, confirming the endothelial identity of the attached cells. Therefore, partial re-endothelialization of the vessels in the peripheral nerve ECMS was successful.

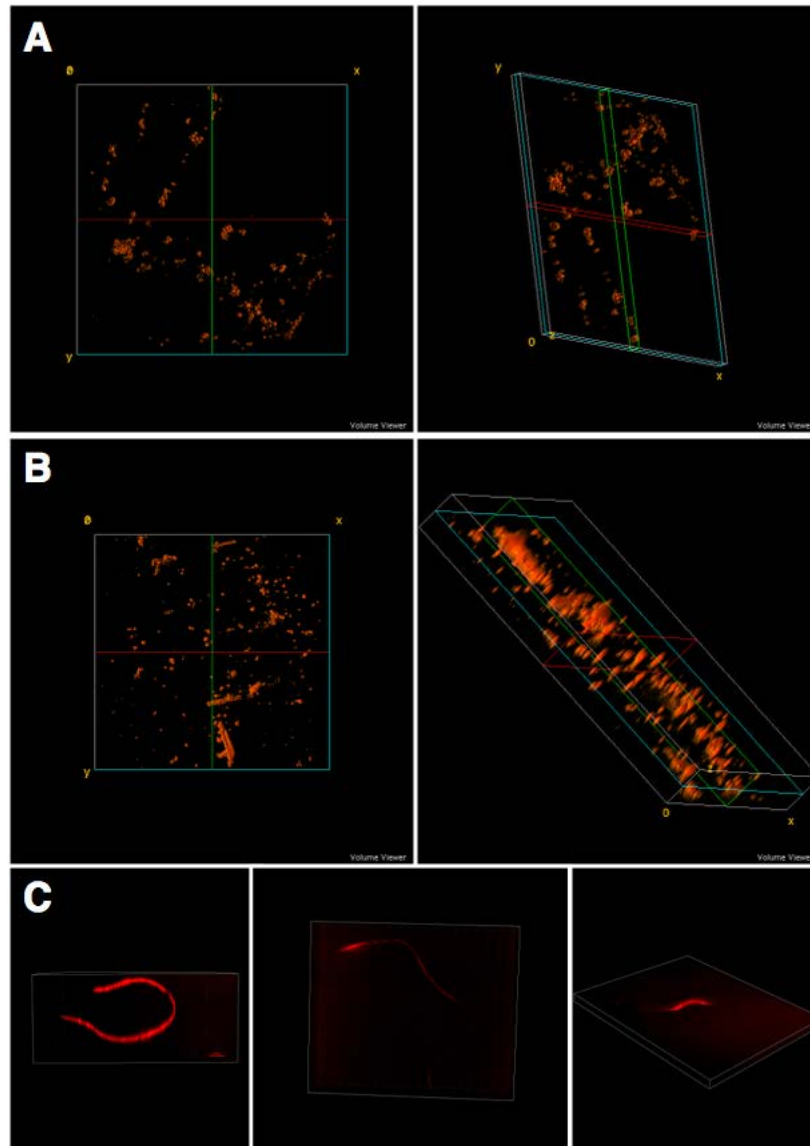


**Figure 28. Re-endothelialization of the vascular tree of the peripheral nerve ECMS.** *wtPAEC* were stained with PKH26 membrane labelling agent and seeded into the nerve ECMS under flow. Seeded cells were analyzed at different time points by spinning disk microscopy. **A) Day 0:** Representative images of seeded PAEC immediately after injection into the vascular tree. The left and the right picture are snapshots from the same 3D model, shown in different angles. **B) Day 1:** Representative images of seeded PAEC after 24 hours of cell culture under vascular flow. The cells had begun to adapt into their environment and started to show smoother cell surfaces, with formation of cell aggregates and groups. In the left snapshot of the 3D model, three elongated structures were visible. On the right snapshot of row B, the angle is different, and the structural vessel-like alignment of the cells can be anticipated. **C) Day 7:** Several vessel-shaped structures appeared in the nerve tissue suggesting the formation of a continuous endothelial cell layer in the recellularized ECMS.

## Immunofluorescent staining of re-endothelialized vessels

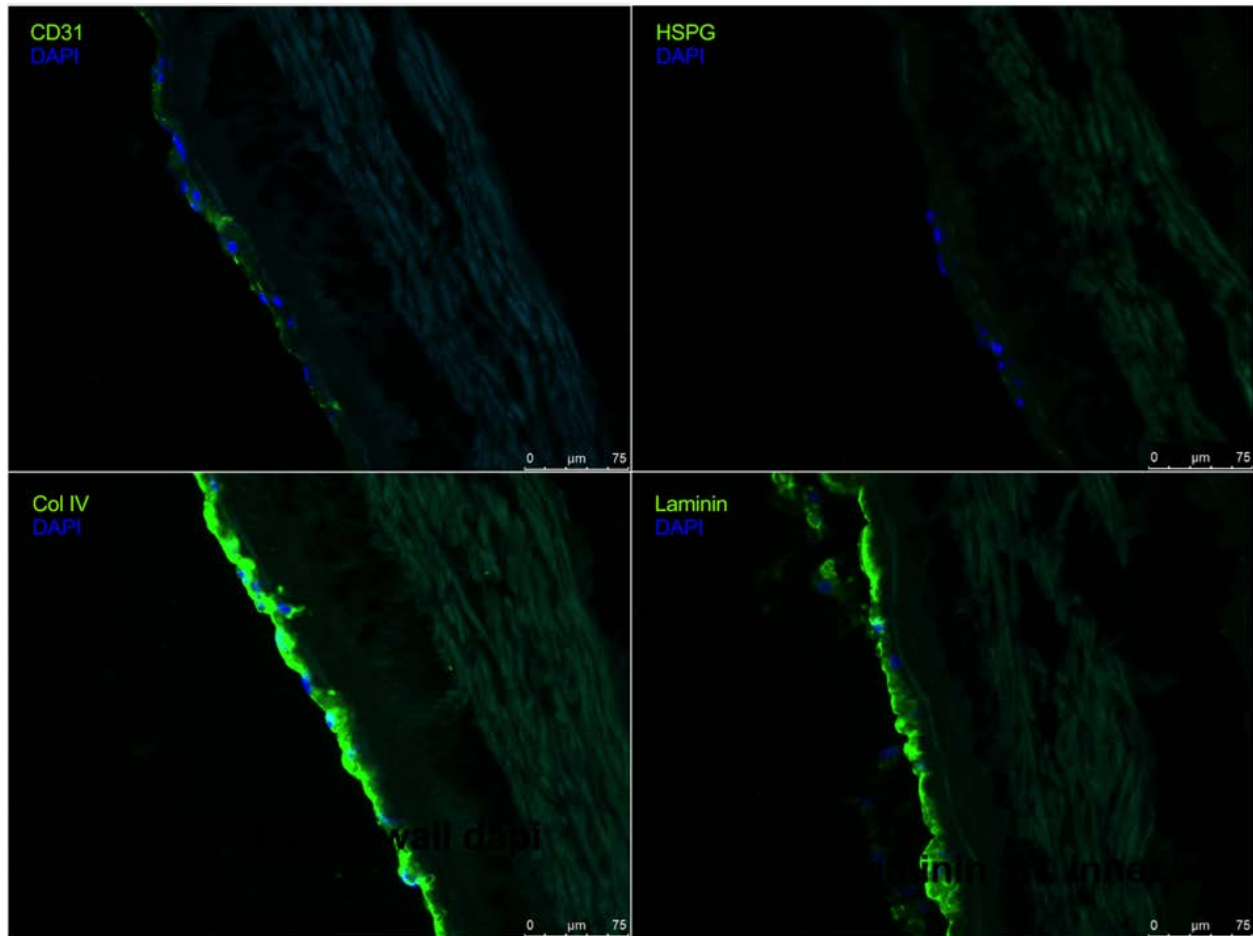


**Figure 29.** Immunofluorescence staining of CD31, HSPG, collagen type IV and laminin in the re-endothelialized vessels of the peripheral nerve ECMS. **Top left:** CD31 (green) staining was positive and co-located with cell nuclei (blue), confirming the endothelial phenotype of the settled cells. **Top right:** HSPG (green) staining was negative and no co-location with cell nuclei was found. **Bottom left:** collagen type IV (green) staining was strongly positive where cells had settled, more than in areas where no cells were found. **Bottom right:** Laminin (green) was highly positive in areas where cells were overserved, unlike elsewhere where no cells had been able to attach. Our data proved, that recellularization was successful in vessels that were in close proximity to the pedicle, however no re-endothelialized capillaries in the periphery of the nerve were observed (n=2).

## 6. Discussion

Tissue engineering is a promising approach to find less immunogenic alternatives for organ and VCA transplantation. However before it can be implemented into clinical application, the protocols for the generation and development of engineered organs, need to be adjusted and accredited thoroughly. This can be done only by careful evaluation of the decellularization protocol specifically designed for each organ, and a careful evaluation of the effects of the process on the integrity and molecular composition of the ECMS. This will allow for enhanced designing of graft conditioning and recellularization steps necessary before implantation.

In this thesis we characterized the ECMS of human vascularized composite grafts (i.e. ear and face) to better understand how different tissues respond to decellularization protocols, and what the molecular composition of the matrix in terms of cytokines and growth factors is. Our data suggest, that decellularized VCA scaffolds present distinct patterns of chemokine preservation in different types of tissues. Interestingly, preservation of proliferative cytokines was higher as compared to pro-inflammatory cytokines, in both grafts. These results will help to design recellularization protocols in the new era of vascularized composite tissue engineering.

Overall, our results raised several issues and limitations, that need to be discussed further. Therefore, in this part of the thesis, we will discuss the principal points raised by our study on engineered VCE.

## 6.1 Discussion of VCE results

### 6.1.1 Preservation of Cytokines after decellularization

In order to obtain information on the impact of the applied protocol on the biologic composition of the ECMS, we performed an extensive analysis of the cytokine levels. Our data showed that our perfusion decellularization protocol was able to decellularize the VCA grafts efficiently, and that all the analyzed tissues of the scaffolds had the capacity to retain cytokines and growth factors. The level of retention however, was dependent on the type of tissue, and to a minor extent, partially on the type of graft. Our study showed that cytokines of different function and nature are preserved to a measurable extent and therefore, contribute to the favorable characteristics VCA-ECMS. Overall, newly colonizing cells come across a cell-friendly environment, akin to physiologic conditions in the ECM. ECMS obtained via perfusion-decellularization are therefore very likely to increase the success rate of cell-reseeding.

### 6.1.2 Body parts show individual preservation patterns

We used two different ECMS, i.e. the ear and the face, to have a consistent idea on the obtained results of the vascularized composite grafts after. The highly significant retention of growth factors in the VCA-ECMS seems to be a promising characteristic for regrowing cells in the scaffold and hence promoting tissue regeneration. The original pattern of intrinsic biochemical cues of the ECMS potentially helps to increase identity of the tissues in a graft. In all three tissues of the ear ECMS, i.e. skin, fat and cartilage, growth factors were the most retained group of cytokines, followed by chemokines in skin and fat, and pro-inflammatory cytokines in cartilage, respectively. Cytokine retention levels in the face ECMS were generally lower but nevertheless, well detectable. According to cytokine retention levels, the applied perfusion decellularization protocol was very efficient, except for the fat tissue. This indicates, that not all tissues respond in the same way to perfusion decellularization and, that according to body part of origin, internal structures may vary. The composition and origin of the graft should therefore be considered when designing the experiment and maybe, an additional decellularization step for certain tissues might be necessary.

### 6.1.3 Analyzing different layers of the VCE

In the analysis, we focused on the response of different tissues in order to better understand how single layers of the graft responded to our TE approach. Our data confirmed that skin in our applied perfusion decellularization protocol is comparable between face and ear ECMS and that the outcome of cytokine retention levels in both cases is similar. Fat conversely, differs significantly from each other in ear and face ECMS after decellularization. The same applied for cartilage in ear and face ECMS. The reason for this dissimilar behavior in certain tissues might be due to the (lacking) vascularization according to different locations of the human body. Therefore, the distribution of the decellularizing agents is not exactly the same and the amounts of fluid to pass through the tissue may vary. Cartilage in its extreme case, shows very little to no vascularization at all and therefore, the influence of fluid accessibility and general motion (i.e. agitation) of the graft play an important role in the decellularization protocol. However, native versus decellularized samples did significantly differ in both face and ear ECMS confirming our perfusion protocol to successfully have affected cartilage. Nevertheless, this was not the case for fat tissue of face and ear ECMS and they showed an indifferent behavior from skin and cartilage.

Our analysis of cytokine retention levels was very systematic and thorough, and the cytokine retention patterns were well described between the different tissues. Such deep characterization and molecular understanding of VCE grafts is very innovative and a new approach to TE for transplantation grafts. Our data proved, that VCA-ECMS retain many cytokines that possibly could enhance regrowth of functional tissue. Therefore, the protocols could potentially be adjusted to favor retention of certain cytokine classes, enhancing the clinical outcome.

### 6.1.4 Coagulation associated factors in the ear ECMS

In order to extend the analytical range of VCE, we opted for a first insight on the effect of the applied perfusion decellularization protocol on the pro- and anti-coagulative status of the ECMS and performed a pilot analysis on the decellularized ear ECMS, assessing the expression of several pro- and anti-coagulation factors after decellularization. It has been shown that pro-coagulative factors like FGL-2 are associated with coagulation in transplanted grafts and that a deficiency of the FGL-2 can prolong graft survival<sup>145</sup>. Therefore, low levels of coagulation factors like FGL-2 and PAI-1 may be beneficial for ECMS, favoring the outcome of in vivo implantation by helping to decrease the risk of coagulation within the graft. On the other hand, some factors might be beneficial because their intrinsic function

is, to reduce or prevent coagulation. Our data showed a significant decrease of FGL-2 levels after decellularization (91.3% reduction). Moreover, soluble PAI-1 was cleared very efficiently with a low level of protein retention. tPA, HSPG and TF showed a slight signal increase in either the pre-detergent or the final decellularized group, which is attributed to higher background signals in the treated samples, as the tissue structure got slightly changed during the decellularization and cryosectioning process. tPA is a tissue-associated anti-coagulative protein found in proximity to endothelial cells. It reduces coagulation and has been found to decrease ischemic-related graft failures in liver transplantation<sup>146</sup>. Therefore, preservation of tPA may contribute to enhanced “smartness” of the ECMS and its retention may therefore be desirable. Our data showed tPA preservation of 82.5% after perfusion decellularization, which is a relatively high retention level, as compared to the general protein content decrease associated with the decellularization process. However, as many proteins exhibit pleiotropic functions in a living system, there are some potential down-sides of extended protein preservation. The level of TF was found to not be significantly influenced by decellularization. High retention levels of TF, for example, can lead to an increased risk of coagulation in the graft. However, on the other hand it also increases angiogenic activities and might lead to a better and faster vascularization of the graft, which can lead to a better healing and biologic acceptance. The exact function of each retained agent in an ECMS must therefore be carefully assessed in *in vivo* experiments. The dependence on the nature of the factor (e.g. tissue-bound or soluble), plays a major role in protein retention rates. For example, tPA which is a tissue-associated factor, presented a high percentage of retention (82.5%). ATIII and PAI-1 on the other hand, were shed away very efficiently, as they are soluble factors that are found in the plasma. Therefore, not only the function but also the location of the protein is important for retention of pro- and anti-coagulative proteins.

### 6.1.5 Limitations of the study

In order to understand the meaning of the cytokine retention levels, we divided the cytokines into three groups according to their functional activities (i.e. pro-inflammatory cytokines, chemokines and growth factors). However, due to the big pleiotropy of cytokines, it is difficult to anticipate the *in vivo* effect of each cytokine and their combinatory effects *in vivo*. It is a known fact, that cytokine expression patterns may vary upon certain triggers (e.g. infection<sup>147</sup>, autoimmune diseases<sup>148</sup>, cancer<sup>149</sup> etc.) and also, according to different locations in the body (e.g. different parts of the lymphatic system<sup>150</sup>) and different tissues<sup>151,152,153</sup>. For instance, it has been described, that IL-6 in the muscular tissue may lead to enhanced growth, therefore acting as growth factor rather than inflammatory agent<sup>154,151</sup>.

Both datasets, the ear and the face ECMS, have been published or submitted for publication. In this thesis, we mainly focused on the characterization of the cytokine content, and the presented results are only a part of the entire projects. More information about the studies can be found in the published works<sup>71,72</sup>.

## 6.2 Discussion of the engineered vascularized peripheral nerve ECMS

In the presence of significant peripheral nerve injuries with gaps of over 2-3 cm, tension-free anastomosis might not be practicable<sup>116</sup>. In such cases autologous nerve grafting is considered the gold standard although it comes at a high cost for the individual. Disadvantages like a second surgery with tissue loss, limited graft availability, donor site morbidity, scarcity and mismatching nerve morphologies can be restricting factors. Alternatively, autologous grafts can be modified and decellularized in order to engineer an acellular nerve graft, serving as regeneration conduit. Currently there is only one decellularized nerve product on the market (Avance<sup>®</sup> Nerve Graft, AxoGen). Studies with this decellularized nerve from cadaveric source demonstrated promising results for large nerve gaps of 2-3 cm<sup>132,133</sup> and calibers of over 5 mm<sup>134</sup>. Despite remarkable results, they still do not overcome the current limit of significant gaps (> 3 cm)<sup>132,133,134</sup>. However, in order to improve decellularized nerve allografts and the clinical outcome of the patients, we hypothesized, that an engineered allograft with re-endothelialized vasculature could help to ameliorate and speed up the healing process by distributing nutrients directly into the tissue. The importance of a good blood supply in nerve regeneration has been observed before<sup>137,138,139,140</sup>. It has been shown that the direct supply of nutrients and other important regenerative agents like oxygen is a key factor in nerve regeneration<sup>137,138</sup>. This could be achieved by direct anastomosis of recellularized vessels from the nerve graft to the recipient, rather than via passive vascularization from surrounding tissues.

Using TE protocols we designed and developed a new vascularized peripheral nerve ECMS for the repair of peripheral nerve injuries. We isolated, decellularized and re-endothelialized porcine vascularized peripheral nerves as a type of nerve conduits. In this model, the vascularization may provide an advantage for axonal outgrowth and nerve regeneration as compared to non-vascularized nerve conduits. In order to characterize our engineered vascularized peripheral nerve graft, we performed a variety of analysis that will be discussed in the following paragraphs.

### 6.2.1 Structural assessment

Macroscopic inspection revealed no significant differences in shape and size of the decellularized graft. However, the graft presented sponge-like characteristics after decellularization, originating from the fact, that the cell-empty graft had less structural stability and was behaving like a 3D mesh-network that had a higher capacity to retain water due to lack of connecting and filling components (i.e. cells) between the ECM molecules.

This phenomenon had been reported before in decellularized grafts and is of no complication for further procurement. As discussed earlier, perfusion decellularization protocols are a very gentle way to decellularize tissue grafts and to preserve their 3D structure. Our macroscopic, histologic and immunologic evaluations came to the same conclusion and a consistent preserved tissue architecture was achieved (macroscopically and microstructurally). The graft did not change its overall shape during decellularization and therefore, could potentially be applied to replace a missing structure in another individual. The microscopic structural similarity to native ECM on the other hand, indicates a potentially supporting environment for new nerve cells that could possibly grow along the axonal tunnels which were proven to be partially preserved.

### 6.2.2 Vasculature

Angiography and micro-CT of the decellularized nerve grafts showed that the vascular tree was very well preserved and remained perfusable, and intact small bifurcated vessels inside the nerve were observed. The maintenance of the microvasculature is a very important feature to the regenerative aspect of the scaffold; the capillaries reach deep into the endoneurium of the nerve tissue. This is where the separation zone of spontaneous regeneration and non-regeneration is located. On the one side, there is the triad of the basement membrane, the epithelium and the myelin sheath produced by the Schwann cells which is able to regenerate spontaneously after injury. Adjacent lies the stromal layer, also known as endoneurium which surrounds the nerve fascicles. The endoneurium in its turn is not capable of spontaneous regeneration<sup>120,121</sup>. This is where the here presented scaffolds might have an advantage over non-vascularized scaffolds. The regeneration of the nerve could naturally be nurtured by providing nutrients to the growing axons from proximal to distal, potentially even in the non-self-regenerative zone (endoneurium) where the capillaries end. Like this, the axonal growth is expected to be facilitated and the regeneration process to speed up, which overall might result in a better functional restoration.

### 6.2.3 Decellularization and DNA content

In order to be in consistency with the suggested guidelines by Crapo et. al<sup>36</sup> (see paragraph “Decellularization”), we performed immunofluorescence and H&E staining to confirm the absence of nuclei and quantified the DNA content of native and decellularized samples. Although the DNA levels were significantly reduced, the measured concentrations were above the suggested threshold of 50 ng/mg tissue in the decellularized samples ( $74.37 \pm 39.76$ , mean  $\pm$  SD). Therefore, a gelelectrophoresis was performed in order to

determine the length of the DNA fragments. As shown in figure 22C, the length did not majorly differ between native and decellularized DNA fragment samples, indicating, that some fragmented DNA and some complete cell nuclei must have been preserved in the tissue. By analyzing the microscopic pictures of the immunofluorescence and the histologic slide scans of the H&E staining we came to the conclusion, that a few nuclei of the outermost connective tissue layer of the graft were not entirely cleared out and remained in the ECMS as artifacts (figure 20 C, D). This is assumed to be due to an incoherent vascularization of the internal and external parts of the nerve. Hence, the external connective tissue was not directly perfused with decellularization agents and therefore, some nuclei remained resident in the ECMS. As discussed in the section of decellularizing technologies, in such a case, adding gentle agitation or friction during the decellularizing protocol could reduce nucleic acid retention in the superficial connective and epineural tissue.

#### **6.2.4 Preservation of nerve structures**

An observed decrease in collagen type IV and laminin levels of the basal lamina was likely due to the described structural changes occurred during decellularization. Overall, besides the lack of cellular components that were able to maintain the nerve structure, we observed very well-preserved collagen and laminin structures, confirming that the decellularization protocol did not affect the components of the extracellular matrix, that are responsible for the structural organization of the peripheral nerve. In agreement with this hypothesis there was no observed decrease of sGAG levels, another major ECM molecule class. Therefore, our data proved, that the molecular preservation of ECM molecules and the associated basal lamina was successfully provided in the applied perfusion decellularization protocol.

#### **6.2.5 Characterization of cytokine retention patterns**

In order to characterize the immunologic and regenerative abilities of the decellularized peripheral nerve ECMS, different cytokines, angiogenesis inducers and growth factors were analyzed. Two assays were carried out, a nerve growth factor specific and a homemade assay, that included pro-inflammatory cytokines, coagulation factors, angiogenic and two other proteins. The nerve factors were measured to be retained more abundantly than any other protein group, possibly due to the fact that the assay was specifically manufactured for nerve tissue. However, when comparing the different cytokine groups, no significant difference in expression levels could be detected. This was possibly due to the fact, that the number of the analytes within the groups was low (e.g. coagulation factors and “other proteins” each n=2). Therefore, a direct comparison between both 11plexes resulted in a

nonsignificant difference of preservation levels. Overall, the growth factors were the most retained cytokine group in the peripheral nerve ECMS, indicating an environment that might be very supportive for cellular growth and tissue regeneration. However, in order to find out about the biologic activity of the retained cytokines and to exclude the risk of growth factor associated diseases (i.e. cancer and uncontrolled tissue growth), this has to be further assessed by in vivo experiments.

### 6.2.6 Re-endothelialization

The settlement of the porcine aortic endothelial cells (PAEC) in the vascular structure of the decellularized peripheral nerve ECMS was observed to increase over the course of the culture of seven days under flow. Hence, it has been proven, that the environment of the engineered ECMS was not cytotoxic, as the cells survived for at least a week inside the scaffold. As the immunofluorescence staining confirmed, the PAECs begun to reshape their environment by secretion of new ECM molecules (collagen type IV and laminin) and hence, recreating their own niche. They maintained their endothelial phenotype, as confirmed by CD31 staining, and were able to form an incoherent endothelial cell layer within the round, vascular structures of the decellularized graft. However, this phenomenon was observed only in proximity to the vascular pedicle where the arterial inlet to the blood vessels was located. Therefore, it is assumed that the technique of cell introduction into the graft was not efficient enough to reach the distant vessels, and has potential to be refined. Nevertheless, our data proved that the re-endothelialization of the perfusion decellularized peripheral nerve ECMS is possible and therefore, potentially could increase the healing rate of gapped nerves while at the same time present enhanced functionality by provision of oxygen and nutrient supply. Therefore, the production of re-vascularized peripheral nerve ECMS is a promising candidate for successful therapy of peripheral nerve gaps of significant distances (>3 cm).

All the data from the re-endothelialized peripheral nerve development project were, at the time of writing this thesis, being processed in a manuscript and about to be submitted<sup>155</sup>.

## 7. Conclusion

Tissue engineering brings new approaches and possible solutions to medical, therapeutic and immunologic challenges that up to date, have not been solved. Nevertheless, the anatomical and functional complexity of VCE grafts represents the challenge that needs to be tackled in the near future. Conversely, simpler structures as the described ear and revascularized nerve scaffolds, could lead to successful application in the clinic within the next few years.

### 7.1 VCA experiments

Our results proved that the different tissues within the composite grafts presented distinct cytokine preservation patterns. This means, that each tissue, according to its characteristics (i.e. degree of vascularization, density etc.) responds differently to the decellularization protocol and some cytokine groups might be preserved better than others. Moreover, if grafts from different locations of the body are compared (i.e. ear vs. face), it becomes obvious that they respond differently to the perfusion decellularization protocol. Therefore, an exact protocol that is adjusted to each specific graft is needed. The decellularization process has to be tailor-made for each of the different VCA grafts, considering the composition of the tissues.

### 7.2 Peripheral nerve experiments

Our results showed a good maintenance of the vascular tree after decellularization, as well as vessel patency and perfusability. Moreover, growth factors and angiogenic proteins were very well preserved and partial re-endothelialization was achieved. Therefore, we conclude that it is possible to engineer re-endothelialized decellularized nerve grafts in order to bridge significant peripheral nerve gaps.

Hitherto existing decellularized peripheral nerve scaffolds do not show any internal vascularization and rely completely on passive revascularization from the surrounding tissue, that is limited to approximately 10 mm in depth. Therefore, our engineered re-endothelialized peripheral nerve have a potential advantage over the hitherto existing standard treatment, that might have a crucial impact on improved therapy outcome. Hence, it is very important to investigate further on the creation of such grafts.

## 8. Outlook

### 8.1 Vascularized composite engineering

VCE present several future challenges such as the selection of the right cell types and the establishment of protocols for cell culturing according to type of tissue, their location and function in the ECMS. As VCE grafts are composed of many different types of tissues, a lot of work will be required to establish protocols that successfully grow composed body parts in a bioreactor. Several protocols will have to be tested and additionally, different approaches will have to be evaluated (e.g. growing different cell types in a full VCA-ECMS versus growing cell layers with subsequent assembly of the produced tissue layers into the VCE) Moreover, further investigation on a molecular level, for example like the above analyzed coagulation proteins, have to be intensified in order to improve the biologic characterization of VCE. Furthermore, it is very important to have a precise knowledge of the graft, starting from the molecular composition and biologic compatibility and ending in functional and aesthetic outcome after implantation. In order to create competitive alternatives to modern standard treatments, it is very important to have an exact characterization of engineered grafts. Moreover, basic tissue and developmental research questions will have to be addressed. How does communication between tissues work? How can we apply functionality to a multilayers graft? And how could we possibly upscale the whole process, in order to make it available to the public?

Therefore, success of engineered grafts is depending very much on the type of tissue, structure and function that they have to replace. As body parts have different purposes and present varying levels of complexity, the TE challenges vary along with the graft's complexity. For clinical application it is crucial to understand the biologic interaction of the graft with the recipient and if the overall outcome is improved when compared to traditional therapies. Hence, biocompatibility studies should be implemented in the future, too.

### 8.2 Peripheral nerve engineering

For the future of the engineered vascularized nerve experiments, it is crucial to not only characterize the molecular composition, but also to find an efficient protocol for re-endothelialization. Overcoming the peripheral recellularization barrier is crucial for nerve scaffolds that are created for replenish large gaps. Therefore, a precise standardized protocol for the nerve surgery (graft acquisition) as well as the recellularization processed should be established. Furthermore, biologic compatibility should be investigated in an animal model

and clinical outcomes as well as the ability of tissue restoration and function of re-vascularized versus non-vascularized decellularized peripheral nerve ECMS should be compared. This would bring the project “engineered revascularized decellularized peripheral nerve graft” a step further towards a successful application in human patients.

In terms of the simple structured engineered grafts (e.g. peripheral nerves, auricles, vessels, bladders etc.) clinical application might become real in the near future. Such grafts have already been used in clinical first in human studies and have shown promising results. The main focus should therefore be concentrating on establishing a sustainable upscaling of the whole graft production process, in order to make the grafts accessible to the clinical application.

## 9. References

1. Skalak, R. Richard Skalak Institute for Biomedical Engineering. 1112–1113
2. Vacanti, C. A. The history of tissue engineering. *J. Cell. Mol. Med.* 10, 569–576 (2006).
3. Mason, C. & Dunnill, P. A brief definition of regenerative medicine. *Regen. Med.* 3, 1–5 (2008).
4. Kefalopoulou, Z., Politis, M., Piccini, P. & al, et. Long-term clinical outcome of fetal cell transplantation for parkinson disease: Two case reports. *JAMA Neurol.* 71, 83–87 (2014).
5. Agency, E. medicines. EPAR: Holoclar. 44, 0–2 (2015).
6. Bakker, A. C. & Langer, B. Zelltherapeutika – eine innovative Therapieoption in der Ophthalmologie: Stammzellen zur Behandlung von Hornhauterkrankungen. *Bundesgesundheitsblatt - Gesundheitsforsch. - Gesundheitsschutz* 58, 1259–1264 (2015).
7. Carrel, A. & Lindbergh, C. A. The Culture of Whole Organs. *Science (80-. )*. 81, 621 LP-623 (1935).
8. Nobel prize. The Nobel Prize in Physiology or Medicine 1912: Alexis Carrel. 15–16 (2013).
9. Green, W. T. J. Articular cartilage repair. Behavior of rabbit chondrocytes during tissue culture and subsequent allografting. *Clin. Orthop. Relat. Res.* 237–250 (1977).
10. Burke, J. F., Yannas, I. V., Quinby, W. C. J., Bondoc, C. C. & Jung, W. K. Successful use of a physiologically acceptable artificial skin in the treatment of extensive burn injury. *Ann. Surg.* 194, 413–428 (1981).
11. Bell, E. *et al.* The Reconstitution of Living Skin. *Journal of Investigative Dermatology* 81, S2–S10 (1983).
12. Vacanti, J. P. *et al.* Selective cell transplantation using bioabsorbable artificial polymers as matrices. *J. Pediatr. Surg.* 23, 3–9 (1988).
13. Vacanti, J. P. Beyond Transplantation: Third Annual Samuel Jason Mixter Lecture. *Arch. Surg.* 123, 545–549 (1988).
14. Cao, Y., Vacanti, J. P., Paige, K. T., Upton, J. & Vacanti, C. A. Transplantation of chondrocytes utilizing a polymer-cell construct to produce tissue-engineered cartilage in the shape of a human ear. *Plastic and Reconstructive Surgery* 100, 297–304 (1997).
15. Crapo, P. M., Gilbert, T. W. & Badylak, S. F. An overview of tissue and whole organ decellularization processes. *Biomaterials* 32, 3233–3243 (2011).
16. Özbek, S., Balasubramanian, P. G., Chiquet-Ehrismann, R., Tucker, R. P. & Adams, J. C. The Evolution of Extracellular Matrix. *Molecular Biology of the Cell* 21, 4300–4305 (2010).
17. Daley, W. P., Peters, S. B. & Larsen, M. Extracellular matrix dynamics in development and regenerative medicine. *J. Cell Sci.* 121, 255–264 (2008).
18. Nelson, C. M. *et al.* Of Extracellular Matrix, Scaffolds, and Signaling: Tissue Architecture Regulates Development, Homeostasis and Cancer. *J. Phys.* 22, 16–19 (2010).
19. Barkan, D., Green, J. E. & Chambers, A. F. Extracellular matrix: A gatekeeper in the transition from dormancy to metastatic growth. *Eur. J. Cancer* 46, 1181–1188 (2010).
20. Vorotnikova, E. *et al.* Extracellular matrix-derived products modulate endothelial and progenitor cell migration and proliferation in vitro and stimulate regenerative healing in vivo. *Matrix Biol.* 29, 690–700 (2010).

21. Bedore, J., Leask, A. & Séguin, C. A. Targeting the extracellular matrix: Matricellular proteins regulate cell-extracellular matrix communication within distinct niches of the intervertebral disc. *Matrix Biol.* 37, 124–130 (2014).
22. Biology, V., Opinion, C. & Biology, C. Matricellular proteins : extracellular modulators of cell function Paul Bornstein and E Helene Sage. 608–616
23. Mecham, R. P. Overview of extracellular matrix. *Curr. Protoc. cell Biol.* Chapter 10, Unit 10.1 (2001).
24. Streuli, C. Extracellular matrix remodelling and cellular differentiation. *Curr. Opin. Cell Biol.* 11, 634–640 (1999).
25. Mouw, J. K., Ou, G. & Weaver, V. M. Extracellular matrix assembly: a multiscale deconstruction. *Nat. Rev. Mol. Cell Biol.* 15, 771–785 (2014).
26. Schaefer, L. & Schaefer, R. M. Proteoglycans: from structural compounds to signaling molecules. *Cell Tissue Res.* 339, 237–246 (2010).
27. Pankov, R. & Yamada, K. M. Fibronectin at a glance. *J. Cell Sci.* 115, 3861–3863 (2002).
28. Yurchenco, P. D., Smirnov, S. & Matus, T. Analysis of basement membrane self-assembly and cellular interactions with native and recombinant glycoproteins. *Methods Cell Biol.* 69, 111–144 (2002).
29. Frantz, C., Stewart, K. M. & Weaver, V. M. The extracellular matrix at a glance. *J. Cell Sci.* 123, 4195–4200 (2010).
30. Gordon, M. K. & Hahn, R. A. Collagens. *Cell Tissue Res.* 339, 247–257 (2010).
31. Szpak, P. Fish bone chemistry and ultrastructure: implications for taphonomy and stable isotope analysis. *J. Archaeol. Sci.* 38, 3358–3372 (2011).
32. Gershlak, J. R. *et al.* Crossing kingdoms: Using decellularized plants as perfusable tissue engineering scaffolds. *Biomaterials* 125, 13–22 (2017).
33. Levenberg, S. *et al.* Engineering vascularized skeletal muscle tissue. *Nat. Biotechnol.* 23, 879–884 (2005).
34. Wanjare, M., Kusuma, S. & Gerecht, S. Perivascular cells in blood vessel regeneration. *Biotechnol. J.* 8, 434–447 (2013).
35. Jain, R. K., Au, P., Tam, J., Duda, D. G. & Fukumura, D. Engineering vascularized tissue. *Nat. Biotechnol.* 23, 821–823 (2005).
36. Crapo, P. M., Gilbert, T. W. & Badylak, S. F. An overview of tissue and whole organ decellularization processes. *Biomaterials* 32, 3233–3243 (2011).
37. Gallie, W. E. The use of boiled bone in operative surgery. *JBJS* s2-16, (1918).
38. Wilson, P. D. Experiences with a bone bank. *Ann. Surg.* 126, 932–946 (1947).
39. Matsumoto, T. *et al.* A study of inverted intestinal graft in the major veins. *Angiology* 17, 842–850 (1966).
40. Herberhold, C., Franz, B. & Breipohl, W. Chemisch-konservierte menschliche Trachea als Prothesenmaterial zur Deckung trachealer Defekte\* TT - Chemical-conserved Human Trachea as Prosthesis in Covering Tracheal Defects - First Experiences. *Laryngo-Rhino-Otol* 59, 453–457 (1980).
41. Macchiarini, P. *et al.* Clinical transplantation of a tissue-engineered airway. *Lancet* 372, 2023–2030 (2008).
42. Chen, F., Yoo, J. J. & Atala, A. Acellular collagen matrix as a possible ‘off the shelf’ biomaterial for urethral repair. *Urology* 54, 407–410 (1999).
43. Sutherland, R. S., Baskin, L. S., Hayward, S. W. & Cunha, G. R. Regeneration of Bladder Urothelium, Smooth

- Muscle, Blood Vessels and Nerves Into an Acellular Tissue Matrix. *J. Urol.* 156, 571–577 (1996).
44. Ott, H. C. *et al.* Perfusion-decellularized matrix: using nature's platform to engineer a bioartificial heart. *Nat. Med.* 14, 213–221 (2008).
  45. Bioreactor. *IUPAC Compend. Chem. Terminol.* 143, 2014 (2014).
  46. Meyer, S. R. *et al.* Comparison of aortic valve allograft decellularization techniques in the rat. *J. Biomed. Mater. Res. A* 79, 254–262 (2006).
  47. Yang, B. *et al.* Development of a Porcine Bladder Acellular Matrix with Well-Preserved Extracellular Bioactive Factors for Tissue Engineering. *Tissue Eng. Part C Methods* 16, 1201–1211 (2010).
  48. Petersen, T. H. *et al.* Tissue-engineered lungs for in vivo implantation. *Science* 329, 538–541 (2010).
  49. Lundy, S., Hu, C. Y., Lee, K., Schmidt, C. E. & Ph, D. and Supports Regeneration. *Tissue Eng.* 10, (2004).
  50. Hodde, J. *et al.* Effects of sterilization on an extracellular matrix scaffold: Part I. Composition and matrix architecture. *J. Mater. Sci. Mater. Med.* 18, 537–543 (2007).
  51. Gilbert, T. W. *et al.* Collagen fiber alignment and biaxial mechanical behavior of porcine urinary bladder derived extracellular matrix. *Biomaterials* 29, 4775–4782 (2008).
  52. Dong, X. *et al.* RGD-modified acellular bovine pericardium as a bioprosthetic scaffold for tissue engineering. *J. Mater. Sci. Mater. Med.* 20, 2327–2336 (2009).
  53. Reing, J. E. *et al.* The effects of processing methods upon mechanical and biologic properties of porcine dermal extracellular matrix scaffolds. *Biomaterials* 31, 8626–8633 (2010).
  54. Xu, C. C., Chan, R. W. & Tirunagari, N. A biodegradable, acellular xenogeneic scaffold for regeneration of the vocal fold lamina propria. *Tissue Eng.* 13, 551–566 (2007).
  55. Brown, B. N. *et al.* Comparison of Three Methods for the Derivation of a Biologic Scaffold Composed of Adipose Tissue Extracellular Matrix. *Tissue Eng. Part C Methods* 17, 411–421 (2011).
  56. Flynn, L. E. The use of decellularized adipose tissue to provide an inductive microenvironment for the adipogenic differentiation of human adipose-derived stem cells. *Biomaterials* 31, 4715–4724 (2010).
  57. Grauss, R. W. *et al.* Histological evaluation of decellularised porcine aortic valves: matrix changes due to different decellularisation methods. *Eur. J. Cardiothorac. Surg.* 27, 566–571 (2005).
  58. Yang, M., Chen, C.-Z., Wang, X.-N., Zhu, Y.-B. & Gu, Y. J. Favorable effects of the detergent and enzyme extraction method for preparing decellularized bovine pericardium scaffold for tissue engineered heart valves. *J. Biomed. Mater. Res. B. Appl. Biomater.* 91, 354–361 (2009).
  59. Xu, H. *et al.* Host response to human acellular dermal matrix transplantation in a primate model of abdominal wall repair. *Tissue Eng. Part A* 14, 2009–2019 (2008).
  60. Gillies, A. R., Smith, L. R., Lieber, R. L. & Varghese, S. Method for decellularizing skeletal muscle without detergents or proteolytic enzymes. *Tissue Eng. Part C. Methods* 17, 383–389 (2011).
  61. Jackson, D. W. *et al.* The effects of processing techniques on the mechanical properties of bone-anterior cruciate ligament-bone allografts. An experimental study in goats. *Am. J. Sports Med.* 16, 101–105 (1988).
  62. Elder, B. D., Kim, D. H. & Athanasiou, K. A. Developing an articular cartilage decellularization process toward facet joint cartilage replacement. *Neurosurgery* 66, 722–7; discussion 727 (2010).
  63. Hopkinson, A. *et al.* Optimization of amniotic membrane (AM) denuding for tissue engineering. *Tissue Eng.*

- Part C. Methods* 14, 371–381 (2008).
64. Azhim, A. *et al.* Preparation of decellularized meniscal scaffolds using sonication treatment for tissue engineering. *Conf. Proc. ... Annu. Int. Conf. IEEE Eng. Med. Biol. Soc. IEEE Eng. Med. Biol. Soc. Annu. Conf.* 2013, 6953–6956 (2013).
  65. Phillips, M., Maor, E. & Rubinsky, B. Nonthermal irreversible electroporation for tissue decellularization. *J. Biomech. Eng.* 132, 91003 (2010).
  66. Wang, Y. *et al.* Recent Advances in Decellularization and Recellularization for Tissue-Engineered Liver Grafts. *Cells Tissues Organs* 204, 125–136 (2017).
  67. Fu, R. H. *et al.* Decellularization and recellularization technologies in tissue engineering. *Cell Transplant.* 23, 621–630 (2014).
  68. Wainwright, J. M. *et al.* Preparation of cardiac extracellular matrix from an intact porcine heart. *Tissue Eng. Part C. Methods* 16, 525–532 (2010).
  69. Uygun, B. E. *et al.* Organ reengineering through development of a transplantable recellularized liver graft using decellularized liver matrix. *Nat. Med.* 16, 814–820 (2010).
  70. Liu, C. *et al.* [Preparation of whole-kidney acellular matrix in rats by perfusion]. *Nan Fang Yi Ke Da Xue Xue Bao* 29, 979–982 (2009).
  71. Duisit, J. *et al.* Bioengineering a Human Face Graft. *Ann. Surg.* XX, 1 (2017).
  72. Duisit, J. Perfusion-decellularization of human ear grafts enables ECM-based scaffolds for auricular vascularized composite tissue engineering. (2018).
  73. Sawada, K., Terada, D., Yamaoka, T., Kitamura, S. & Fujisato, T. Cell removal with supercritical carbon dioxide for acellular artificial tissue. *J. Chem. Technol. Biotechnol.* 83, 943–949 (2008).
  74. Lehr, E. J. *et al.* Decellularization reduces immunogenicity of sheep pulmonary artery vascular patches. *J. Thorac. Cardiovasc. Surg.* 141, 1056–1062 (2011).
  75. Woods, T. & Gratzer, P. F. Effectiveness of three extraction techniques in the development of a decellularized bone-anterior cruciate ligament-bone graft. *Biomaterials* 26, 7339–7349 (2005).
  76. Mardhiyah, A., Sha'ban, M. & Azhim, A. Evaluation of histological and biomechanical properties on engineered meniscus tissues using sonication decellularization. in *2017 39th Annual International Conference of the IEEE Engineering in Medicine and Biology Society (EMBC)* 2064–2067 (2017). doi:10.1109/EMBC.2017.8037259
  77. Stern, M. M. *et al.* The influence of extracellular matrix derived from skeletal muscle tissue on the proliferation and differentiation of myogenic progenitor cells *ex vivo*. *Biomaterials* 30, 2393–2399 (2009).
  78. Karabekmez, F. E., Duymaz, A. & Moran, S. L. Early clinical outcomes with the use of decellularized nerve allograft for repair of sensory defects within the hand. *Hand* 4, 245–249 (2009).
  79. Kim, J. K., Koh, Y. Do, Kim, J. O. & Seo, D. H. Development of a decellularization method to produce nerve allografts using less invasive detergents and hyper/hypotonic solutions. *J. Plast. Reconstr. Aesthetic Surg.* 69, 1690–1696 (2016).
  80. Guo, S.-Z., Ren, X.-J., Wu, B. & Jiang, T. Preparation of the acellular scaffold of the spinal cord and the study of biocompatibility. *Spinal Cord* 48, 576–581 (2010).
  81. Ozeki, M. *et al.* Evaluation of decellularized esophagus as a scaffold for cultured esophageal epithelial cells. *J. Biomed. Mater. Res. Part A* 79A, 771–778 (2006).

82. Atala, A. Future perspectives in reconstructive surgery using tissue engineering. *Urol. Clin. North Am.* 26, 157–65, ix–x (1999).
83. Atala, A. Tissue engineering of human bladder. *Br. Med. Bull.* 97, 81–104 (2011).
84. Kates, M. *et al.* Tissue-engineered urinary conduits. *Curr. Urol. Rep.* 16, 8 (2015).
85. Patterson, J. T. Tissue-engineered vascular grafts for use in the treatment of congenital heart disease: from the bench to the clinic and back again. 7, 409–419 (2012).
86. Koç, O. N. & Gerson, S. L. Akt helps stem cells heal the heart. *Nat. Med.* 9, 1109–1110 (2003).
87. Arslan-Yildiz, A. *et al.* Towards artificial tissue models: past, present, and future of 3D bioprinting. *Biofabrication* 8, 14103 (2016).
88. Murphy, S. V & Atala, A. 3D bioprinting of tissues and organs. *Nat. Biotechnol.* 32, 773–785 (2014).
89. Munarin, F. *et al.* Pectin-based injectable biomaterials for bone tissue engineering. *Biomacromolecules* 12, 568–577 (2011).
90. Czaja, W., Krystynowicz, A., Bielecki, S. & Brown, R. M. Microbial cellulose--the natural power to heal wounds. *Biomaterials* 27, 145–151 (2006).
91. Ferreira, L. M., Sobral, C. S., Blanes, L., Ipolito, M. Z. & Horibe, E. K. Proliferation of fibroblasts cultured on a hemi-cellulose dressing. *J. Plast. Reconstr. Aesthet. Surg.* 63, 865–869 (2010).
92. Modulevsky, D. J., Lefebvre, C., Haase, K., Al-Rekabi, Z. & Pelling, A. E. Apple derived cellulose scaffolds for 3D mammalian cell culture. *PLoS One* 9, (2014).
93. Modulevsky, D. J., Cuerrier, C. M. & Pelling, A. E. Biocompatibility of Subcutaneously Implanted Plant-Derived Cellulose Biomaterials. *PLoS One* 11, 1–19 (2016).
94. Cui, F.-Z. & Mikos, A. G. Important Topics in the Future of Tissue Engineering: Comments from the participants of the 5th International Conference on Tissue Engineering at Kos, Greece. *Regenerative Biomaterials* 1, 103–106 (2014).
95. Molitor, M. Transplantation of Vascularized Composite Allografts. Review of Current Knowledge. *Acta Chir. Plast.* 58, 18–28
96. Petruzzo, P., Sardu, C., Lanzetta, M. & Dubernard, J. M. Report ( 2017 ) of the International Registry on Hand and Composite Tissue Allotransplantation ( IRHCTT ). 294–303 (2017).
97. Shores, J. T., Brandacher, G. & Lee, W. P. A. Hand and upper extremity transplantation: an update of outcomes in the worldwide experience. *Plast. Reconstr. Surg.* 135, 351e–60e (2015).
98. Salminger, S. *et al.* Functional and psychosocial outcomes of hand transplantation compared with prosthetic fitting in below-elbow amputees: A multicenter cohort study. *PLoS One* 11, 1–13 (2016).
99. Biddiss, E. A. & Chau, T. T. Upper limb prosthesis use and abandonment: a survey of the last 25 years. *Prosthet. Orthot. Int.* 31, 236–257 (2007).
100. Gaetz, W. *et al.* Massive cortical reorganization is reversible following bilateral transplants of the hands: Evidence from the first successful bilateral pediatric hand transplant patient. *Ann. Clin. Transl. Neurol.* (2017). doi:10.1002/acn3.501
101. McDiarmid, S. V., Levin, L. S. & Luskin, R. S. Vascularized Composite Tissue Allografts (VCA): the Policy Side. *Curr. Transplant. Reports* 3, 50–56 (2016).

102. Kueckelhaus, M. *et al.* Vascularized composite allotransplantation: current standards and novel approaches to prevent acute rejection and chronic allograft deterioration. *Transpl. Int.* 29, 655–662 (2016).
103. Fischer, S. *et al.* Acute rejection in vascularized composite allotransplantation. *Curr. Opin. Organ Transplant.* 19, 531–544 (2014).
104. Kaufman, C. L. *et al.* Monitoring and long-term outcomes in vascularized composite allotransplantation. *Curr. Opin. Organ Transplant.* 18, 652–658 (2013).
105. Weissenbacher, A. *et al.* Antibody-mediated rejection in hand transplantation. *Transpl. Int.* 27, 13–17 (2014).
106. Chandraker, A. *et al.* The management of antibody-mediated rejection in the first presensitized recipient of a full-face allotransplant. *Am. J. Transplant* 14, 1446–1452 (2014).
107. Petruzzo, P. *et al.* Long-term follow-up in composite tissue allotransplantation: In-depth study of five (hand and face) recipients. *Am. J. Transplant.* 11, 808–816 (2011).
108. Lian, C. G. *et al.* Biomarker evaluation of face transplant rejection: Association of donor T cells with target cell injury. *Mod. Pathol.* 27, 788–799 (2014).
109. Schön, M. R. *et al.* Liver Transplantation After Organ Preservation With Normothermic Extracorporeal Perfusion. *Annals of Surgery* 233, 114–123 (2001).
110. Vallabhajosyula, P. *et al.* Tissue-specific exosome biomarkers for noninvasively monitoring immunologic rejection of transplanted tissue. *J. Clin. Invest.* 127, 1375–1391 (2017).
111. Bueno, E. M. *et al.* Vascularized composite allotransplantation and tissue engineering. *J. Craniofac. Surg.* 24, 256–263 (2013).
112. Davis, G. & Curtin, C. M. Management of Pain in Complex Nerve Injuries. 32, 2016 (2016).
113. Wilson, A. D. H., Hart, A., Brannstrom, T., Wiberg, M. & Terenghi, G. Primary sensory neuronal rescue with systemic acetyl-L-carnitine following peripheral axotomy. A dose-response analysis. *Br. J. Plast. Surg.* 56, 732–739 (2003).
114. Pollins, A. C., Kim, J. S., Boyer, R. B. & Thayer, W. P. Mass spectrometry comparison of nerve allograft decellularization processes. *J. Mater. Sci. Mater. Med.* 28, (2017).
115. Biazar, E., Keshel, S. H., Sahebalzamani, A. & Heidari, M. Design of Oriented Porous PHBV Scaffold as a Neural Guide. *Int. J. Polym. Mater. Polym. Biomater.* 63, 753–757 (2014).
116. Panagopoulos, G. N., Megaloikonomos, P. D. & Mavrogenis, A. F. The Present and Future for Peripheral Nerve Regeneration. *Orthopedics* 40, e141–e156 (2017).
117. Siemionow, M. & Sonmez, E. Nerve Allograft Transplantation: A Review. *J reconstr Microsurg* 23, 511–520 (2007).
118. Gao, Y. *et al.* Nerve autografts and tissue-engineered materials for the repair of peripheral nerve injuries: a 5-year bibliometric analysis. *Neural Regen. Res.* 10, 1003 (2015).
119. Chamberlain, L. J. Influence of Implant Parameters on the Mechanisms of Peripheral Nerve Regeneration. (1998).
120. Yannas, I. V. Tissue and Organ Regeneration in Adults. *Saudi Med J* 33, 3–8 (2015).
121. Chamberlain, L. J., Yannas, I. V., Hsu, H. P., Strichartz, G. & Spector, M. Collagen-GAG substrate enhances the quality of nerve regeneration through collagen tubes up to level of autograft. *Exp. Neurol.* 154, 315–329 (1998).

122. Archibald, S. J., Shefner, J., Krarup, C. & Madison, R. D. Monkey median nerve repaired by nerve graft or collagen nerve guide tube. *J. Neurosci.* 15, 4109–4123 (1995).
123. Fawcett, J. W. & Keynes, R. J. Peripheral Nerve Regeneration. *Annu. Rev. Neurosci.* 13, 43–60 (1990).
124. Madison, R. D., da Silva, C., Dikkes, P., Sidman, R. L. & Chiu, T. H. Peripheral nerve regeneration with entubulation repair: comparison of biodegradable nerve guides versus polyethylene tubes and the effects of a laminin-containing gel. *Exp. Neurol.* 95, 378–390 (1987).
125. Madison, R. D., Da Silva, C. F. & Dikkes, P. Entubulation repair with protein additives increases the maximum nerve gap distance successfully bridged with tubular prostheses. *Brain Res.* 447, 325–334 (1988).
126. Bailey, S. B., Eichler, M. E., Villadiego, A. & Rich, K. M. The influence of fibronectin and laminin during Schwann cell migration and peripheral nerve regeneration through silicon chambers. *J. Neurocytol.* 22, 176–184 (1993).
127. Bryan, D. J., Miller, R. A., Costas, P. D., Wang, K. K. & Seckel, B. R. Immunocytochemistry of skeletal muscle basal lamina grafts in nerve regeneration. *Plast. Reconstr. Surg.* 92, 927–940 (1993).
128. Ohbayashi, K. *et al.* Peripheral nerve regeneration in a silicone tube: effect of collagen sponge prosthesis, laminin, and pyrimidine compound administration. *Neurol. Med. Chir. (Tokyo).* 36, 428–433 (1996).
129. Yannas, I. V. Facts and theories of induced organ regeneration. *Adv. Biochem. Eng. Biotechnol.* 93, 1–38 (2005).
130. Harley, B. A. *et al.* Optimal degradation rate for collagen chambers used for regeneration of peripheral nerves over long gaps. *Cells. Tissues. Organs* 176, 153–165 (2004).
131. Hussey, G. S., Keane, T. J. & Badylak, S. F. The extracellular matrix of the gastrointestinal tract: a regenerative medicine platform. *Nat. Rev. Gastroenterol. & Hepatol.* 14, 540 (2017).
132. Rinker, B. *et al.* Use of Processed Nerve Allografts to Repair Nerve Injuries Greater Than 25 mm in the Hand. *Ann. Plast. Surg.* 78, S292–S295 (2017).
133. Justicia, J. *et al.* To print this article, please use the print button in the bottom toolbar of the web reader. *J. Clin. Nurs.* 19, 3274–3290 (2004).
134. Isaacs, J. & Safa, B. A Preliminary Assessment of the Utility of Large-Caliber Processed Nerve Allografts for the Repair of Upper Extremity Nerve Injuries. *HAND* 12, 55–59 (2016).
135. Liu, G., Jin, Y., Zhang, Q. & Li, R. Peripheral nerve repair: a hot spot analysis on treatment methods from 2010 to 2014. *Neural Regen. Res.* 10, 996 (2015).
136. Ray, W. Z. & Mackinnon, S. E. Management of nerve gaps: Autografts, allografts, nerve transfers, and end-to-side neurorrhaphy. *Experimental neurology* 223, 77–85 (2010).
137. Terzis, J. K. & Kostopoulos, V. K. Vascularized nerve grafts and vascularized fascia for upper extremity nerve reconstruction. *Hand* 5, 19–30 (2010).
138. Terzis, J. K., Skoulis, T. G. & Soucacos, P. N. Vascularized nerve grafts. A review. *Int. Angiol.* 14, 264–277 (1995).
139. Griffin, J. W., Hogan, M. V., Chhabra, A. B. & Deal, D. N. Peripheral Nerve Repair and Reconstruction. *J. Bone Jt. Surg.* 95, 2144–2151 (2013).
140. Kline, D. G. Nerve Surgery as It Is Now and as It May Be. *Neurosurgery* 46, 1285 (2000).
141. Scarrit, M. E. A review of cellularization strategies for tissue engineering of whole organs. *Front. Bioeng. Biotechnol.* 3, 1–17 (2015).
142. Bongoni, A. K., Lanz, J., Rieben, R. & Banz, Y. Development of a bead-based multiplex assay for the simultaneous

- detection of porcine inflammation markers using xMAP technology. *Cytom. Part A* 83, 636–647 (2013).
143. Lertkiatmongkol, P., Liao, D., Mei, H., Hu, Y. & Newman, P. J. Endothelial functions of platelet/endothelial cell adhesion molecule-1 (CD31). *Curr. Opin. Hematol.* 23, 253–259 (2016).
  144. Sarrazin, S., Lamanna, W. C. & Esko, J. D. Heparan Sulfate Proteoglycans. *Cold Spring Harbor Perspectives in Biology* 3, (2011).
  145. Ning, Q. *et al.* Role of fibrinogen-like protein 2 prothrombinase/fibrinolytic in experimental and human allograft rejection. *J. Immunol.* 174, 7403–7411 (2005).
  146. Hashimoto, K. *et al.* Use of tissue plasminogen activator in liver transplantation from donation after cardiac death donors. *Am. J. Transplant* 10, 2665–2672 (2010).
  147. Puren, A. J., Feldman, C., Savage, N., Becker, P. J. & Smith, C. Patterns of cytokine expression in community-acquired pneumonia. *Chest* 107, 1342–1349 (1995).
  148. Kunz, M. & Ibrahim, S. M. Cytokines and cytokine profiles in human autoimmune diseases and animal models of autoimmunity. *Mediators Inflamm.* 2009, (2009).
  149. Ellsworth, S. G. *et al.* Principal component analysis identifies patterns of cytokine expression in non-small cell lung cancer patients undergoing definitive radiation therapy. *PLoS One* 12, e0183239 (2017).
  150. Dean, G. A. & Pedersen, N. C. Cytokine Response in Multiple Lymphoid Tissues during the Primary Phase of Feline Immunodeficiency Virus Infection. *Journal of Virology* 72, 9436–9440 (1998).
  151. Pedersen, B. K., Steensberg, A. & Schjerling, P. Muscle-derived interleukin-6: Possible biological effects. *Journal of Physiology* 536, 329–337 (2001).
  152. Lutosławska, G. Interleukin-6 as an adipokine and myokine: The regulatory role of cytokine in adipose tissue and skeletal muscle metabolism. *Hum. Mov.* 13, 372–379 (2012).
  153. Lundberg, I., Ulfgrén, K., Nyberg, P., Andersson, U. & Klareskog, L. Cytokine production in muscle tissue of patients with idiopathic inflammatory myopathies. *Arthritis Rheum.* 40, 865–874 (1997).
  154. Muñoz-Cánoves, P., Scheele, C., Pedersen, B. K. & Serrano, A. L. Interleukin-6 myokine signaling in skeletal muscle: a double-edged sword? *The Febs Journal* 280, 4131–4148 (2013).
  155. T. Wüthrich *et al.* Development of a vascularized extracellular matrix nerve scaffold using perfusion decellularization and re-endothelialization. (2018).
  156. Schaad, L. *et al.* Correlative Imaging of the Murine Hind Limb Vasculature and Muscle Tissue by MicroCT and Light Microscopy. *Sci. Rep.* 7, 1–12 (2017).

# 10. Declaration of consent

## Declaration of consent

on the basis of Article 28 para. 2 of the RSL05 phil.-nat.

Name/First Name: Wüthrich Tsering

Matriculation Number: 11-103-165

Study program: Master of Science in Molecular Life Sciences with  
special qualification in Microbiology/Immunology

Bachelor  Master  Dissertation

Title of the thesis:

**Engineering Extracellular Matrix Scaffolds Derived from Vascularized Composite  
Allografts and Vascularized Peripheral Nerves Grafts**

Supervisor:

Prof. Dr. R. Rieben

Dr. phil. nat. A. Taddeo

I declare herewith that this thesis is my own work and that I have not used any sources other than those stated. I have indicated the adoption of quotations as well as thoughts taken from other authors as such in the thesis. I am aware that the Senate pursuant to Article 36 para. 1 lit. r of the University Act of 5 September, 1996 is authorised to revoke the title awarded on the basis of this thesis. I allow herewith inspection in this thesis.

Place/Date

Signature

# 11. Acknowledgements

I would like to thank Prof. Dr. Robert Rieben from the Department of Biomedical Research (DBMR, University of Bern) and Prof. Dr. med. Esther Vögelin from the Clinic for Plastic and Hand Surgery (Inselspital, University Hospital Bern) for the opportunity to complete my master thesis in a very productive environment of close collaboration between their research groups. I also speak my sincerest gratitude to Dr. phil. nat. Adriano Taddeo, who was the most inspiring supervisor and teacher and from whom I have learnt a lot during my time in the laboratory. He truly is a role model, not only in a scientific, but also in a personal way. Further acknowledgement I would like to dedicate to all the persons that were involved in the projects that became part of my master thesis. This includes the team of Prof. Dr. med. Benoit Lengelé at the Université Catholique de Louvain, especially Dr. med. MD-PhD Jérôme Duisit, for a good collaboration, study design and inspiration. Special thanks go to the members of the Plastic Surgery team of the Inselspital Bern, Dr. med. Radu Olariu and Dr. med. Ioana Lese for their sacrificed holidays, their surgical skills as well as scientific support and inspiration. Further thanks go to all the lab members that have introduced me to scientific techniques, the lab life and the apéro-culture on the roof top terrace. I have learnt a lot, scientifically as well as personally, and it has been a great pleasure for me to be part of this group. I sincerely enjoyed my time in this lab - thank you all from the bottom of my heart.

I also thank my peers from the study program, for having created many beautiful memories during the time of our studies, and having shared the good times, the coffee breaks and the mozzarella sticks, as well as the lessons learnt in the lectures, courses and the lab, and for having mentally supported each other at times when motivation was at risk of running low.

Last but not least, I thank my closest friends and family to have always supported me by creating a perfect balance to lab life. I thank you for all the good conversations, for cheering me up, filling me with motivation and dancing the nights away. Thank you for your interest and excuse me, if I was not always able to explain to you in simple German words, what I was actually doing all day long. Without you, life would be pointless.